ABSTRACT

Title of Dissertation: Estimating High Spatial Resolution Clear-Sky Land Surface Longwave Radiation Budget from MODIS and GOES Data

Wenhui Wang, Doctor of Philosophy, 2008

Dissertation directed by: Dr. Shunlin Liang, Professor
Department of Geography

The surface radiation budget (SRB) is important in addressing a variety of scientific and application issues related to climate trends, hydrological and biogeophysical modeling, and agriculture. The three longwave components of SRB are surface downwelling, upwelling, and net longwave radiation (LWDN, LWUP, and LWNT). Existing surface longwave radiation budget (SLRB) datasets have coarse spatial resolution and their accuracy needs to be greatly improved.

This study develops new hybrid methods for estimating instantaneous clear-sky high spatial resolution land LWDN and LWUP from the Moderate Resolution Imaging Spectroradiometer (MODIS, 1km) and the Geostationary Operational Environmental Satellites (GOES, 2-10 km) data. The hybrid methods combine extensive radiation transfer (physical) and statistical analysis (statistical) and share the same general framework. LWNT is derived from LWDN and LWUP.

This study is the first effort to estimate SLRB using MODIS 1 km data. The new hybrid methods are unique in at least two other aspects. First, the radiation transfer simulation accounted for land surface emissivity effect. Second, the surface pressure

effect in LWDN was considered explicitly by incorporating surface elevation in the statistical models.

Nonlinear models were developed using the simulated databases to estimate LWDN from MODIS TOA radiance and surface elevation. Artificial Neural Network (ANN) models were developed to estimate LWUP from MODIS TOA radiance. The LWDN and LWUP models can explain more than 93.6% and 99.6% of variations in the simulated databases, respectively. Preliminary study indicates that similar hybrid methods can be developed to estimate LWDN and LWUP from the current GOES-12 Sounder data and the future GOES-R data.

The new hybrid methods and alternative methods were evaluated using two years of ground measurements at six validation sites from the Surface Radiation Budget Network (SURFRAD). Validation results indicate the hybrid methods outperform alternative methods. The mean RMSEs of MODIS-derived LWDN, LWUP, and LWNT using the hybrid methods are 16.88, 15.23, and 17.30 W/m^2. The RMSEs of GOES-12 Sounder-derived LWDN and LWUP are smaller than 23.70 W/m^2. The high spatial resolution MODIS and GOES SLRB derived in this study is more accurate than existing datasets and can be used to support high resolution numerical models.

Estimating High Spatial Resolution Clear-Sky Land Surface Longwave Radiation Budget from MODIS and GOES Data

By

Wenhui Wang

Dissertation submitted to the Faculty of the Graduate School of the
University of Maryland, College Park, in partial fulfillment
of the requirements for the degree of
Doctor of Philosophy
2008

Advisory Committee:

Dr. Shunlin Liang, Chair
Dr. Ivan Csiszar
Dr. Ralph Dubayah
Dr. Samuel Goward
Dr. Zhanqing Li

DEDICATION

To my family and my parents

ACKNOWLEDGEMENTS

I would like to thank my dissertation advisor, Dr. Shunlin Liang. During the past four years, Dr. Liang has given me countless support, guiding my academic research and providing with funding for my PhD studies at the University of Maryland (UMD). I also want to thank Dr. Ivan Csiszar, Dr. Ralph Dubayah, Dr. Samuel Goward, and Dr. Zhanqing Li for serving on my dissertation committee and for providing valuable suggestions and recommendations for my research. I also owe a debt of gratitude to my previous PhD advisor, Dr. Mark Gahegan, at the Geography Department of the Pennsylvania State University, for introducing me to the field of geography and remote sensing.

During the past five and a half years (including one and a half years at the Pennsylvania State University), my family, particularly my husband, has provided valuable support to my academic pursuit and has always accommodated the schedule of my study and research. Without their support and encouragement, I would not have achieved the goal of obtaining a PhD.

I also want to acknowledge the assistance provided to my research by the following researchers or PhD students at the Geography Department at UMD. They are Dr. Hongliang Fang, Dr. Tao Zhang, Mr. Dongdong Wang, and Ms. Hye-Yun Kim. Thanks also go to Dr. Kaicun Wang, an associate researcher at the Geography Department, for his valuable suggestions for my research. Last, but not the least, I want to thank Dr. Alex Ritter for proofreading the draft of this dissertation.

TABLE OF CONTENTS

LIST OF TABLES

LIST OF FIGURES

LIST OF ABBREVIATIONS

AIRS – Atmosphere Infra-Red Sounder
ANN – artificial neural network
ARM – Atmospheric Radiation Measurement
AVHRR – Advanced Very High Resolution Radiometer
CEOS – Committee on Earth Observation Satellites
CERES – Clouds and the Earth's Radiant Energy System
EOS – Earth Observation System
GCOS – Global Climate Observation System
GEWEX – Global Energy and Water Cycle Experiments
GOES – Geostationary Operational Environmental Satellite
HIRS – High Resolution Infrared Radiation Sounder
ISCCP – International Satellite Cloud Climatology Project
JHU – John Hopkins University
LST – land surface temperature
LWDN – surface downwelling longwave radiation
LWNT – surface net longwave radiation
LWUP – surface upwelling longwave radiation
MODIS – Moderate Resolution Imaging Spectroradiometer
MODTRAN4 – Moderate Resolution Transmittance Code Version 4
RMSE – root mean squared error
SURFRAD – Surface Radiation Budget Network
TIR – thermal infra-red
TIROS – Television and InfraRed Observation Satellite
TOA – top of atmosphere
TOVS – TIROS Operational Vertical Sounder
TRMM – Tropical Rainfall Measuring Mission
UCSB – University of California Santa Barbara
VAS -- VISSR Atmosphere Sounder
VISSR -- Visible and Infrared Spin Scan Radiometer
WCRP – World Climate Research Programme
WMO – World Meteorological Organization

Chapter 1 Introduction

The surface radiation budget plays important roles in determining the thermal conditions of the atmosphere, ocean, and land. It shapes the main characteristics of the Earth's climate (Ellingson, 1995; Gupta & Wilber, 1992; Schmetz, 1989) and is valuable in addressing a variety of scientific and application issues related to climate trends, hydrological and biogeophysical modeling, and agriculture. The surface radiation budget is dominated by longwave radiation at night and at most times of the year in polar regions (Curry et al., 1996). The three longwave (4 – 100 μm) components are surface downwelling longwave radiation (LWDN), surface upwelling longwave radiation (LWUP), and surface net longwave radiation (LWNT). Since LWNT is simply the difference between downwelling and upwelling longwave radiation, estimating surface longwave radiation budget can be reduced to the problem of estimating LWDN and LWUP.

LWDN is a direct measure of the radiative heating of the surface by the atmosphere (Inamdar & Ramanathan, 1997). LWUP is an indicator of how warm the Earth's surface is. Both downwelling and upwelling longwave radiation are diagnostic parameters for numerical weather prediction models. The former is an input parameter and the latter is a prediction in land surface models for ecological, hydrological, and atmospheric studies. LWNT is one of the two components (the other one is surface net shortwave radiation) needed for estimating surface net radiation, which is the key driving force for evapotranspiration.

Regional and global surface longwave radiation budget can only be estimated from satellite data. Quantifying surface longwave radiation budget with high accuracy is a fundamental prerequisite for reliable weather prediction, climate simulation, and land surface modeling (Wild et al., 2001). The meteorological, hydrological, and agricultural research communities require an accuracy of 5 - 10 W/m^2 for surface longwave radiation budget retrieved from satellite data at the 25 - 100 km spatial resolution and 3-hour - daily temporal resolution (CEOS & WMO, 2000; GCOS, 2006; GEWEX, 2002).

1.1 Existing Surface Longwave Radiation Budget Datasets

Four major long-term surface longwave radiation budget datasets are currently available. The first dataset is derived using the Clouds and the Earth's Radiant Energy System (CERES), onboard the NASA Earth Observing System (EOS) Terra and Aqua satellites and the Tropical Rainfall Measuring Mission (TRMM) satellite (Inamdar & Ramanathan, 1997; Wielicki et al., 1996; Gupta et al., 1997). The second long-term surface longwave radiation budget dataset is provided by the NASA World Climate Research Programme/ Global Energy and Water Cycle Experiments (WCRP/GEWEX) using the Geostationary Operational Environmental Satellites (GOES) data (ASDC, 2006). The third dataset is an 18-year surface longwave radiation budget dataset derived using the International Satellite Cloud Climatology Project (ISCCP) data (Zhang et al., 2004; Zhang & Rossow, 2002; Zhang et al., 1995). The fourth dataset is a 22-year LWDN datasets for the Arctic (Francis & Secora, 2004). Table 1-1 summarized the spatial resolution, temporal coverage, satellite instrument, instrument footprint, and stated accuracy of the four datasets.

	CERES	WCRP/GEWEX	ISCCP	ARCTIC LWDN
Products Available & spatial resolution	LWDN&LWUP 1°	LWDN&LWUP 1°	LWDN&LWUP 280 km	LWDN 100 km
Temporal Coverage	1998 -present	1983-2005	1983-2001	1979-2002
Satellite	TRMM, EOS Terra/Aqua	GOES	TOVS	TOVS
Instrument Footprint (km)	20	10 x 40	40	40
Stated Accuracy Monthly Avg. (W/m^2)	21	33.6	20-25	30

Table 1-1 Summary of existing surface longwave radiation budget datasets.

1.2 The Need to Estimate Surface Longwave Radiation Budget Using High Spatial Resolution Satellite Data

Existing datasets do not achieve the required accuracy. The random errors in surface longwave radiation budget components will be reduced when they are aggregated spatially and temporally. User communities require an accuracy of 5-10 W/m^2 at 3-hour to daily temporal resolution and 25-100 km spatial resolution. However, the achieved accuracy is from 21 to 33.6 W/m^2 at the monthly timescale and at 100 - 280 km spatial resolution.

Current datasets are all derived from coarse spatial resolution satellite data. Surface longwave radiation budget components vary at the finer spatial scales, especially for LWUP. One approach to improve the accuracy of surface longwave radiation budget estimates is to use high spatial resolution satellite observation that can provide more detailed information about the atmosphere and the Earth's surface. High spatial resolution satellite atmospheric and surface observations (down to 1 km) are routinely available

today. However, few studies have estimated surface longwave radiation budget using these data.

Another issue is that no dataset is currently available to support high spatial resolution numerical models. In recent years, high resolution (down to 1 km) land surface models and numerical weather prediction models have been widely studied and applied in short range forecasting, natural hazards warning, and mesoscale land surface and atmospheric modeling (Soci & Fischer, 2006; Guan et al., 2000; Christensen & Christensen, 1998). However, current surface longwave radiation budget datasets are all designed for large scale models and cannot capture the detailed variation on the land surface. Without high resolution surface longwave radiation budget datasets, the accuracy of the models is compromised.

1.3 The Purpose of This Study

The purpose of this study is to develop new methods to estimate instantaneous clear-sky land surface longwave radiation budget using high spatial resolution satellite data. The definitions of high spatial resolution vary according to application areas. In this study, the application areas are land surface models and numerical weather prediction models. High spatial resolution is defined as surface longwave radiation budget with a spatial resolution from 1 km to 10 km.

The goal of this study is to estimate the clear-sky surface longwave radiation budget. The outgoing radiance received by a satellite sensor is decoupled from the surface when opaque cloud cover exists. Different methods are needed for estimating

surface longwave radiation budget under cloudy-sky conditions using passive thermal infrared remote sensing techniques.

High spatial resolution satellite data from two sources were used in this study. The first data source is the Moderate Resolution Imaging Spectroradiometer (MODIS) onboard the NASA Terra and Aqua EOS satellites. MODIS provides unique opportunities for estimating surface longwave radiation budget at 1 km spatial resolution. Although MODIS is not a true sounding instrument, it has 16 channels in the 3.6 to 15 μm spectral range (Barnes et al., 1998; Guenther et al., 1998). The two MODIS instruments provide four observations over any locations on the surface of the Earth daily, with more observations over high latitude regions.

The surface longwave radiation budget estimated from MODIS data alone is inadequate for deriving diurnal cycle in low latitude regions. The second data source is the sounding instruments onboard the NOAA Geostationary Operational Environmental Satellite (GOES). The current GOES satellites provide diurnal coverage of the Earth Surface between ±60º latitude, with a half-hour temporal resolution. Data from GOES-12 Sounder were used in this study. It has a spatial resolution of 10 km in thermal infrared (TIR) channels. Moreover, the feasibility of estimating clear-sky surface longwave radiation budget using the future GOES-R Advanced Baseline Imager (ABI) data was also studied.

New hybrid methods were developed for estimating clear-sky high spatial resolution LWDN and LWUP using MODIS, GOES-12 Sounder, and GOES-R data. LWNT was derived using LWDN and LWUP. All hybrid methods share the same general

framework and combine extensive radiative transfer simulation (physical) and statistical analysis (statistical). They are the first such methods designed to estimate surface longwave radiation budget using MODIS and the current and future GOES data. The new hybrid methods differ from previous methods in at least two other aspects. First, land surface emissivity effect was accounted for in the radiative transfer simulation. Second, the surface pressure effect in LWDN was considered by incorporating surface elevation in the statistical models developed using the simulated databases.

This dissertation is organized as follows. The theoretical basis and the review of previous studies are provided in Chapter 2. Chapter 3 describes data employed in this study. Chapter 4 presents the framework of the hybrid methods for estimating LWUP and LWDN from MODIS and GOES data. Chapters 5 and 6 are devoted to estimating LWDN, LWUP, and LWNT from MODIS data. Products intercomparision between MODIS and CERES surface longwave radiation budget and the methods for estimating LWDN and LWUP from GOES-12 Sounder and the future GOES-R data are presented in Chapter 7. Chapter 8 summarizes this study and provides suggestions for future research.

Chapter 2 Theoretical Background and Literature Review

2.1 Top of Atmosphere Radiance

For a plane parallel, horizontally homogeneous non-scattering atmosphere and a flat Lambertain surface, the Top of Atmosphere (TOA) radiance measured by a satellite sensor at a TIR channel can be expressed by the following equation (Liang, 2004):

$$L_i = L_i^p + t_i\left(\varepsilon_i B(T_s) + (1-\varepsilon_i)\frac{F_{i,d}}{\pi}\right) \tag{2-1}$$

where i is channel number; L_i is spectral radiance; L_i^p is thermal path radiance; t_i is surface to TOA transmittance; ε_i is channel *i* narrow band emissivity; T_s is surface temperature; $B(T_s)$ is Planck function; $F_{i,d}$ is the narrow band LWDN at channel i. Clear-sky TOA radiance contains information about both atmosphere and surface.

2.2 Surface Downwelling Longwave Radiation (LWDN)

LWDN is the result of atmosphere absorption, emission, and scattering. Clear-sky LWDN depends on the vertical profiles of atmosphere temperature, moisture, and other gases (Lee, 1993; Lee & Ellingson, 2002; Ellingson, 1995) :

$$F_d = \int_{\lambda_1}^{\lambda_2}\int_0^1 I_\lambda(z=0,\mu)\mu d\mu d\lambda \tag{2-2}$$

where λ_1 and λ_2 is the spectral range of LWDN (4-100 μm); λ is wavelength; z is the altitude above surface; $\mu = \cos(\theta)$ and θ is local zenith angle; $I_\lambda(z=0,\mu)$ is downward spectral radiance at surface and is expressed as:

$$I_\lambda(z=0,\mu) = -\int_0^{z_t} B(T_z)\frac{\partial T_\lambda(0,z,-\mu)}{\partial z}dz \tag{2-3}$$

where $B(T_z)$ is Planck function evaluated at altitude z ; z_t is the altitude of satellite; T_λ is transmittance from surface to altitude z .

LWDN is dominated by the radiation from a shallow layer close to the surface of the Earth. The atmosphere above 500 meters from the surface only accounts for 16-20% of total LWDN. The contribution of the lowest 10 meters atmosphere accounts for 32-36% of total LWDN (Schmetz, 1989). Previous studies indicate that atmospheric temperature and moistures profiles are the most important parameters in estimating clear-sky LWDN. It is sufficient to use climatological CO_2 and O_3 mass mixing ratios because variations in the mixing ratios of the two gases have small impacts on LWDN. A 50% change in the mixing ratio of the two species only modifies LWDN by 1 W/m^2 (Smith & Wolfe, 1983).

During the past decades, many studies have estimated clear-sky LWDN from satellite data. Comprehensive reviews about these studies are available from the literature (Niemela et al., 2001; Diak et al., 2004; Ellingson, 1995; Schmetz, 1989). Methods used in previous studies are either physical or hybrid. The physical method is straightforward, i.e., calculating LWDN using a radiative transfer model (or highly parameterized equations) and atmosphere temperature/moisture profiles. The merit of physical methods is their basis on physics. Their major disadvantage is that errors in the input parameters (atmosphere profiles for clear-sky cases) affect the accuracy of the LWDN estimated.

Hybrid methods are based on extensive radiative transfer simulation and statistical analysis. First, LWDN and TOA radiance, for a particular instrument, are simulated using a radiative transfer model and a large number of clear-sky atmosphere profiles. Then empirical relationship between TOA radiance (or brightness temperature) and LWDN are established using statistical analysis. Hybrid methods are less sensitive to errors in the atmosphere profiles. The physics of LWDN is embedded in the radiative transfer simulation processes. More details about the hybrid method are provided in Chapter 4.

Smith and Woolf (1983) used a linear regression analysis on 1200 *in-situ* soundings to obtain relations between the Visible and Infrared Spin Scan Radiometer (VISSR) Atmosphere Sounder (VAS) TOA radiance and surface longwave radiation budget at 1000 hPa pressure level for both clear-sky and cloudy-sky conditions. They found that window channels were the most important predictors in both cases. Their statistical models for clear-skies explain 98.1% of variances in the simulated database, with standard error of 10.3 W/m^2.

Darnell (1983) used a radiative transfer model with input data from the Television and InfraRed Observation Satellite (TIROS) Operational Vertical Sounder (TOVS) products to calculate LWDN for both clear and cloudy skies. Frouin et al. (1989) developed a radiative transfer technique for estimating LWDN over ocean using TOVS temperature and moisture profiles and cloud parameters derived from VISSR data. Gupta et al. (Gupta, 1989; Gupta & Wilber, 1992; Gupta et al., 1997) developed highly parameterized equations for computing LWDN globally using TOVS meteorological data.

Morcrette and Deschamps (1986) estimate LWDN using regression equations from the second High Resolution Infrared Sounder (HIRS/2) TOA radiance under clear-sky conditions. The results were compared with hourly ground measurements over three sites in Western Europe. Standard errors ranged from 16 -30 W/m^2.

Clouds and the Earth's Radiant Energy System (CERES) science team adopted two plans for estimating clear-sky LWDN. In plan A, a hybrid method uses TOA longwave fluxes and other correlated meteorological variables (total column water vapor, surface temperature, and near-surface temperature) to estimate LWDN under clear-sky conditions. TOA and surface longwave fluxes were simulated using a radiative transfer model, which uses soundings from ships as input. Window and non-window components of downward flux were fitted using TOA fluxes and other meteorological variables. In plan B, total-sky LWDN is estimated using parameterized equations (Gupta et al., 1997). The input parameters to the algorithm are surface temperature and emissivity, temperature and humidity profiles, fractional cloud cover, and cloud top height.

Zhou and Cess (2001) developed an hybrid method for retrieving LWDN using ground measurements from the Atmosphere Radiation Measurements (ARM) program at the U.S. Southern Great Plain (SGP) and Tropical Western Pacific (TWP) sites. Their study demonstrated that clear-sky LWDN could be largely determined by LWUP and column precipitable water vapor.

Lee and Ellingson (2002) found that linear model for estimating LWDN using the HIRS brightness temperatures cannot account for the variation of water vapor burden sufficiently, with increasing model residuals as the water vapor burden increases. They

proposed nonlinear statistical models for both clear and cloudy-sky conditions. The results showed that model fitting standard errors are about 9 W/m^2 for clear-sky conditions and 4-8 W/m^2 for cloudy-sky conditions. The method can produce unbiased estimations over large range of meteorological conditions. However, the method was not validated using *in situ* measurements.

2.3 Surface Upwelling Longwave Radiation (LWUP)

Theoretically, LWUP consists of two components: surface longwave emission and reflected LWDN (Liang, 2004):

$$F_u = \varepsilon \int_{\lambda_1}^{\lambda_2} \pi B(T_s) d\lambda + (1 - \varepsilon) F_d \quad (2\text{-}4)$$

where F_u is LWUP, ε is surface broadband emissivity, T_s is surface temperature, $B(T_s)$ is Planck's function, λ_1 and λ_2 are the spectral range of LWUP (4-100 μm), and F_d is LWDN. LWUP is dominated by surface longwave emission. Three parameters are required to estimate land surface LWUP accurately: surface temperature, broadband emissivity, and LWDN.

Two methods have been used for estimating LWUP from satellite data. The first method is to calculate LWUP using satellite-derived surface temperature and emissivity products and LWDN based on Equation 2-4. Because surface longwave emission dominates LWUP, this method is called temperature-emissivity method in the rest of the text. Some studies ignore the reflected LWDN; LWUP is estimated using surface temperature and emissivity only. Many algorithms have been developed to estimate land

surface temperature (LST) and emissivity from satellite data (Sobrino et al., 2004; Wan, 1999; Wan & Dozier, 1996; Wan & Li, 1997; Gabarró et al., 2004; Gillespie et al., 1998; Gillespie et al., 1999; Prata, 2002; Sobrino & Romaguera, 2004). In CERES products, clear-sky LWUP is estimated from MODIS LST and emissivity products (Inamdar & Ramanathan, 1997; Gupta et al., 1997).

The second method is the hybrid method, similar to the hybrid method used for estimating LWDN (see Chapter 4 for more details). The hybrid method has mainly been used to estimate LWDN. Smith and Woolf (1983) used a hybrid method to estimate both LWDN and LWUP from the NOAA geostationary satellites VISSR VAS TOA radiance at 1000 hPa pressure level. Meerkoetter and Grassl (1984) used the hybrid method to estimate LWUP and LWNT from the Advanced Very High Resolution Radiometer (AVHRR) split-window radiance.

2.4 Limitations of Previous Studies

Hybrid methods had been developed to estimate surface longwave radiation budget for various satellite instruments. However, the spatial resolutions of these instruments are coarse. While MODIS and GOES-12 Sounder data provide new opportunities to estimate high spatial resolution surface longwave radiation budget at 1 km and 10 km resolution, no study has been conducted until today.

Previous studies have focused on estimating surface longwave radiation budget over sea surfaces. Constant emissivity was assumed because the sea surface is mostly uniform and water emissivity is less variable. Surface emissivity is more important in estimating LWUP over land because land surface emissivity varies widely over time.

Beside LWUP, emissivity scheme also affects the simulated TOA radiance in the hybrid method. The purpose of this study is to derive the surface longwave radiation budget over land surfaces. The land surface emissivity effect must be sufficiently considered.

Surface pressure is an important factor in estimating land LWDN because of the effect of the pressure broadening of the spectral lines (Lee & Ellingson, 2002). The atmosphere is thinner over high elevation surfaces. There is less atmosphere emission at higher elevations when air temperatures are the same. Previous studies typically estimated LWDN only at sea level. Existing methods must be modified to account for the surface pressure effect over land surfaces at high elevations.

Chapter 3 Data for Methods Development and Evaluation

A variety of datasets were used in this work to facilitate method development and evaluation. The hybrid methods for estimating LWDN and LWUP from TOA radiance require representative atmosphere profiles in radiative transfer simulation. The physical method for estimating LWDN requires atmosphere profiles as input parameters. Emissivity spectra are needed to account for the surface emissivity effect over the land surface. Surface temperature and emissivity products are required to calculate LWUP using the temperature-emissivity method. MODIS and GOES 12-Sounder TOA radiance products, cloud products (for identifying clear-sky observations), and ground-measured LWDN and LWUP are needed for methods evaluation. Table 3-1 summarizes all datasets used in this work. Major datasets are described in the following subsections. All MODIS and GOES products are available online from the NASA Level 1 and Atmosphere Archive and Distribution System (http://ladsweb.nascom.nasa.gov), the NASA Earth Observing System Data Gateway (http://edcimswww.cr.usgs.gov/pub/imswelcome/), the NASA Langley Cloud and Radiation Research Group (http://www-angler.larc.nasa.gov/), and the NOAA Comprehensive Large Array-data Stewardship System (http://www.class.ngdc.noaa.gov/).

Datasets	Short Name	Version	Spatial Resolution. (km)	Parameters Used	References
MODIS Terra Atmosphere Product	MOD07_L2	5	5	Atmosphere profile, surface temperature, column water vapor, surface pressure, and elevation	(Menzel et al., 2002; Seemann et al., 2003)
MODIS LST/Emissivity Product 1	MOD11_L2(Terra) MYD11_L2(Aqua)	4	1	Land surface temprature	(Wan, 1999; Wan & Dozier, 1996)
MODIS LST/Emissivity Product 2	MOD11B1(Terra) MYD11B1(Aqua)	4	5	Narrow band emissivity	(Wan, 1999; Wan & Li, 1997)
MODIS Land Cover Product	MOD11C3	5	5	Plant function type	(Strahler et al., 1999)
University of California Santa Barbara Emissivity Library	--	--	--	Emissivity spectra	(Wan, 1999)
John Hopkins University Emissivity Library	--	--	--	Emissivity spectra	(ASTER, 1999; Salisbury & D'Aria, 1992; Salisbury & Milton, 1988)
MODIS TOA Radiance Product	MOD021KM(Terra) MYD021KM(Aqua)	5	1	TOA radiance	(Toller et al., 2006)
MODIS Cloud Product	MOD06_L2 (Terra) MYD06_L2 (Aqua)	5	1	Cloud mask	(Ackerman et al., 2002)
GOES-12 Sounder TOA Radiance Product	--	--	10	TOA radiance	--
GOES-12 Cloud Product	--	--	4	Cloud mask	(Minnis et al., 2004)
SURFRAD Ground Measurements	--	--	--	LWDN, LWUP, surface air temperature	(Augustine et al., 2000)

Table 3-1 Major datasets used in this study.

3.1 MODIS Terra Atmosphere Product

Several methods used in this study require atmosphere profiles: the physical method for estimating LWDN and the hybrid methods for estimating LWDN and LWUP. The MODIS science team provides atmospheric product routinely (Seemann et al., 2003; Menzel et al., 2002). MODIS-Terra atmosphere product was used in this study. Temperature, moisture, pressure, and geopotential height profiles are provided at 20 fixed pressure levels (1000, 950, 920, 850, 800, 700, 620, 500, 400, 300, 250, 200, 150, 100, 70, 50, 30, 20, 10, 5 hPa) in the product. Validation study indicated that MODIS retrievals are similar to ground observations for the atmosphere with fairly monotonic, smooth temperature and moisture distributions (Seemann et al., 2003). Besides atmosphere profiles, surface temperature, surface pressure, surface elevation, and column water vapor corresponding each profile are also available in the product. They were used to facilitate method development.

3.2 MODIS LST/Emissivity Products

Estimating LWUP using the temperature-emissivity method requires surface temperature and emissivity products as input parameters. The MODIS science team provides multiple daily LST and emissivity products operationally at 1 and 5 km spatial resolution. The Land Surface Temperature/Emissivity Daily 5-Min L2 Swath 1 km product is the source of surface temperature in this study. In the product, LST is retrieved using a generalized split-window algorithm (Wan, 1999; Wan & Dozier, 1996) at 1 km spatial resolution. Constant emissivity based on land cover types is used in the algorithm.

This LST product has been validated in previous studies (Wan et al., 2004; Coll et al., 2005; Wan et al., 2002; Wang et al., 2007). Its accuracy is 1 °C for the surfaces with known emissivity and the greatest difference between MODIS retrieved LST and ground-measured LST are ~ 2 °C. MOD11_L2 LST product was also evaluated using long-term continuous nighttime measurements over fixed points in this study. The differences between MOD11_L2 LST and ground-measured LST are less than 1.7 °C at most U.S. sites (Wang et al., 2008).

The broadband emissivity data required by the temperature-emissivity method is derived using the narrow band emissivities from the Land Surface Temperature/ Emissivity Daily L3 Global 5 km SIN Grid 5 km products (MOD11B1 and MYD11B1). In this product, narrow band emissivities are retrieved based on a day/night algorithm at 5 km spatial resolution (Wan, 1999; Wan & Li, 1997). The accuracy of the MODIS narrow band emissivity is reported to be 0.01 (Wan et al., 2004; Wan et al., 2002; Wang et al., 2004).

3.3 Emissivity Libraries

To estimate surface longwave radiation budget over land surface in high accuracy, emissivity spectra are needed to characterize the spectral features and ranges of the emissivities of terrestrial, natural, and manmade materials. Two emissivity libraries were used in this work: the John Hopkins University (JHU) Emissivity Library that is currently part of the ASTER emissivity library (ASTER, 1999; Salisbury & D'Aria, 1992; Salisbury & Milton, 1988) and the University of California Santa Barbara (UCSB) Emissivity Library (Wan, 1999).

The JHU Emissivity Library provides single emissivity spectra for conifers, deciduous, grass, dry grass, ice, snow, and water in the spectral range of 2 – 14 μm. The library contains multiple soil spectra to represent different types of soil. The averaged soil emissivity spectrum was calculated and used as the emissivity spectra of soil in this study. The modified JHU Emissivity Library was used in developing the hybrid method for estimating LWDN. LWDN is less sensitive to surface characteristics compared to LWUP (see Chapter 5). Therefore, a smaller emissivity library was used to reduce data volume and computational time.

The UCSB Emissivity Library consists of 150 spectral emissivity measurements for both natural and man-made materials. Some emissivity spectra are very similar. To reduce the amount of calculation needed, similar emissivity spectra in the original library were combined. A total of 59 spectra representing different land surfaces were used to develop the hybrid methods for estimating LWUP (see Chapter 6).

3.4 Surface Radiation Budget Network Ground Measurements

Two years (2005 and 2006) of ground data from the Surface Radiation Budget Network (SURFRAD, see Figure 3-1) (Augustine et al., 2000; Augustine et al., 2005) were used to evaluate the methods developed in this work. SURFRAD ground measurements are organized into daily files of three-minute averaged values. The land cover types of these sites include grassland, cropland, and desert. The surface elevation of SURFRAD sites ranges from 213 to 1689 meters. SURFRAD data is widely used for satellite-derived land surface and atmospheric products validation (Fang et al., 2007;

Zhou et al., 2007; Gupta et al., 2004). Table 3-2 summarizes the latitude, longitude, land cover type, and elevation of the six SURFRAD sites used in this study.

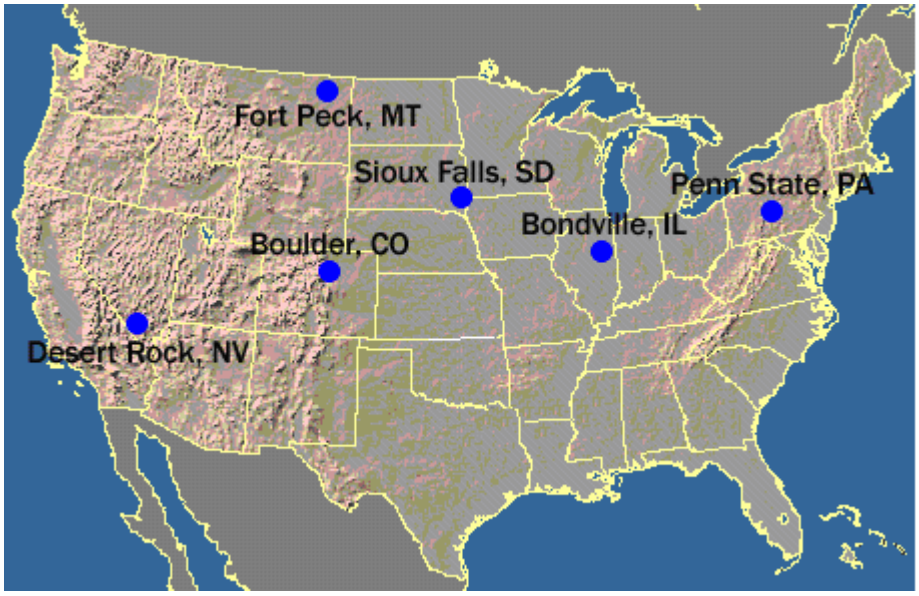

Figure 3-1 Map showing locations of SURFRAD validation sites used in this research.

Site Name	Lat & Lon	Land cover	Elevation (m)
Bondville, IL	40.05, -88.37	Cropland	213
Sioux Falls, SD	43.73, -96.62	Grassland	473
Penn State, PA	40.72, -77.93	Cropland	376
Desert Rock, NV	36.63, -116.02	Desert	1007
Fort Peck, MT	48.31, -105.10	Grassland	634
Boulder, CO	40.13, -105.24	Grassland	1689

Table 3-2 SURFRAD validation sites.

LWUP and LWDN were measured using the Precision Infrared Radiometer (model PIR, Eppley Laboratories) at the SURFRAD sites (The Eppley Laboratory, 2007). The PIRs are elevated ~8 meters above the surface and the maximum signal comes from 45 degrees. SURFRAD has three standard PIRs that are calibrated annually at the World Radiation Center's Physikalisch-Meteorologisches Observatorium in Davos (PMOD), Switzerland. The PMOD blackbody infrared radiation calibration unit was chosen

because it performed well in a round-robin test that involved a blind comparison of several comparable devices (Philipona et al., 1998). After the SURFRAD standard PIRs are calibrated in the blackbody, their calibrations are fine tuned by running them outdoors against PMOD's World Pyrgeometer Standard Group. Field instruments are calibrated by running them next to the three standard PIRs and using the simultaneous data to transfer the mean calibration of the three standard PIRs to the field instrument. During the daytime, a shade ball shades the PIR dome to minimize errors associated with inward infrared emission from the dome to the thermopile. Albrecht and Cox's method (Albrecht & Cox, 1977) is used to correct for dome emission and compute the longwave irradiance. The accuracy of ground instruments is within 1% (Philipona et al., 2001).

Chapter 4 Framework of the Hybrid Methods for Estimating LWDN and LWUP Using MODIS and GOES Data

In this study, multiple methods were developed to estimate LWDN and LWUP from MODIS, GOES-12 Sounder, and GOES-R ABI TOA radiance. The physical method for calculating LWDN and the temperature-emissivity method for calculating LWUP from MODIS data are straightforward. The hybrid methods were developed to estimate LWDN and LWUP directly from MODIS, GOES-12 Sounder, and GOES-R ABI TOA radiance. This chapter presents the general framework shared by all hybrid methods. Chapters 5, 6, and 7 present the details of individual hybrid methods.

Figure 4-1 shows the flowchart of this general framework. LWDN (4-100 μm) is directly simulated using a radiative transfer model. It is used in deriving statistical models to predict LWDN using TOA radiance. It is also used to account for the reflected LWDN in the synthesized LWUP. Spectral LWDN is the surface downwelling longwave radiation at specific wavelengths from 3.6 to 15 μm. It is used to synthesize TOA radiance. Atmosphere profile database is an input for calculating surface longwave emission because surface temperature is assigned based on surface air temperature in each atmosphere profile. Ancillary parameters include surface temperature, surface air temperature, surface pressure, surface elevation, column water vapor, and broadband emissivity (from atmosphere profile database and emissivity library). The detailed procedure of radiative transfer simulation is presented in Section 4.2.

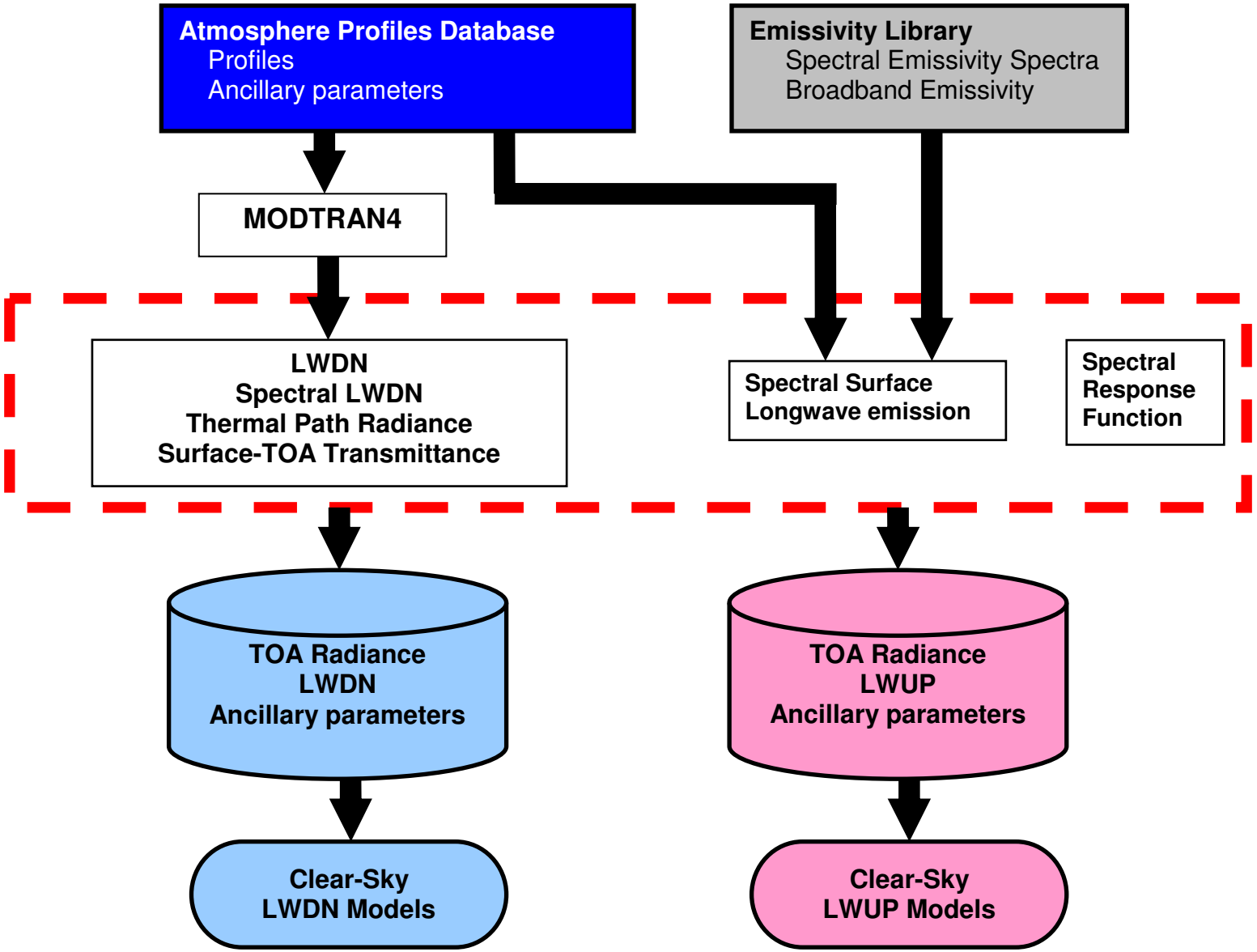

Figure 4-1 Flowchart of the framework shared by all hybrid methods.

A hybrid method consists of two steps. The first step is radiative transfer simulation. The input parameters required in this step are a large number of representative atmosphere profiles and emissivity spectra of different land surfaces. Simulated databases consist LWDN (or LWUP), TOA radiance, and supporting variables to facilitate statistical analysis. The sources of atmosphere profiles and emissivity spectra employed in this study are described in Chapter 3. Section 4.1 in this chapter is dedicated to generating atmosphere profile database. The second step is the statistical analysis. The goal is to establish the statistical relationship between LWDN (or LWUP) and TOA radiance using the simulated databases.

4.1 Generating Atmosphere Profile Databases

Radiative transfer simulation requires a large number of atmosphere temperature and moisture profiles, representing a wide range of atmosphere conditions. In this study, the latest version (version 5) of MODIS Terra-retrieved atmosphere product (MOD07_L2) in 2001 and 2004 over the North American continent were used to build the atmosphere profile database required for the radiative transfer simulation. Besides atmosphere profiles, MOD07_L2 also provides surface temperature, surface pressure, column water vapor, and elevation corresponding to each profile. They were stored in the database to facilitate method development and evaluation.

Representative profiles over the North America continent were selected by comparing new profiles to those already in the database. For each profile, the temperature and moisture values in layers below 10 km were resampled to fixed altitude levels. The similarities of two profiles in terms of temperature and moisture are defined as:

$$S_T = \sum_{i=0}^{n} \left(W_i \left| T_{1,i} - T_{2,i} \right| \right) \tag{4-1}$$

$$S_M = \sum_{i=0}^{n} \left(W_i \left| M_{1,i} - M_{2,i} \right| \right) \tag{4-2}$$

$$W_i = \frac{1}{(z_i + 1)} \tag{4-3}$$

where S_T is the similarity in temperature; S_M is the similarity in moisture; W_i is the weight at altitude i; z is altitude above the ground; $T_{1,i}$ and $T_{2,i}$ are the temperatures of the two profiles at altitude i (unit Kelvin); $M_{1,i}$ and $M_{2,i}$ are moistures of the two profiles at altitude i (unit ppmv). Two profiles are similar if the calculated S_T is smaller than 1 K and S_M is less than 200 ppmv). The thresholds are decided by the target size of database; the thresholds are smaller for a larger database. The profile database used in this study consists of more than 7000 profiles. Figure 4-2 shows the statistics of surface temperature and moisture values of the database. This atmosphere profile database was used to develop the hybrid methods for estimating LWDN from MODIS and GOES data.

A second atmosphere profile database that has only ~2000 profiles was created on the basis of the first atmosphere database by using larger threshold values. This smaller database was used to develop the hybrid methods for estimating LWUP from MODIS and GOES data. The underlying rationale is presented in Chapter 6.

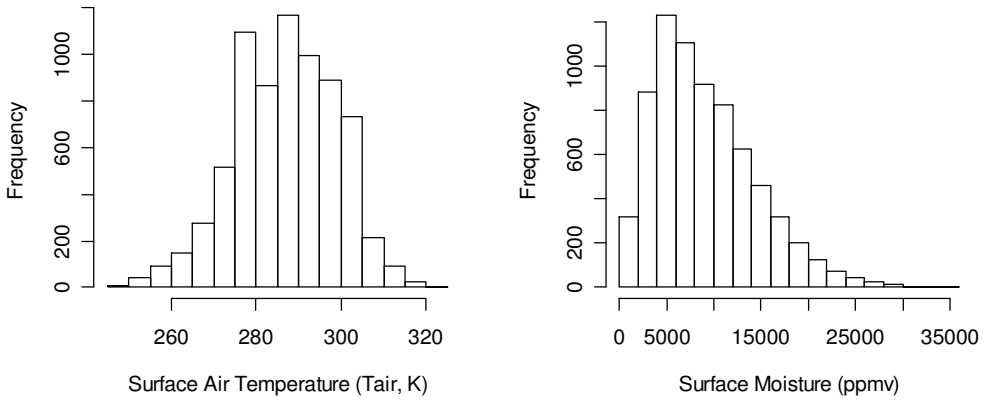

Figure 4-2 Statistics of surface air temperature and moisture in the first atmosphere profile database.

4.2 Radiative Transfer Simulation

The Moderate Resolution Transmittance Code Version 4 (MODTRAN4) was used to simulate LWDN, spectral LWDN, thermal path radiance, and surface to TOA transmittance for each atmosphere profile (see Figure 4-1). The scientific community widely uses MODTRAN4 to calculate the transmission and emission of the atmosphere and surface at wavelengths from the optical to the sub-millimeter range. MODTRAN4 provides various standard atmospheric models, and also allows users to define the atmosphere profiles (Berk et al., 1999).

The radiative transfer simulation assumes that all surfaces are Lambertian. A constant CO_2-mixing ratio of 365 ppmv and constant column O_3 of 355 Dobson were assumed in the radiative transfer simulation. Simulated databases were generated using MODTRAN4, atmosphere profile database, and emissivity library, based on the following steps:

1. Simulating spectral LWDN, thermal path radiance, and transmittance for each profile using MODTRAN4. Path radiance and transmittance are calculated at five sensor view zenith angles (0°, 15°, 30°, 45°, and 60°). Surface temperature is assigned based on the surface air temperature from the temperature profile.

2. Simulating LWDN for each profile using MODTRAN4.

3. Calculating spectral and integrated surface emissions for each profile using the Planck function. Eleven surface temperatures are assigned to each profile to simulate the surface condition for different land cover under similar atmospheric conditions. The difference between surface temperature and surface air temperature are -10, -8, -6, -4, -2, 0, 2, 4, 6, 8, and 10 °C. UCSB or JHU emissivity spectra were used to account for the surface emissivity effect (see Chapters 5 and 6 for further information).

4. Synthesizing LWUP based on Equation 2-4. Broadband emissivity is derived for each emissivity spectra.

5. Synthesizing TOA radiance based on Equation 4-4:

$$L = \int_{\lambda_1}^{\lambda_2} \left(\left(\mathrm{L}_{\downarrow \lambda} \left(1 - \varepsilon_{\lambda} \right) + \varepsilon_{\lambda} B(T_s) \right) \tau_{\lambda} + L_{p\lambda} \right) SRF \, d\lambda \qquad (4\text{-}4)$$

where λ is wavelength; $\mathrm{L}_{\downarrow \lambda}$ is spectral LWDN; ε_{λ} is emissivity; T_s is surface temperature; $B(T_s)$ is Planck function; τ_{λ} is surface-TOA transmittance; $L_{p\lambda}$ is

thermal path radiance; SRF is spectral response function of a particular sensor channel; and λ_1 and λ_2 are the spectral range of the channel.

Table 4-1 shows the structure of the simulated databases. Besides TOA radiance and LWDN/LWUP, broadband emissivity, surface elevation, surface temperature, surface air temperature, and column water vapor corresponding to each profile are also stored in the simulated databases. Only TOA radiance is dependent on sensor view zenith angles among all fields in the database.

Fields	**0°**	**15°**	**30°**	**45°**	**60°**
TOA Radiance (channels 1… n)					
LWDN or LWUP	Independent of sensor view zenith angle				
Surface elevation (H)					
Surface temperature(Ts)					
Surface air temperature(Tair)					
Column water vapor					
Broad band emissivity					

Table 4-1 The structure of the simulated databases for developing LWDN and LWUP models.

4.3 Uncertainty in Radiative Transfer Simulation

Previous studies have evaluated the accuracy of MODTRAN4 radiative transfer model. The MODTRAN4 calculated surface downward longwave irradiances are close to 2 W/m^2 to the absolute sky-scanning radiometer measurements and line-by-line radiative transfer model (Philipona et al., 2001).

To reduce the computation time needed for creating the simulated databases, TOA radiance were synthesized using spectral LWDN, thermal path radiance, surface-TOA transmittance, and surface longwave emission, instead of simulated them directly using MODTRAN4. To assess the errors caused by the synthesizing procedure, the synthesized

MODIS TOA radiance were compared to directly simulated values under different atmospheric conditions, sensor view zenith angles, and surface emissivity spectra. The difference between the synthesized and the directly simulated MODIS TOA radiance is less than 0.6% in all TIR channels, except channel 30 (O_3 channel, not used in this study).

4.4 Statistical Analysis

Statistical models for estimating LWDN and LWUP were developed using the simulated databases. First, stepwise regression was employed to identify the channels that are important for estimating LWDN and LWUP for each sensor. The O_3 channels were not considered because climatological column zone was used in the radiative transfer simulation. The physics related to LWDN and LWUP were also considered in channels selections. LWDN is dominated by atmospheric temperature and moisture profiles close to the surface. Therefore, channels related to surface temperature/moisture profiles and surface temperature and emissivity were considered in stepwise regression. Statistical models were developed at five fixed sensor view zenith angles (0°, 15°, 30°, 45°, and 60°). The values at other sensor view zenith angles are derived using linear interpolation.

Based on previous studies, there are strong linear relationships between surface longwave radiation budget components and TIR TOA radiance. Linear LWDN and LWUP models were first considered. Lee and Ellingson's study (2002) indicated nonlinear models produce better model fitting results in estimating LWDN. In this study, nonlinear regression and artificial neural network (ANN) techniques were also employed. The best models were used in estimating LWDN and LWUP.

Chapter 5 Estimating Instantaneous Clear-Sky LWDN Using MODIS Data

Although MODIS is not a true sounding instrument, it provides HIRS-like sounding channels that can estimate surface longwave radiation budget (Wang & Liang, 2008; Wang et al., 2008). Table 5-1 summarizes MODIS Terra TIR channels as well as the primary use for each channel. The channel design of MODIS Aqua is similar to MODIS Terra.

Channel	Bandwidth(μm)	Required NEΔT (K)	Primary Use
20	3.660-3.840	0.05	Surface temperature
21	3.929-3.989	2.00	
22	3.929-3.989	0.07	
23	4.020-4.080	0.07	
24	4.433-4.498	0.25	Temperature profile
25	4.482-4.549	0.25	
27	6.535-6.895	0.25	Moisture profile
28	7.175-7.475	0.25	
29	8.400-8.700	0.05	
30	9.580-9.880	0.25	O_3
31	10.780-11.280	0.05	Surface temperature
32	11.770-12.270	0.05	
33	13.185-13.485	0.25	Temperature profile
34	13.485-13.785	0.25	
35	13.785-14.085	0.25	
36	14.085-14.385	0.35	

Table 5-1 MODIS Terra TIR channels.

In this chapter, the feasibility of estimating LWDN using the physical method was first investigated. Then a new hybrid method for estimating LWDN directly from MODIS TOA radiance and surface elevation was presented. Both the physical method and the new hybrid method were evaluated using SURFARAD ground measurements.

5.1 Physical Method

The calculation of LWDN using atmosphere profiles and the radiative transfer model (physical method) is straightforward. However, the physical method is sensitive to errors in the atmosphere profile. LWDN is dominated by the radiation from the shallow layer close to the surface of the Earth. The atmosphere from the surface to 500 meters contributes ~80% of total LWDN (Schmetz, 1989). The vertical resolution of the MODIS-retrieved atmosphere profiles is coarse. At most, three or four layers are below 500 meters at any location on Earth. Therefore MODIS-derived atmosphere profiels cannot capture the detailed structure of the atmosphere (Seemann et al., 2003).

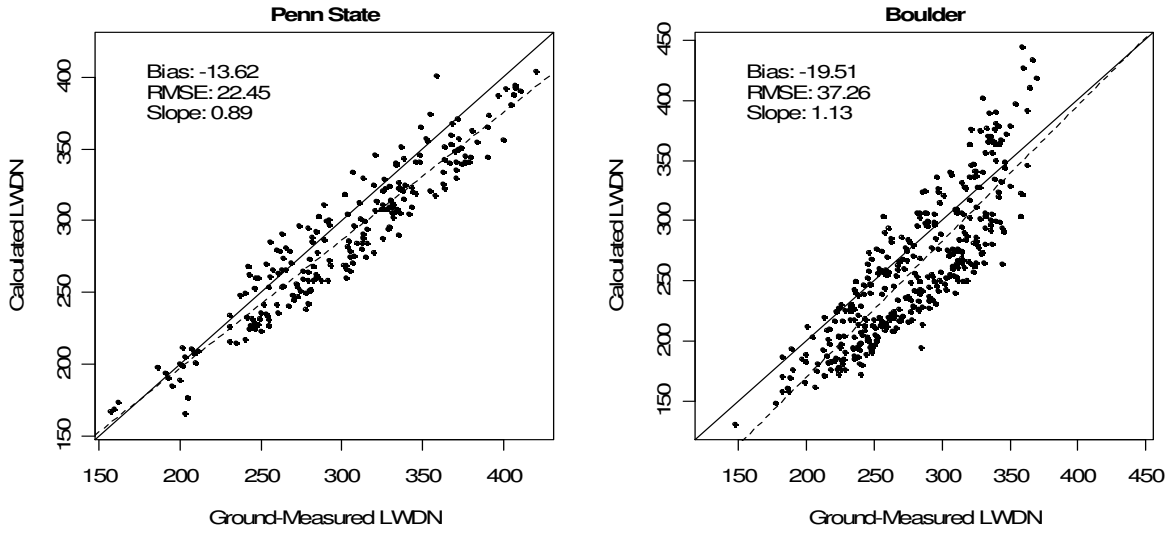

Figure 5-1 Comparing clear-sky LWDN calculated using the physical method and the SURFRAD ground-measured LWDN at the Penn State (376 m) and Boulder (1689 m) sites.

The pilot study showed that LWDN cannot be estimated with acceptable accuracy with the physical method, especially over high elevation surfaces. Figure 5-1 shows the calculated and ground-measured LWDN at two SURFRAD sites: Penn State (376 m) and

Boulder (1689 m). The errors at both sites are larger than 20 W/m^2. The root mean squared error (RMSE) at the Boulder site is as large as 37.26 W/m^2. The hybrid method, which is less sensitive to the errors in atmosphere profiles, may be a better alternative.

5.2 Hybrid Method

5.2.1 Radiative Transfer Simulation

The hybrid method for estimating LWDN from MODIS data follows the general framework described in Chapter 4. The simulated databases were based on the first atmosphere profile database (with ~7000 atmosphere profiles, see Section 4.1) and the MODIS Terra spectral response function, following the procedure described in Section 4.2. LWDN is the result of atmosphere absorption, emission, and scattering. It is less sensitive to surface conditions than LWUP. However, surface emissivity plays an important role in simulating realistic TOA radiance. In this study, plant function type corresponding to each profile was determined using collocated MODIS land cover product. Emissivity spectra from the JHU Emissivity Library (see Section 3.3) were used to approximate the emissivity characteristic of each plant function type. Figure 5-2 shows the flowchart of the MODIS LWDN hybrid method, modified from the general framework presented in Chapter 4.

5.2.2 Developing Linear LWDN Models

Near surface air temperature is one of the dominant factors for clear-sky LWDN. Surface temperature channels are important for estimating LWDN because surface temperature is closely correlated to surface air temperature (see Figure 5-3). However, the relationship between surface temperature and surface air temperatures is not the same

at night as it is during the day, especially over bare ground and/or high elevation surfaces. Therefore, separate models were developed to predict LWDN at daytime and nighttime.

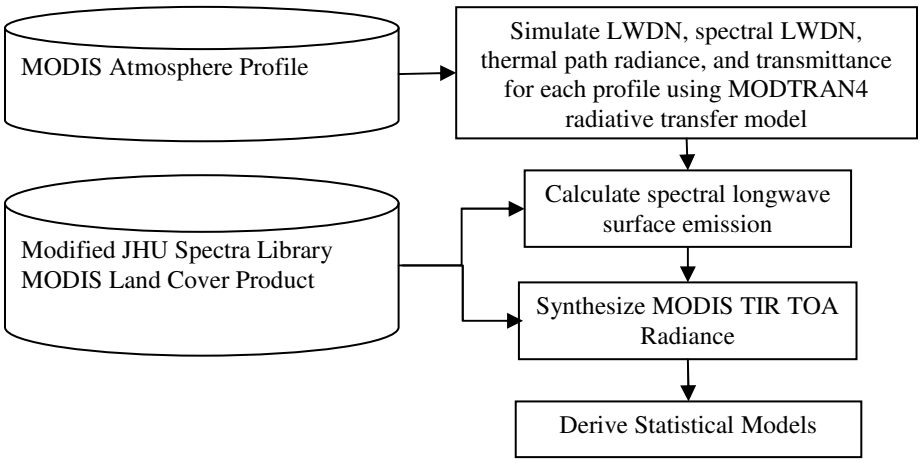

Figure 5-2 Flowchart of the MODIS LWDN hybrid method.

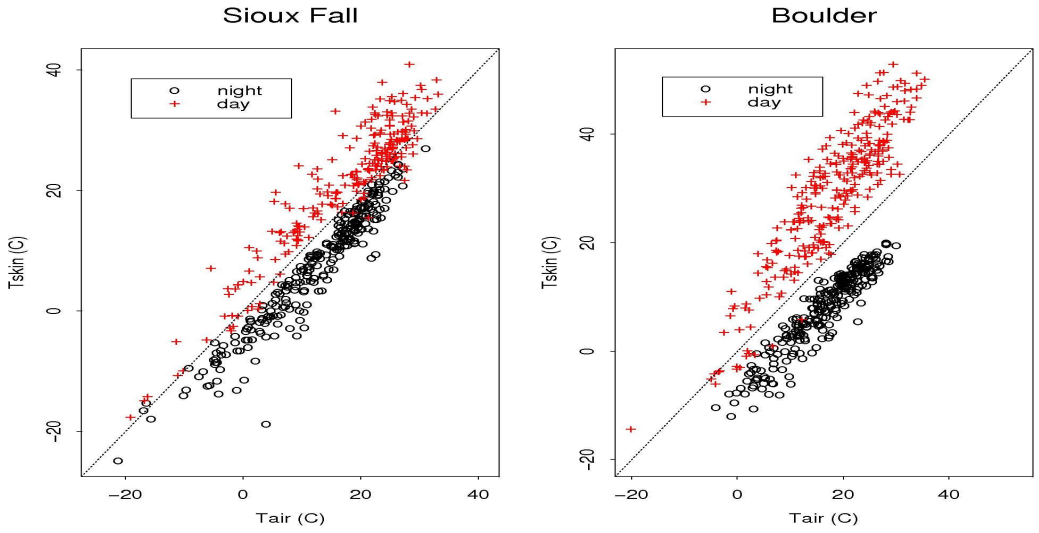

Figure 5-3 The relationship between ground-measured surface air temperature and MODIS-retrieved surface temperature during the day and at night at the Sioux Falls (473 m) and Boulder sites (1689 m).

Surface pressure is another important factor in estimating LWDN because of the effect of pressure broadening of the spectral lines (Lee & Ellingson, 2002). However, the surface pressure has not been considered explicitly in previous studies because they were focused on estimating LWDN over the sea surface. In this study, surface elevation (H) was used as a surrogate to surface pressure to account for the surface pressure effect.

MODIS channels 27-29 and 31-34 predict LWDN from MODIS TOA radiance best. This is consistent with the physics that governs LWDN: 27 and 28 are water vapor channels; 33 and 34 are near surface air temperature profile channels; 29, 31, and 32 are used for retrieving surface temperature. MODIS channels 35 and 36 were not used in the models because they are related to high altitude, instead of near surface, temperature profiles. Equation 5-1 shows the linear models developed:

$$F_d = a_0 + \sum a_i L_i + bH \quad \text{(i=27, 28, 29, 31, 32, 33, 34)} \tag{5-1}$$

where F_d is clear-sky LWDN; a_0, a_i, and b are regression coefficients; L_i are MODIS TOA radiance. Totally ten linear models, corresponding to five sensor viewing zenith angles (0°, 15°, 30°, 45°, and 60°) and two observation times (daytime and nighttime) were developed. Statistics show that the linear models explain more than 92.3 % of the variations in the simulated datasets, with standard errors less than 16.11 (nighttime) and 16.27 (daytime) W/m^2.

5.2.3 Developing Nonlinear LWDN Models

Residuals analysis indicates that LWDN tends to be underestimated under hot and humid conditions and overestimated under cold and dry conditions. Nonlinear LWDN

model was developed to account for the nonlinear effect. The same set of predictor variables used in the linear models was used to develop the nonlinear models:

$$F_d = L_{Tair}\left(a_0 + a_1 L_{27} + a_2 L_{29} + a_3 L_{33} + a_4 L_{34} + b_1 \frac{L_{32}}{L_{31}} + b_2 \frac{L_{33}}{L_{32}} + b_3 \frac{L_{28}}{L_{31}} + c_1 H \right) \qquad (5\text{-}2)$$

where L_{Tair} is equal to L_{31} in the nighttime models and is equal to L_{32} in the daytime models; a_i, b_i, and c_1 are regression coefficients. The nonlinear model can explain more than 93.6 % of variations, with standard errors less than 14.79 (nighttime) and 15.20 (daytime) W/m^2. Table 5-2 shows the linear and nonlinear model fitting results under five sensor view zenith angles. The regression coefficients of the nonlinear models are given in Table 5-3.

	Linear				**Nonlinear**			
	Daytime		**Nighttime**		**Daytime**		**Nighttime**	
	R^2	**Std. Err.**	**R^2**	**Std. Err.**	**R^2**	**Std. Err.**	**R^2**	**Std. Err.**
0º	0.923	16.19	0.930	15.50	0.939	14.44	0.943	13.98
15º	0.923	16.17	0.930	15.52	0.938	14.47	0.942	14.01
30º	0.923	16.13	0.929	15.58	0.938	14.55	0.943	14.10
45º	0.923	16.10	0.928	15.72	0.936	14.74	0.940	14.32
60 º	0.923	16.27	0.924	16.11	0.932	15.20	0.936	14.79

Table 5-2 Linear and nonlinear LWDN model fitting results (unit of standard error: W/m^2).

	Daytime					**Nighttime**				
	0º	**15º**	**30º**	**45º**	**60 º**	**0º**	**15º**	**30º**	**45º**	**60 º**
a0	150.204	153.149	162.142	180.911	214.228	84.143	87.069	95.437	112.646	142.438
a1	4.453	4.344	3.909	3.119	2.129	5.365	5.274	4.899	4.184	3.049
a2	-1.740	-1.800	-1.989	-2.411	-3.279	-1.782	-1.833	-1.993	-2.374	-3.199
a3	-21.030	-20.367	-18.460	-14.022	-3.723	-15.508	-14.870	-13.068	-8.880	0.425
a4	32.217	31.676	30.225	26.553	16.927	27.077	26.520	25.066	21.511	13.061
b1	-150.869	-154.969	-167.043	-192.689	-239.237	-106.529	-110.082	-119.872	-140.713	-177.342
b2	33.176	34.007	35.638	40.589	53.681	62.673	63.050	63.200	64.904	69.793
b3	-26.812	-25.894	-22.376	-16.065	-6.780	-40.546	-39.727	36.611	-30.986	-21.948
c1	-1.911	-1.907	-1.902	-1.914	-1.987	-1.984	-1.977	-1.966	-1.962	-2.001

Table 5-3 Nonlinear LDWN models regression coefficients.

5.3 Validation Results and Discussion

5.3.1 Using MODIS Terra Data

The linear and nonlinear LWDN models were first evaluated using MODIS Terra TOA radiance and collocated SURFRAD ground data. LWDN at a particular senor view zenith angle were derived using linear interpolation. Clear-sky observations were identified using MODIS cloud product. We also examined all data points manually to exclude cloud-contaminated pixels with unreasonably low TOA radiance values in MODIS channel 31.

Table 5-4 summaries the statistics of validation results based on MODIS Terra data. Figure 5-4 and Figure 5-5 show the validation plots for individual sites. The nonlinear models outperform the linear models at five of the six sites, with RMSEs ranging from 14.35 to 20.35 W/m^2 and biases ranging from -6.88 to 9.72 W/m^2. The RMSEs of the linear models range from 15.58 to 25.29 W/m^2 and biases range from –12.18 to 8.79 W/m^2. The mean RMSE of nonlinear models for all sites is 17.60 W/m^2, ~2.5 W/m^2 smaller than that of the linear models.

Preliminary spatial scaling study using only clear-sky observations indicates that RMSEs of MODIS-derived LWDN were further reduced by 2 W/m^2 after the nonlinear model-predicted LWDN was aggregated to 5 km or more. The reduction in error may not be significant compared to the overall error (15-20 W/m^2). The small error reduction may be due to only clear-sky retrievals were used in the spatial scaling. More spatial scaling study is needed after the development of method for estimating cloudy-sky LWDN using MODIS data in the future.

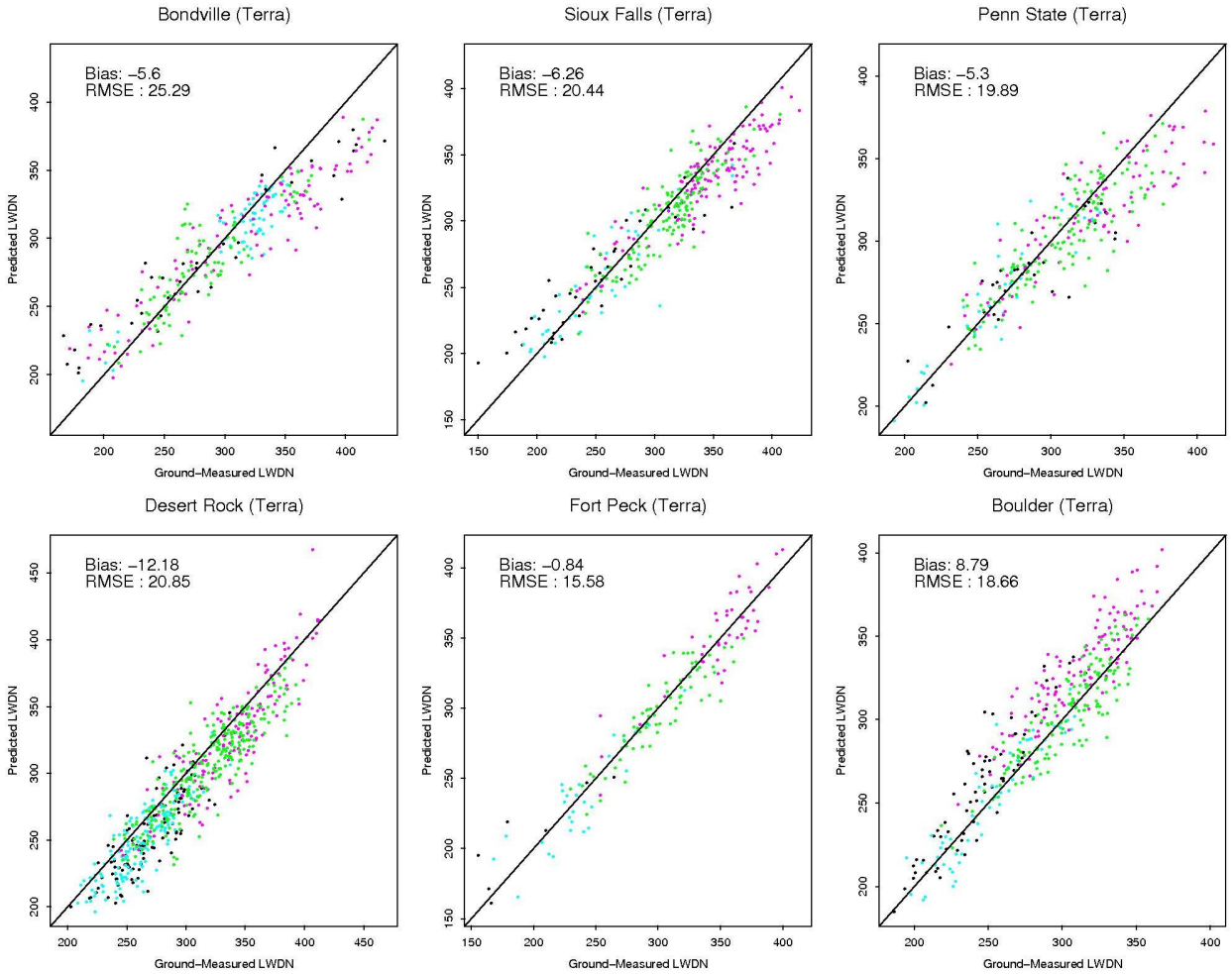

Figure 5-4 Linear LWDN models validation results using MODIS Terra data (black-fallwinter/day; cyan-fallwinter/night; magenta-springsummer/day; green-springsummer/night).

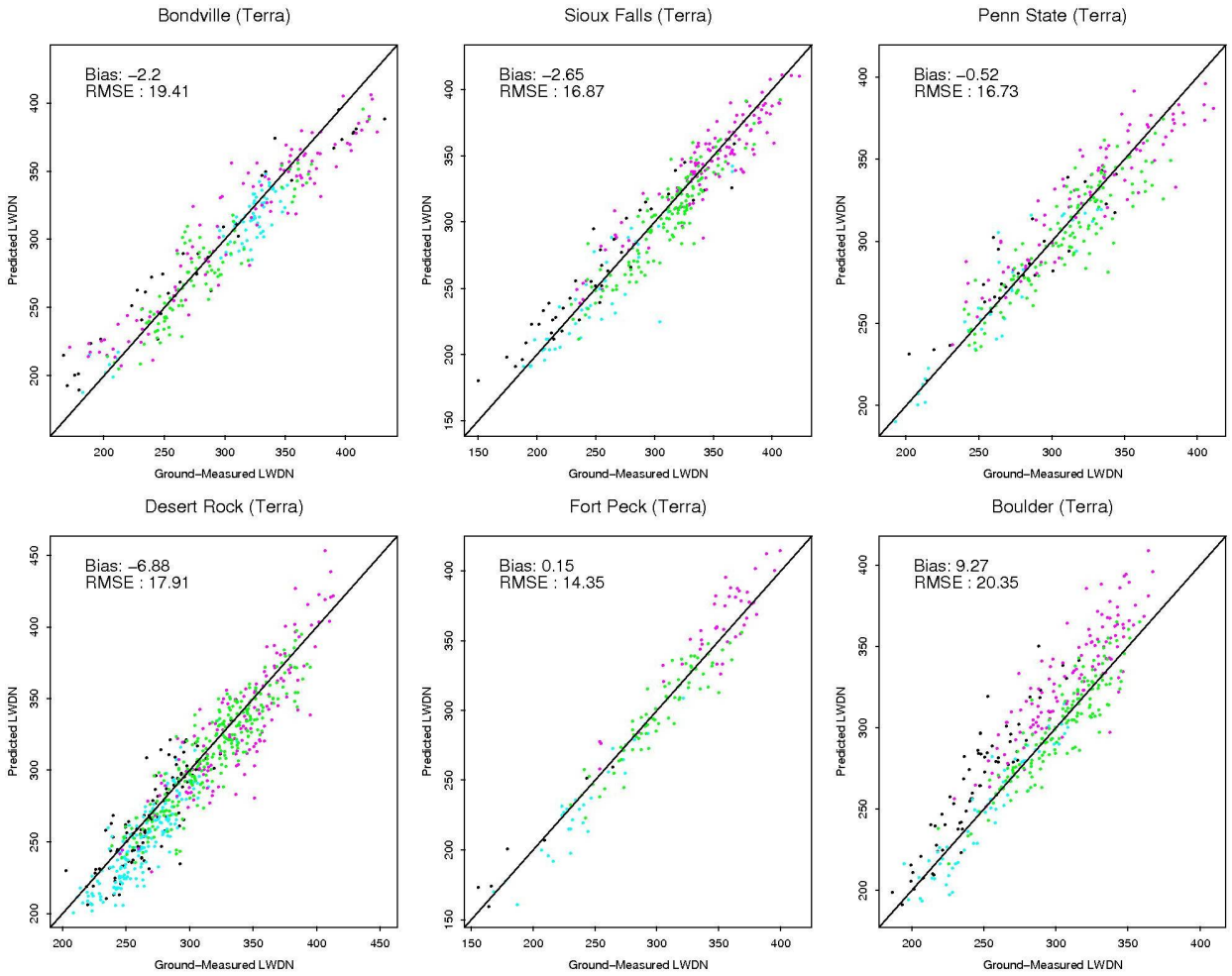

Figure 5-5 Nonlinear LWDN models validation results using MODIS Terra data (black-fallwinter/day; cyan-fallwinter/night; magenta-springsummer/day; green-springsummer/night).

Sites	#Obs.	MODIS Terra (W/m^2)			
		Linear		Nonlinear	
		Bias	RMSE	Bias	RMSE
Bondville	298	-5.60	25.29	-2.20	19.41
Sioux Falls	350	-6.26	20.44	-2.65	16.87
PennState	290	-5.30	19.89	-0.52	16.73
DesertRock	667	-12.18	20.85	-6.88	17.91
FortPeck	153	-0.84	15.58	0.15	14.35
Boulder	383	8.79	18.66	9.27	20.35
Mean	-	-3.57	20.12	-0.47	17.60

Table 5-4 LWDN models validation results using MODIS Terra TOA radiance.

5.3.2 Using MODIS Aqua Data

Although the LWDN models were developed using MODIS Terra-retrieved atmosphere profiles and Terra spectral response functions, the models were also applied (without modification) to two years of MODIS Aqua data (2005 and 2006) because the two sensors have similar designs. Table 5-5 summarizes the validation results using Aqua data. Figure 5-6 and Figure 5-7 show the validation plots. The nonlinear models' biases range from -10.03 to 5.40 W/m^2 and RMSEs range from 13.82 to 18.89 W/m^2. The mean RMSE of nonlinear models for all sites is 16.17 W/m^2, ~4 W/m^2 smaller than that of the linear models. Terra and Aqua have different satellite overpass times: 10:30 am and 10:30 pm versus 1:30 pm and 1:30 am (local time); therefore, the atmosphere and land surface conditions are different for the two sensors. However, the nonlinear model biases and RMSEs for Aqua are generally smaller than Terra. Liu et al. (2006) show that Aqua sensor has smaller detector-dependent systematic errors than Terra in thermal channels, which may contribute to the smaller error in Aqua-derived LWDN. The Aqua validation results indicated that the LWDN models developed in this study are general enough to be applied for both Terra and Aqua observations.

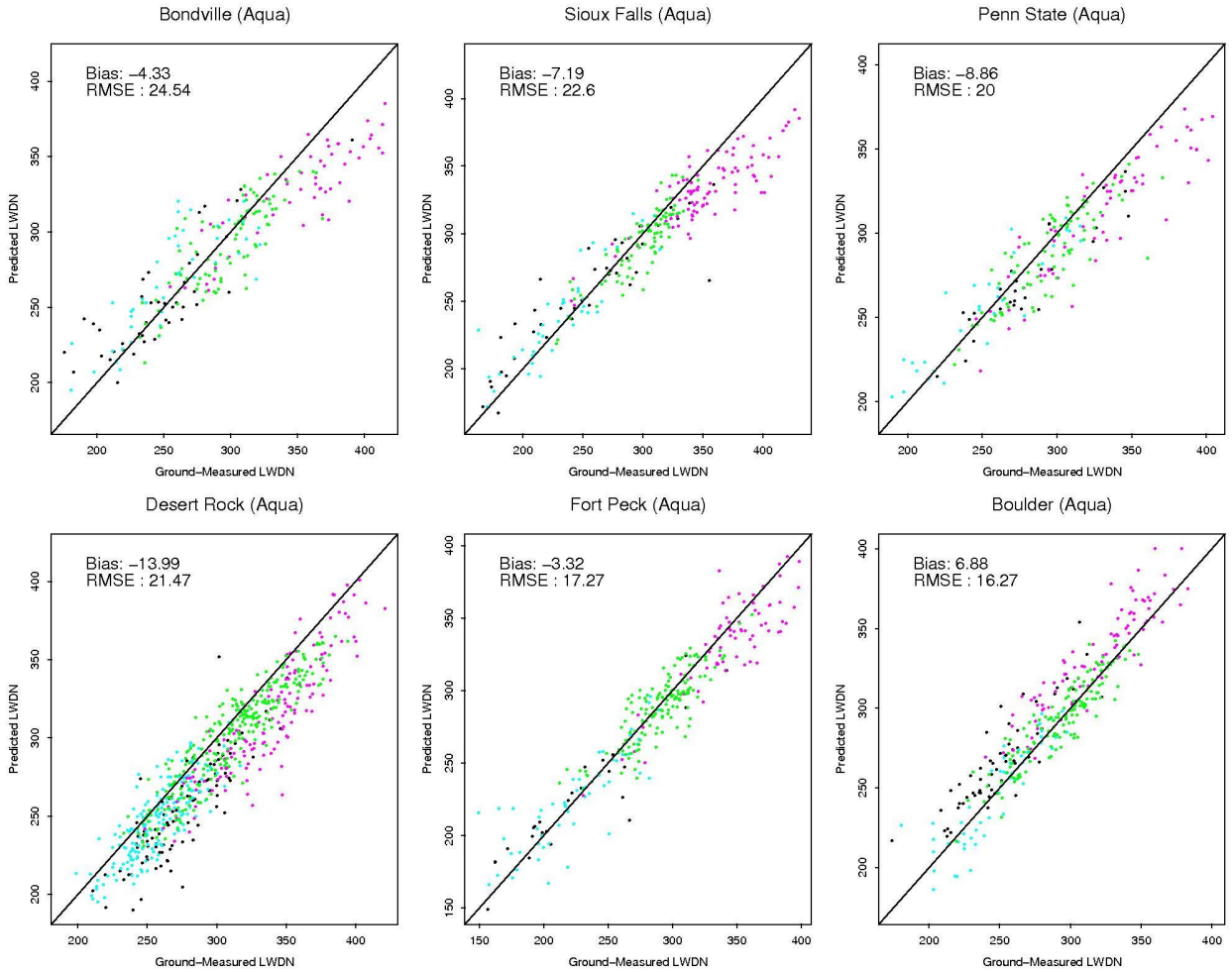

Figure 5-6 Linear LWDN models validation results using MODIS Aqua data (black-fallwinter/day; cyan-fallwinter/night; magenta-springsummer/day; green-springsummer/night).

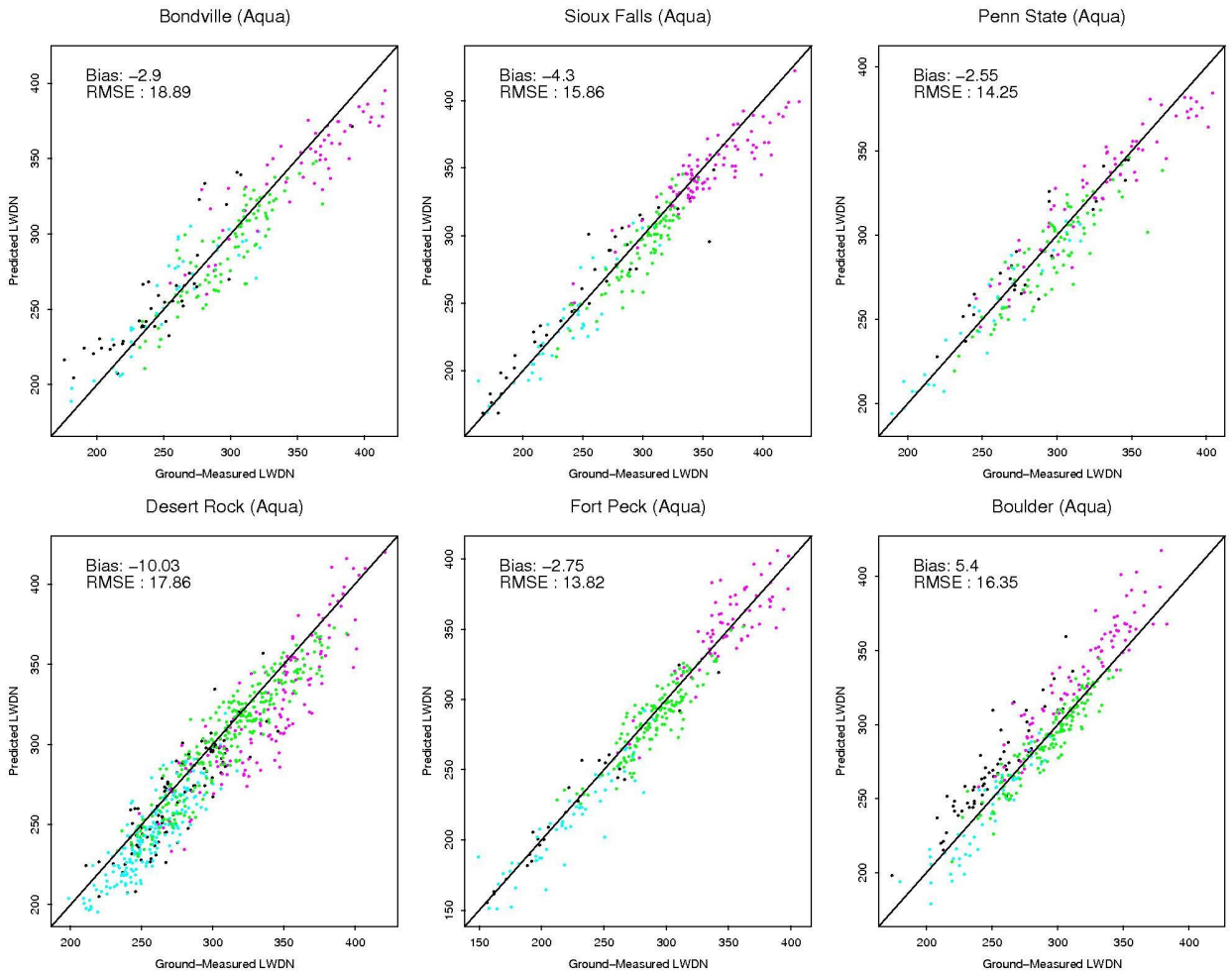

Figure 5-7 Nonlinear LWDN models validation results using MODIS Aqua data (black-fallwinter/day; cyan-fallwinter/night; magenta-springsummer/day; green-springsummer/night).

Sites	#Obs.	MODIS Aqua (W/m^2)			
		Linear		Nonlinear	
		Bias	RMSE	Bias	RMSE
Bondville	228	-4.33	24.54	-2.90	18.89
Sioux Falls	254	-7.19	22.60	-4.30	15.86
PennState	205	-8.86	20.00	-2.55	14.25
DesertRock	681	-13.99	21.47	-10.03	17.86
FortPeck	296	-3.32	17.27	-2.75	13.82
Boulder	341	6.88	16.27	5.40	16.35
Mean	-	-5.14	20.36	-2.86	16.17

Table 5-5 LWDN models validation results using MODIS Aqua TOA radiance.

5.3.3 The Spatial Mismatch Issue

Both Terra and Aqua LWDN validation plots show that daytime observations (in black and magenta colors) typically have larger scatter than nighttime observations (in green and cyan colors). The spatial mismatch between the MODIS footprint (1 km^2 at nadir) and the ground PIR footprint (~ 200 m^2) may be the cause of the larger daytime scatter. The Earth's surface behaves almost as an isothermal and homogeneous surface at night. During the day, surface temperature can exceed surface air temperature by more than 20 °. Although MODIS channel 32, rather than channel 31, was used in the daytime nonlinear models, the LWDN derived is still affected by surface temperature.

5.3.4 Cloud Contamination

Cloud contamination may be a significant source of error in this study. MODIS cloud product cannot mask all clouds, especially cirrus clouds. The TOA radiance of cloud-contaminated pixels is mixtures of surface and cloud-top contributions and will be lower than true clear-sky values. Some data points used in the study may be contaminated by cloud even after manual screening (Wan, 2008; Wang et al., 2007). This is especially

true at the Desert Rock site. Air traffic from Los Angeles produces a considerable amount of cirrus clouds over this site.

5.3.5 Errors Caused by the Atmosphere Profile Database

The nighttime results at the two high elevation sites (Desert Rock and Boulder) indicate that the nonlinear LWDN models account for surface pressure effect reasonably well because surface pressure does not vary significantly between day and night. However, large errors exist at the Boulder site during the day. Statistically, the current profile database lacks hot and humid and high elevation profiles because there are few areas of the North American continent at high elevations. This issue will be addressed in the future.

5.3.6 Uncertainty Caused by CO_2 and O_3 Concentration Assumptions

A constant CO_2 mixing ratio of 365 ppmv was assumed in the radiative transfer simulation. Figure 5-8 shows the MODTRANR4 simulated LWDN under the tropical, mid-latitude summer, and sub-arctic winter atmospheres when the CO_2 mixing ratio varies from 180 to 730 ppmv. For the sub-arctic atmosphere, the change of LWDN is ~2.50 W/m^2 when the CO_2 mixing ratio is reduced by 50% or doubled. For the tropical atmosphere, the change of LWDN is less than 1.50 W/m^2. The variation for other atmospheres should be between these two atmospheres.

Constant column O_3 of 355 Dobson was assumed in the radiative transfer simulation. The uncertainty in LWDN caused by O_3 was studied using MODTRAN4 under three standard atmospheres: tropical, mid-latitude summer, and sub-arctic winter. LWDN changes less than 1.5 W/m^2 when the default column O_3 was reduced by 50% or

doubled (see Figure 5-9). The uncertainty caused by CO_2 and O_3 assumptions is minor when compared to the errors caused by the scale mismatch, ground instruments, and cloud contamination and therefore can be ignored in this study.

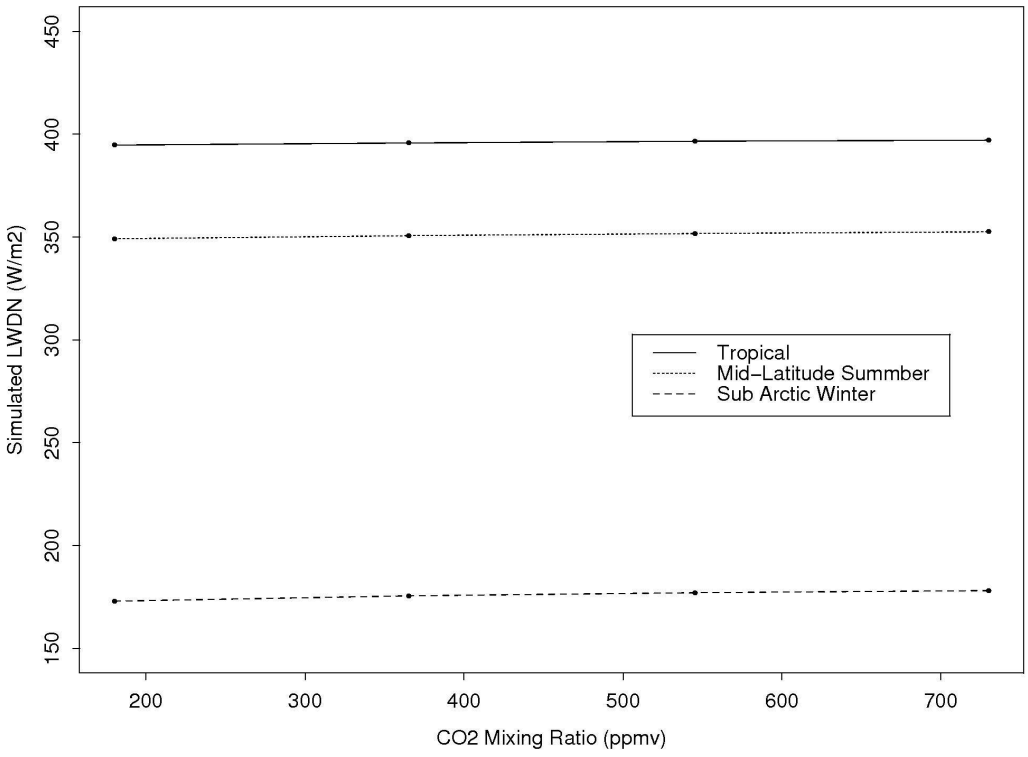

Figure 5-8 The change of the simulated LWDN when the CO_2 mixing ratio varies from 180 ppmv to 730 ppmv.

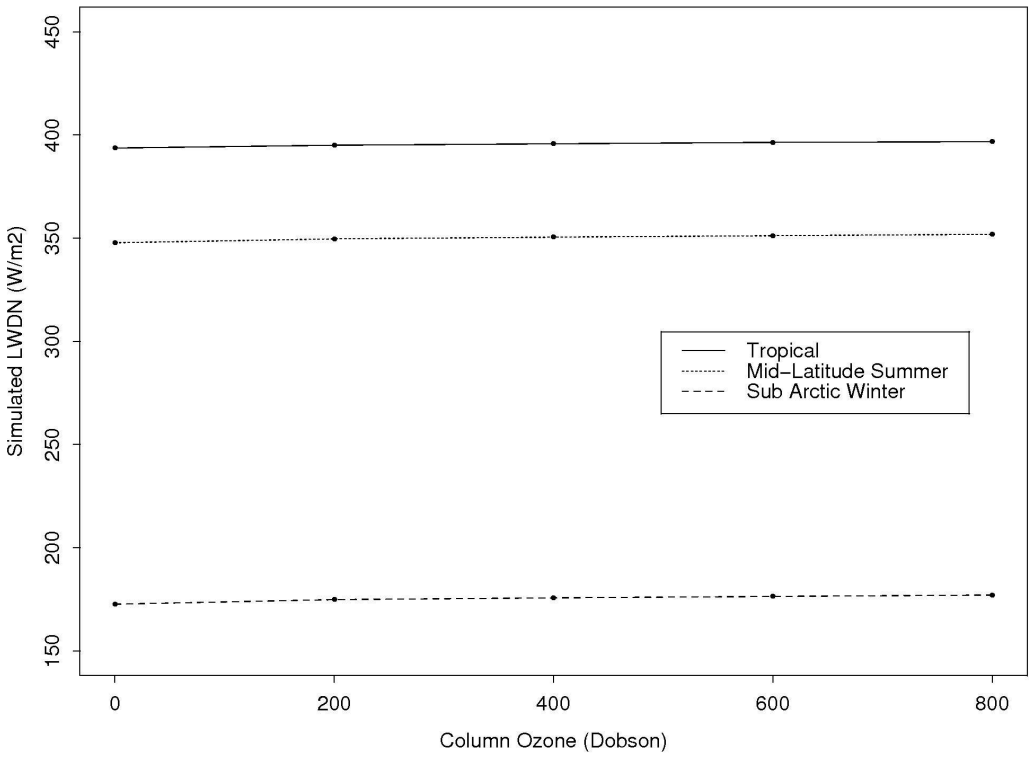

Figure 5-9 The change of the simulated LWDN when the O_3 mixing ratio varies from 0 to 800 Dobson.

5.4 Summary

This chapter describes a new hybrid method for estimating instantaneous clear-sky LWDN over land from MODIS 1 km data. Linear and nonlinear LWDN models were developed based on extensive radiative transfer simulations and statistical analysis. Land surface emissivity effect was considered by incorporating the JHU Emissivity Library in the radiative transfer simulation. The statistical models incorporated surface elevation to account for the surface pressure effect. The linear models explain more than 92.3 % of variations of the simulated databases, with standard errors less than 16.27 W/m^2 for all

sensor view zenith angles. The nonlinear models explain more than 93.6 % of variations, with standard errors less than 15.20 W/m^2.

The LWDN models were evaluated using two years of ground measurements at six SURFRAD sites. The nonlinear models outperform the linear models, with mean RMSE of 17.60 (Terra) and 16.17 (Aqua) W/m^2. The mean RMSE of the nonlinear models is ~2.5 W/m^2 smaller than that of the linear models. The validation results indicate that the models developed in this study can be applied to both Terra and Aqua observations.

The potential sources of errors were analyzed. The spatial mismatch between MODIS and ground instrument footprints and cloud contamination may produce errors in the validation results. Moreover, the insufficient number of hot, humid, and high elevation profiles may cause errors. This issue needs to be addressed in the future. The errors caused by using constant CO_2 and O_3 concentration values are negligible.

Chapter 6 Estimating Instantaneous Clear-Sky LWUP and LWNT Using MODIS Data

In this chapter, two methods were developed to estimate LWUP from MODIS data. One method is the temperature-emissivity method, i.e., estimating LWUP using MODIS-derived LST and emissivity products. A new hybrid method, similar to the hybrid method presented in Chapter 5, was also developed to estimate LWUP from MODIS TOA radiance. The two methods were compared using the SURFRAD ground measurements. LWNT was derived by subtracting LWDN from LWUP.

6.1 Temperature-Emissivity Method

The temperature-emissivity method estimates LWUP using MODIS-derived LST and emissivity products based on Equation 2-4. Multiple satellite surface temperature and emissivity products are routinely available at 1 km spatial resolution (Wan, 1999; Dash et al., 2002; Prata, 2002). MODIS 1 km LST products (MOD11_L2 and MYD_11L2) and MODIS 5 km emissivity products (MOD11B1 and MYD11B1, see Section 3.2) were used in this work. Broadband emissivity (4-100 μm) was estimated using MOD11B1 and MYD11B1 narrow band emissivity, using Wang et al.'s method (2005). The maximum error in narrow band to broadband emissivity conversion is 0.006, not including the uncertainty associated with narrow band emissivity retrieval. Ground-measured LWDN was used to account for the reflected LWDN in the Equation 2-4. Therefore, the temperature-emissivity method was independent of the errors in MODIS-derived LWDN.

6.2 Hybrid Method

Clear-sky TOA radiance contains information about surface temperature, emissivity, and LWDN. LWUP can also be estimated using hybrid method that is similar to the hybrid method for estimating LWDN. The hybrid method derives LWUP directly from satellite TOA radiance (or brightness temperature), without estimating the three variables in the right-hand side of Equation 2-4 separately. LWUP and LWDN have the same order of magnitude. The two terms on the right side of Equation 2-4 have opposite signs, which can partly mitigate the errors in surface emissivity (Diak et al., 2000). The advantage of the hybrid method is that the problem of separating LST and emissivity is bypassed. As a result, LWUP is more accurately estimated.

6.2.1 Radiative Transfer Simulation

The hybrid method estimating LWUP from MODIS TOA radiance follows the general framework described in Chapter 4. Figure 6-1 shows the flowchart of the LWUP hybrid method. There are three major differences compared with the LWDN hybrid method presented in Chapter 5. First, a more comprehensive emissivity library, the modified UCSB Emissivity Library with 59 emissivity spectra (see Section 3.3), was used in the radiative transfer simulation because LWUP is sensitive to land surface emissivity variations. Second, the radiative transfer simulation is based on the smaller atmosphere profile database with only ~2000 profiles (see Section 4.1). Using UCSB emissivity spectra significantly increases size of the simulated databases. LWUP is dominated by surface emission. This study shows a smaller but representative profile database reduces the size of the simulated databases, without compromising the

predictability of the statistical models. Third, LWUP is not affected by surface pressure or elevation. Therefore, surface elevation is not a predictor variable in the LWUP models.

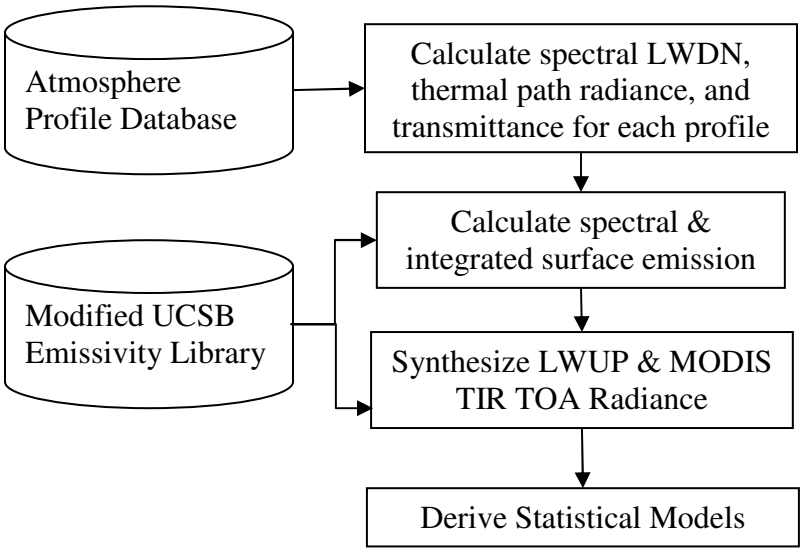

Figure 6-1 Flowchat of the hybrid method for estimating LWUP from MODIS TOA radiance.

6.2.2 Developing Linear LWUP Models

The simulated databases were analyzed to develop models for predicting LWUP from MODIS TOA radiance. Multiple regression analysis was first employed to develop the linear LWUP model. It is found that MODIS bands 29, 31, and 32 predict LWUP best, consistent with the physics that govern LWUP. All three bands are used to retrieve LST and emissivity; band 29 is also sensitive to near surface water vapor amount. Equation 6-1 is the derived linear model:

$$F_u = a_0 + a_1 L_{29} + a_2 L_{31} + a_3 L_{32} \quad (6\text{-}1)$$

where F_u is LWUP; a_0, a_1, a_2, and a_3 are regression coefficients; L_{29}, L_{31}, L_{32} are MODIS channels 29, 31, and 32 TOA radiance. In total, five models were developed for predicting LWUP at 0°, 15°, 30°, 45°, and 60° sensor view zenith angles. Statistical analysis indicates that the linear models account for more than 99% of the variation, with standard errors less than 6.11 W/m^2 for all sensor view zenith angles. Table 6-1 summarizes the model fitting results. Estimating LWUP using the linear models is referred to as the linear model method in the remainder of the text.

Although the linear models explain more than 99% of the variations in the simulated databases, strong non-linear effects are observed in the residuals. LWUP tends to be underestimated at low temperature and overestimated at high temperature and/or high moisture conditions. Some parameterized nonlinear models using both TOA radiance and brightness temperatures were evaluated to reduce the nonlinear effect in the residuals. However, the models were not significantly improved.

6.2.3 Developing ANN LWUP Models

The ANN techniques have proven their ability in modeling nonlinear problems. In this study, LWUP were also modeled using a single hidden layer neural network provided by the S-Plus 7 statistical software package (Insightful, 2005). The inputs to the neural networks were MODIS TOA radiance data from channels 29, 31, and 32, the same TOA radiance set used for developing the linear models.

Table 6-1 also summarizes the statistics of the ANN model fitting results. The ANN models can explain more than 99.6% of variations in the simulated databases, with standard errors less than 3.70 W/m^2 for all sensor view angles. Moreover, the non-linear

effect was significantly reduced. Estimating LWUP using the ANN models is referred to as the ANN model method in the remainder of the test.

	Linear Regression						ANN
θ	a_0	a_1	a_2	a_3	R^2	Std. Err.	Std. Err.
0º	102.7589	10.4963	121.3973	-100.4079	0.993	4.89	3.07
15º	104.5829	10.6894	123.4974	-103.0277	0.993	4.94	3.10
30º	110.4514	11.4267	129.9471	-111.2339	0.992	5.10	3.20
45º	122.3125	13.5455	141.1782	-126.4748	0.991	5.41	3.44
60 º	146.0408	20.5749	157.2946	-152.6469	0.990	6.11	3.70

Table 6-1 Summary of linear and ANN model fitting results (θ – sensor view zenith angle; unit of standard error: W/m^2).

6.3 Validation Results and Discussion

The temperature-emissivity method, the linear model method and the ANN model method were evaluated using two years (2005 and 2006) of clear-sky MODIS Terra and Aqua TOA radiance, LST and emissivity products, and the collocated SURFRAD ground measurements. Linear interpolation was applied to obtain ground values at the time of the satellite overpass. Clear-sky observations were identified using MOD11_L2 and MYD11_L2 quality control information and the MODIS cloud product. All data points were also manually examined to exclude cloud-contaminated pixels with unreasonably low TOA radiance values in MODIS channel 31. LWUP at a particular sensor view zenith angle were derived using linear interpolation in the linear model and ANN model methods.

The sensor viewing zenith angle effect must be considered when using satellite-retrieved surface temperature and emissivity products to estimate LWUP. Both variables depend on sensor viewing zenith angle. However, the surface temperature and emissivity in Equation 2-4 are independent of sensor viewing zenith angle. Because there is only

one observation available for any MODIS overpass time, the angular effect was ignored in this study. To mitigate the angular effect, only MODIS observations with sensor viewing angles equal to or less than 45° are used in the validation. The angular effect was accounted for in the linear model method and the ANN model method. Statistics show the difference in the validation results caused by ignoring observations with sensor view zenith angle larger than 45° is negligible for both methods.

6.3.1 Using MODIS Terra Data

Figure 6-2, Figure 6-3, and Figure 6-4 show the validation results using MODIS Terra Data. The ANN method outperforms the other two methods at all sites, with averaged RMSE ~5 W/m^2 less than the temperature-emissivity method and ~2.5 W/m^2 less than the linear model. The temperature-emissivity method-derived LWUP has the largest errors and biases for all sites, with biases ranging from -13.63 to -27.14 W/m^2 and RMSEs ranging from 16.55 to 28.09 W/m^2. The linear model method biases range from -4.62 to -21.93 W/m^2 and RMSEs range from 12.72 to 25.03 W/m^2. The ANN model method biases range from -4.53 to -16.41 W/m^2 and RMSEs range from 11.79 to 18.70 W/m^2. Table 6-2 summarized the validation results using MODIS Terra data for each site, as well as averaged biases and RMSEs for each method.

Site Name	LST Method		Linear Models		ANN Models	
	Bias	RMSE	Bias	RMSE	Bias	RMSE
Bondville	-14.14	19.02	-9.49	17.75	-6.81	15.54
Sioux Falls	-19.95	22.64	-13.55	17.87	-11.56	16.18
Penn State	-13.63	16.55	-7.32	12.72	-5.67	11.79
Desert Rock	-27.14	28.09	-21.93	25.03	-16.41	18.70
Fort Peck	-16.13	19.62	-8.88	17.46	-7.03	15.75
Boulder	-14.39	19.36	-4.62	19.24	-4.53	17.35
Mean	-17.56	20.88	-10.97	18.35	-8.67	15.89

Table 6-2 Summary of validation results using MODIS Terra data (unit: W/m^2).

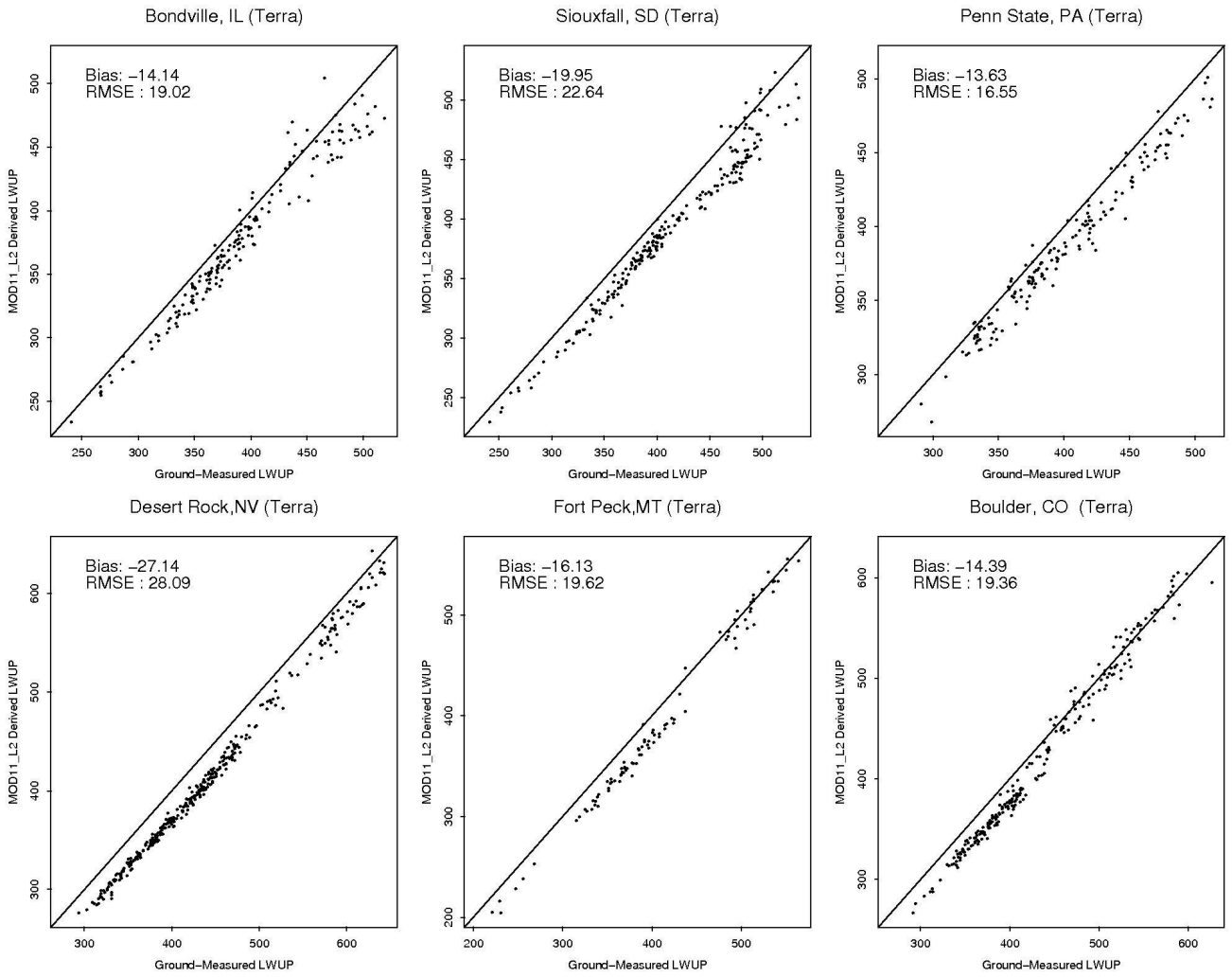

Figure 6-2 The temperature-emissivity method validation results using MODIS Terra LST and emissivity products.

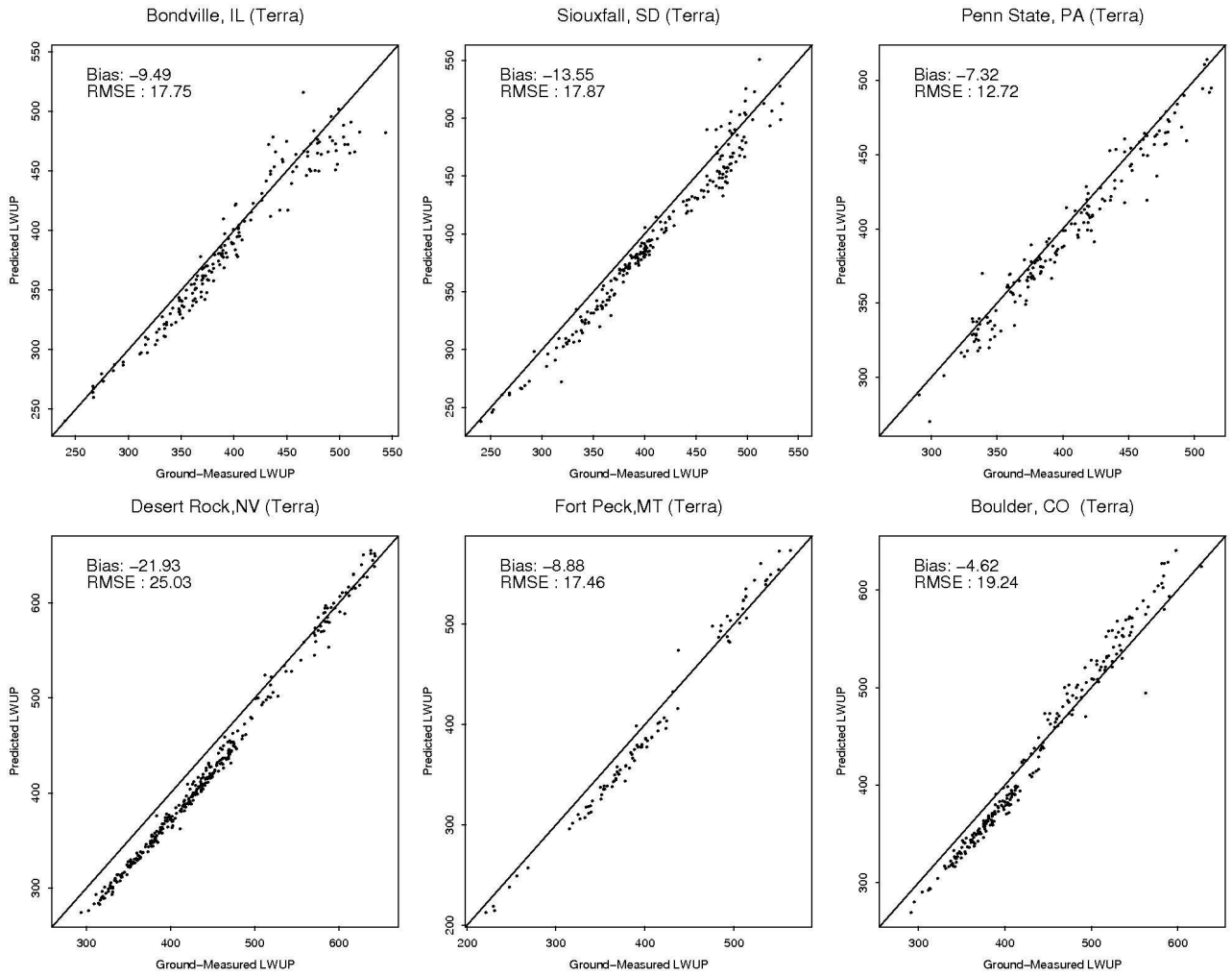

Figure 6-3 The linear model method validation results using MODIS Terra TOA radiance.

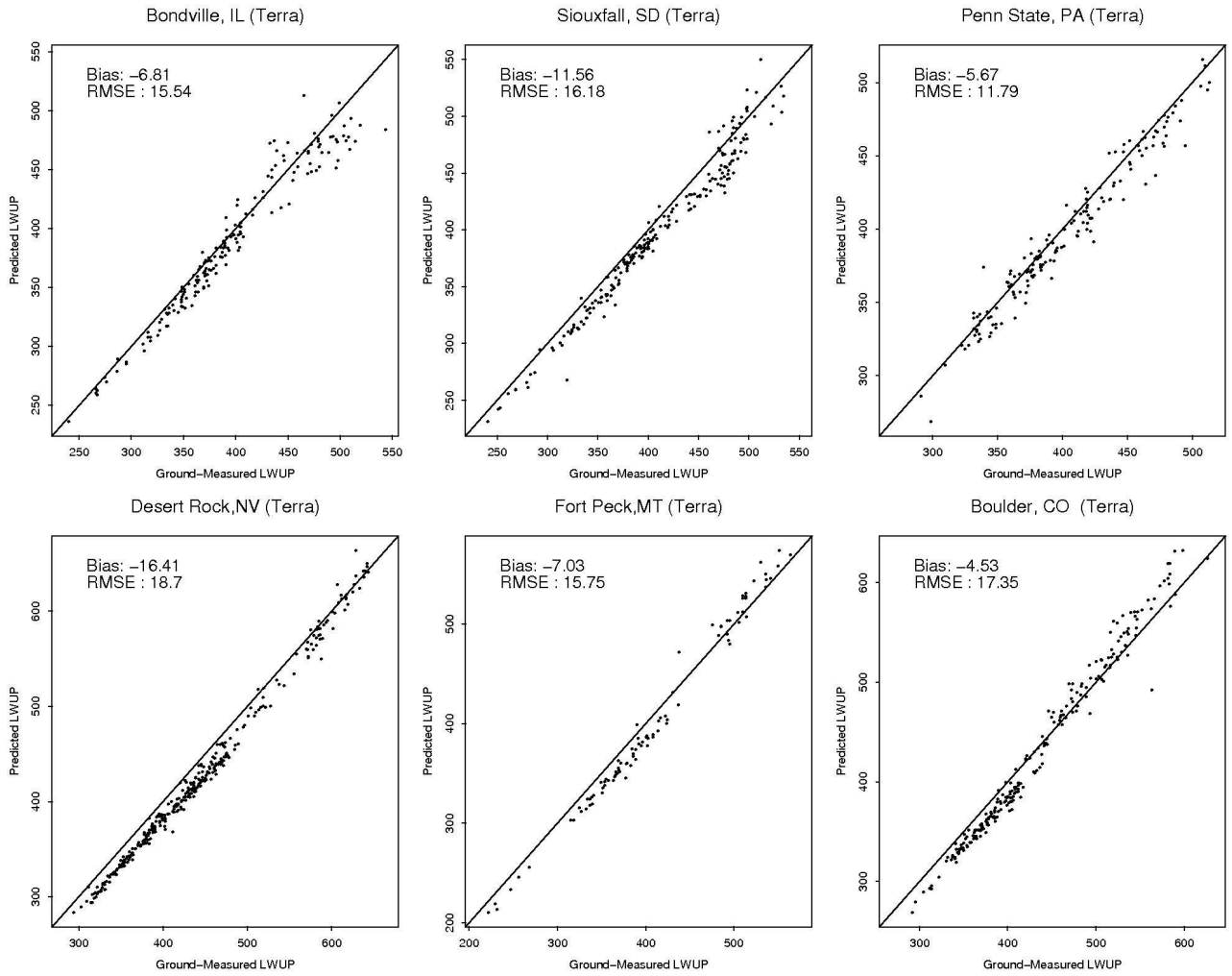

Figure 6-4 The ANN model method validation results using MODIS Terra TOA radiance.

6.3.2 Using MODIS Aqua Data

Although the linear and ANN models were developed using MODIS Terra retrieved atmosphere profiles and spectral response functions, the three methods were also applied (without any modification) to two years of Aqua data (2005 and 2006) because the two sensors have similar designs. The Terra and Aqua validation results are similar. The ANN model method outperforms the other two methods. The temperature-emissivity method biases range from -12.70 to -25.73 W/m^2 and RMSEs range from 16.98 to 26.82 W/m^2. The linear model method biases range from -5.21 to -20.21 W/m^2 and RMSEs range from 10.92 to 23.94 W/m^2. The ANN model method biases range from -3.00 to -15.52 W/m^2 and RMSEs range from 10.04 to 17.83 W/m^2. Figure 6-5, Figure 6-6, and Figure 6-7 show the validation results for individual sites.

Table 6-3 summarizes the validation results using MODIS Aqua data. Similar to LWDN validation results, the RMSEs of Aqua-derived LWUP are generally smaller than the Terra RMSEs at all sites. The Aqua validation results indicated that the LWUP models developed in this study are general enough to be used for both Terra and Aqua observations.

Site Name	LST Method		Linear Models		ANN Models	
	Bias	RMSE	Bias	RMSE	Bias	RMSE
Bondville	-13.17	17.55	-7.36	14.98	-4.07	12.64
Sioux Falls	-19.35	23.00	-12.81	17.74	-11.18	16.17
Penn State	-12.70	16.98	-5.21	10.92	-3.00	10.04
Desert Rock	-25.73	26.82	-20.21	23.94	-15.52	17.83
Fort Peck	-14.87	17.56	-7.33	15.11	-5.02	14.09
Boulder	-15.80	19.66	-5.50	18.76	-4.48	16.65
Mean	-16.94	20.26	-9.74	16.91	-7.21	14.57

Table 6-3 Summary of validation results using MODIS Aqua data (unit: W/m^2).

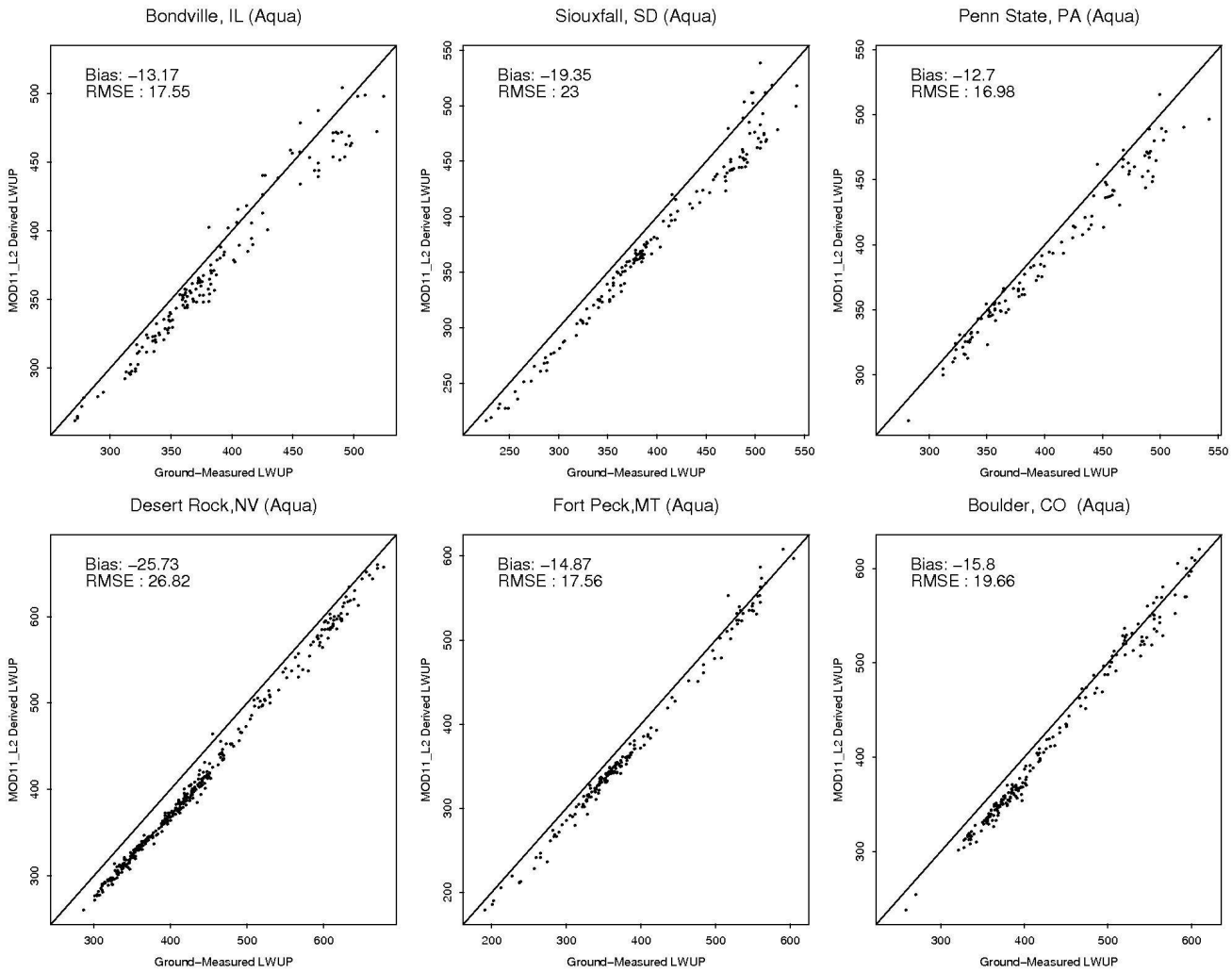

Figure 6-5 The temperature-emissivity method validation results using MODIS Aqua LST and emissivity products.

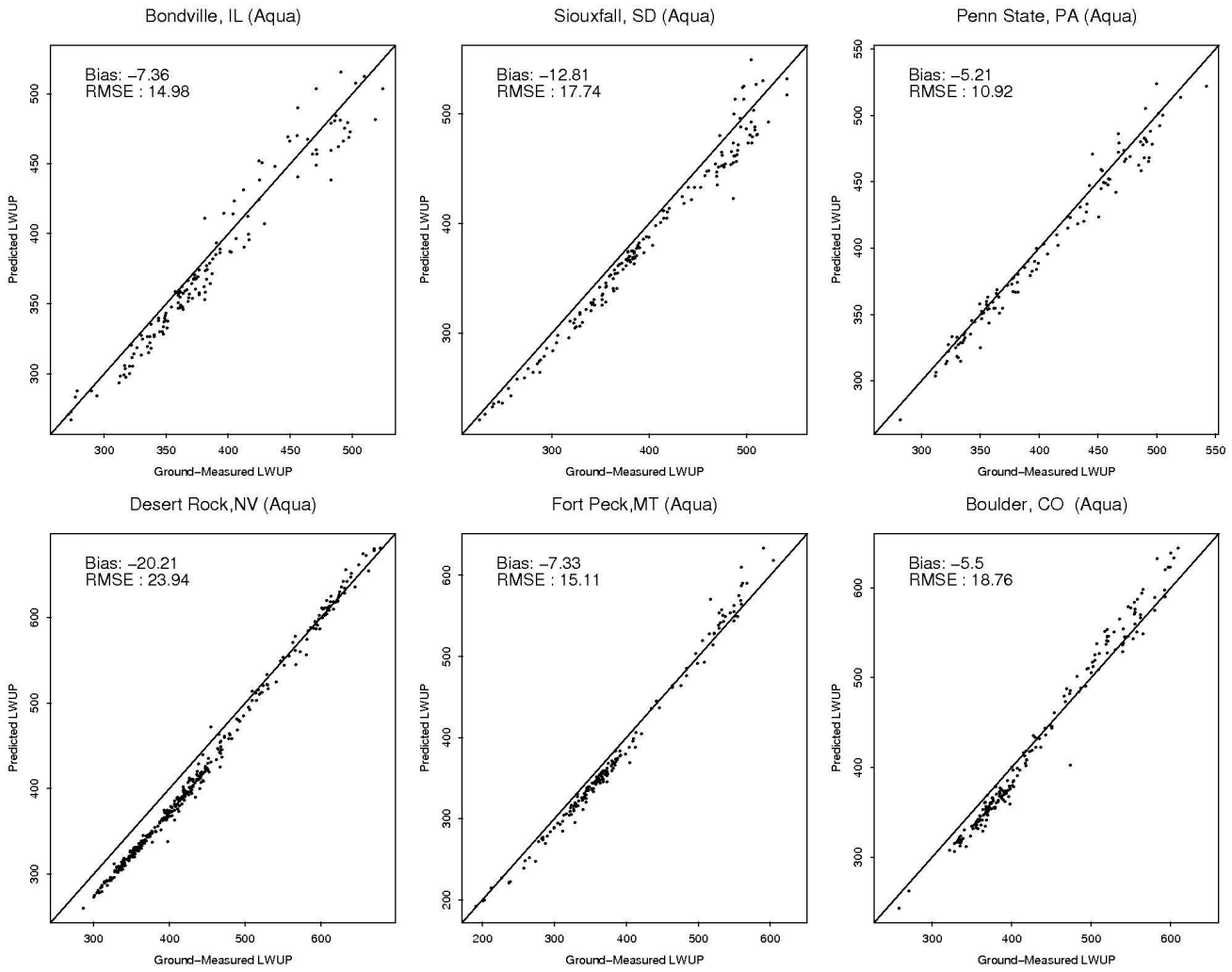

Figure 6-6 The linear model method validation results using MODIS Aqua TOA radiance.

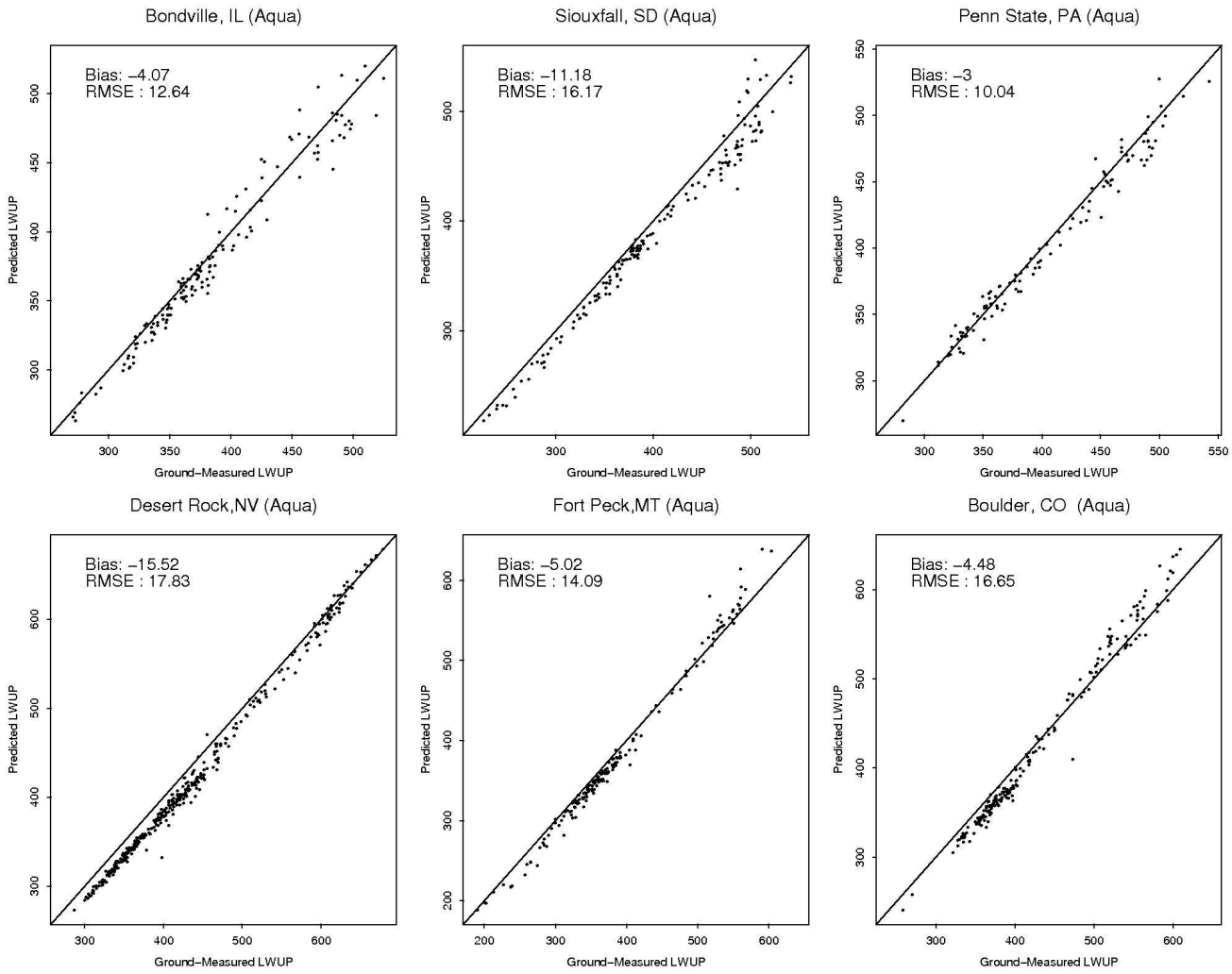

Figure 6-7 The ANN model method validation results using MODIS Aqua TOA radiance.

6.3.3 The Spatial Mismatch Issue

The spatial mismatch issue must be considered when satellite-derived LWUP is compared with SURFRAD ground measurements. Unlike LWDN, LWUP is sensitive to many surface factors that vary over time, such as vegetation cover, snow cover, and soil moisture. The spatial resolution of MODIS-derived LWDN is 1 km at nadir. The footprint of SURFRAD PIRs that measure LWUP is about 200 m^2. Ground data used in this study may be less representative of the MODIS footprint than that measured using multiple ground sensors within the MODIS footprint simultaneously (Coll et al., 2005; Wan et al., 2002). However, SURFRAD station locations are chosen such that the land form around the station is uniform. One major advantage of using data from long-term continuous monitoring sites such as SURFRAD is that a large quantity of point ground measurements over representative sites is available. Two years of data were used in this study. Although it may not suitable for assessing errors in individual observations, useful information can be derived after hundreds of measurements from each sites are compared with MODIS-derived LWUP.

The Earth's surface behaves almost as an isothermal and homogeneous surface at night. The spatial mismatch problem between the MODIS footprint and ground measurements is more severe during daytime. Larger scattering was observed for daytime observations for all three methods.

6.3.4 Results at the Desert Rock Site

The Desert Rock site, a high elevation desert site, has the largest bias and RMSE for the three methods. The Desert Rock site, unlike other sites, is partially vegetated. The errors caused by the Lambertion assumption and spatial mismatch are larger at this site

than at other sites. Moreover, air traffic out of Los Angeles produces abundant cirrus cloud cover over this site. The broadband emissivity of this site is ~ 0.95. Statistics show that 30% of MODIS-derived broadband emissivity is below this value. Cloud contamination is a significant source of error at this site.

6.3.5 The Systematic Biases

The emissivity-temperature, linear model, and ANN model methods all underestimate LWUP, with mean biases ranging from -18 to -7 W/m^2. The biases are larger at low temperatures. Cloud contamination is an important factor that causes negative biases in LWUP. MODIS cloud product cannot mask all cloud cover, especially cirrus clouds. Some pixels used in the study may be cloud-contaminated even after manual screening. Moreover, cloud contamination affects the temperature-emissivity method more than the other two methods because cloud contaminated pixels have both low LST and narrow band emissivity values. Wang et al.'s study (2005) indicated that MODIS retrieved narrow band emissivities are sensitive to cloud contamination which can result in low emissivity retrieval.

Sensor systematic error may be another factor that causes the systematic biases in the MODIS-derived LWUP. The absolute radiometric accuracy and the detector-dependent systematic errors of MODIS Terra TIR channels have been studied in previous studies (Wan et al., 2002; Liu et al., 2006). However, more study is needed in the future to characterize the bias patterns in MODIS channels 29, 31, and 32 to assess the errors caused by the sensor systematic error.

6.4 Estimating LWNT Using MODIS-Derived LWDN and LWUP

LWNT is simply the difference between LWDN and LWUP. In this study, LWNT was calculated using MODIS-derived LWDN and LWUP. LWDN was estimated using the nonlinear LWDN models (see Section 5.2.3); LWUP was estimated using the ANN models (see Section 6.2.3). The ANN models systematically underestimated LWUP over all surfaces. A bias of 8.00 W/m^2 was corrected based on LWUP validation results.

MODIS-derived LWNT was validation using the same two years (2005 and 2006) of SURFRAD ground data that were used to validate LWDN and LWUP. Ground-measured LWNT was derived from LWDN and LWUP ground measurements. Table 6-4 summarizes LWNT validation results. The averaged RMSEs were 17.72 W/m^2 (Terra) and 16.88 W/m^2 (Aqua); the averaged biases are -2.08 W/m^2 (Terra) and 1.99 W/m^2 (Aqua). The RMSEs over all sites are less than 20 W/m^2.

Figure 6-8 and Figure 6-9 illustrate the LWNT validation result at individual sites. Similar to the LWDN and LWUP validation results, larger scatter was observed for daytime observations. The larger scatter may be caused by spatial mismatch between MODIS and ground instruments footprints.

Sites	**Terra**		**Aqua**	
	Bias	RMSE	Bias	RMSE
Bondville	3.97	19.12	7.67	19.74
Sioux Falls	-2.43	17.08	-1.00	15.60
PennState	1.37	18.92	6.19	18.87
DesertRock	-3.88	18.40	-0.09	16.90
FortPeck	-1.79	13.44	4.70	14.44
Boulder	-9.69	19.38	-5.51	15.75
Mean	-2.08	17.72	1.99	16.88

Table 6-4 MODIS-derived LWNT validation results (unit W/m^2).

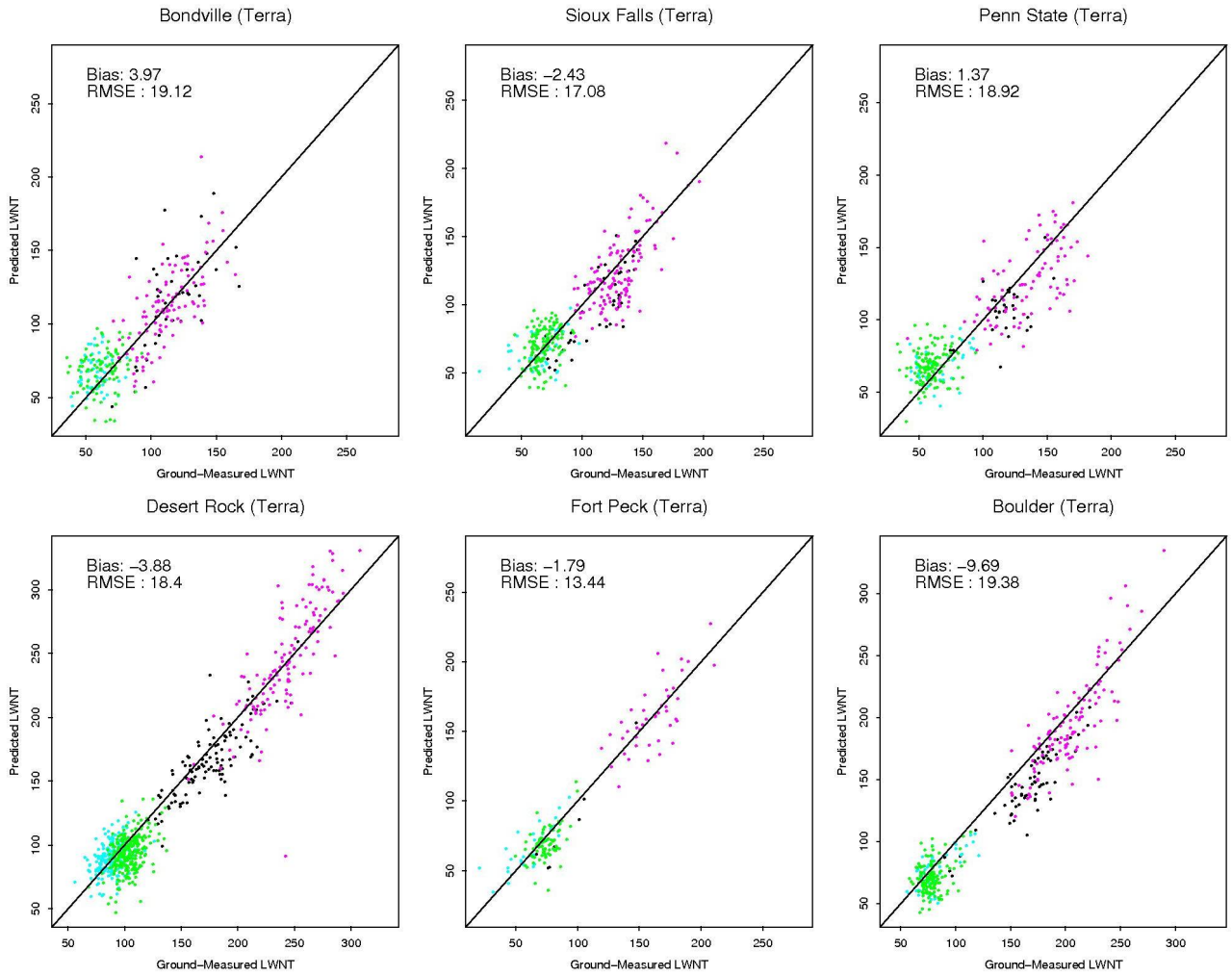

Figure 6-8 MODIS Terra-derived LWNT validation results (black-fallwinter/day; cyan-fallwinter/night; magenta-springsummer/day; green-springsummer/night).

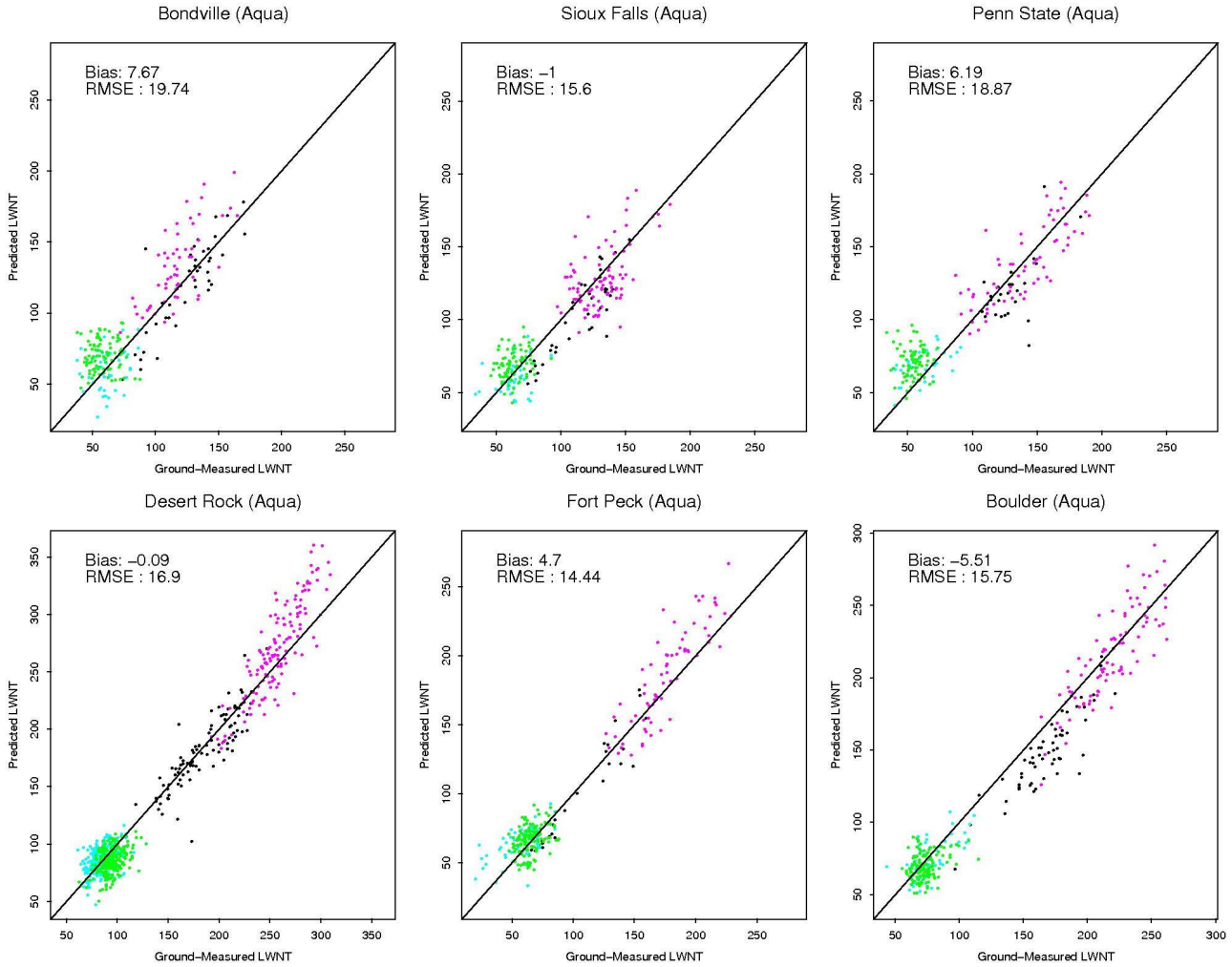

Figure 6-9 MODIS Aqua-derived LWNT validation results (black-fallwinter/day; cyan-fallwinter/night; magenta-springsummer/day; green-springsummer/night).

6.5 Summary

Three methods for estimating clear-sky land LWUP using MODIS data at 1 km spatial resolution were evaluated using SURFRAD ground data. The three methods are: 1) the temperature-emissivity method, 2) the linear model method, and 3) the ANN model method. Methods 2 and 3, derived from the new hybrid method, estimate LWUP directly from MODIS TOA radiance. The linear model method explains more than 99% of variations in the simulated databases, with a standard error less than 6.11 W/m^2. The ANN method explains more than 99.6% of variations in the simulated databases. It has smaller standard errors (<3.70 W/m^2) compared with the linear model method.

The three methods were validated using two years (2005 and 2006) of ground measurements from six SURFRAD sites. Although the linear and ANN models were developed using MODIS Terra data, they were applied to both Terra and Aqua MODIS TOA radiance. The ANN model method outperforms the other two methods, with mean RMSEs of 15.89 (Terra) and 14.57 (Aqua) W/m^2. The temperature-emissivity method has the largest biases and RMSEs at all sites. The mean bias and RMSE of the ANN model method is ~5 W/m^2 smaller than that of the temperature-emissivity method and ~2.5 W/m^2 smaller than that of the linear model method. The validation results indicated that the linear and ANN model methods developed in this study can be applied to both Terra and Aqua observations.

Table 6-5 compares the validation results (combining Terra and Aqua) and input parameters for the three methods. The new hybrid method requires simpler input parameters but achieved a higher accuracy than the temperature-emissivity method. The

former only requires MODIS TOA radiance. The latter requires three input parameters, i.e., surface temperature, emissivity, and LWDN.

	Temperature-Emissivity Method	**Hybrid Method**	
		Linear model	**ANN model**
Avg. RMSE	20.58	17.63	15.23
Avg. Bias	-17.25	-10.46	-7.94
Input Parameters	Surface temp. Emissivity, LWDN	TOA radiance	TOA radiance

Table 6-5 Comparing the three methods for estimating LWUP using MODIS data.

LWNT was estimated using MODIS-derived LWDN and LWUP and validated using the six SURFRAD sites. LWDN was estimated using the nonlinear LWDN models; LWUP was estimated using the ANN models. The averaged RMSEs were 17.72 W/m^2 (Terra) and 16.88 W/m^2 (Aqua); the averaged biases are -2.08 W/m^2 (Terra) and 1.99 W/m^2 (Aqua).

Chapter 7 Products Intercomparision and the hybrid methods for GOES Data

CERES surface longwave radiation budget products (Gupta et al., 1997; Inamdar & Ramanathan, 1998) represent the state-of-the-art surface longwave radiation budget derived from satellite data. The spatial resolution of CERES instruments is 20 km at nadir (Wielicki et al., 1996). In this Chapter, MODIS-derived surface longwave radiation was compared to the CERES instantaneous clear-sky product to further evaluate the MODIS hybrid methods developed in Chapters 5 and 6.

MODIS can only provide four observations over low latitude regions. Surface longwave radiation budget components estimated from MODIS data alone are inadequate for deriving the diurnal cycle. Data from geostationary satellites, which provide high temporal resolution observations over low attitude regions, do not have this disadvantage. The GOES satellites provide diurnal coverage of the Earth's surface between ±60º latitude. GOES data from the current GOES-12 Sounder has a spatial resolution of 10 km in TIR channels, with a half-hour temporal resolution (Space Systems-Loral, 1996). The future GOES-R ABI will have a spatial resolution of 2 km in TIR channels, with a 5-mininute temporal resolution (Schmit et al., 2005). In this study, preliminary hybrid methods, similar to the MODIS hybrid methods presented in Chapter 5 and Chapter 6, were developed for estimating LWDN and LWUP from the GOES-12 Sounder and GOES-R ABI data.

7.1 MODIS versus CERES Surface Longwave Radiation Budget– A Case Study

A case study was conducted to compare the MODIS and CERES derived clear-sky instantaneous LWNT over the Washington D.C. - Baltimore Metropolitan Area on April 10, 2007 (18:10 UTC). Both MODIS and CERES instruments involved in the case study are onboard of NASA EOS Aqua satellite. The CERES surface longwave radiation products are estimated using two plans. In Plan A, clear-sky LWDN is derived using a hybrid method (Inamdar & Ramanathan, 1997); In Plan B, total-sky LWDN is retrieved using a physical-based method based on highly parameterized equations; LWUP is derived using MODIS LST and emissivity products and aggregated to CERES footprint (Gupta et al., 1997). The CERES Plan B retrieval was used in the intercomparision because the Plan A retrieval is not available in the CERES product used in the study.

Figure 7-1 shows the CERES and MODIS LWNT images over the study area. Retrievals over water surface were set to zero to facilitate understanding. Because the spatial resolution of CERES is 20 km, the CERES LWNT image was more monotonous. The MODIS-derived LWNT image reveals more details throughout the scene, including urban hot spots and cool spots near the water. MODIS-derived LWNT was generally higher than CERES-derived LWNT. Figure 7-2 (a) shows the histogram of the differences between MODIS- and CERES-retrieved LWNT. The averaged difference is ~ 23 W/m^2.

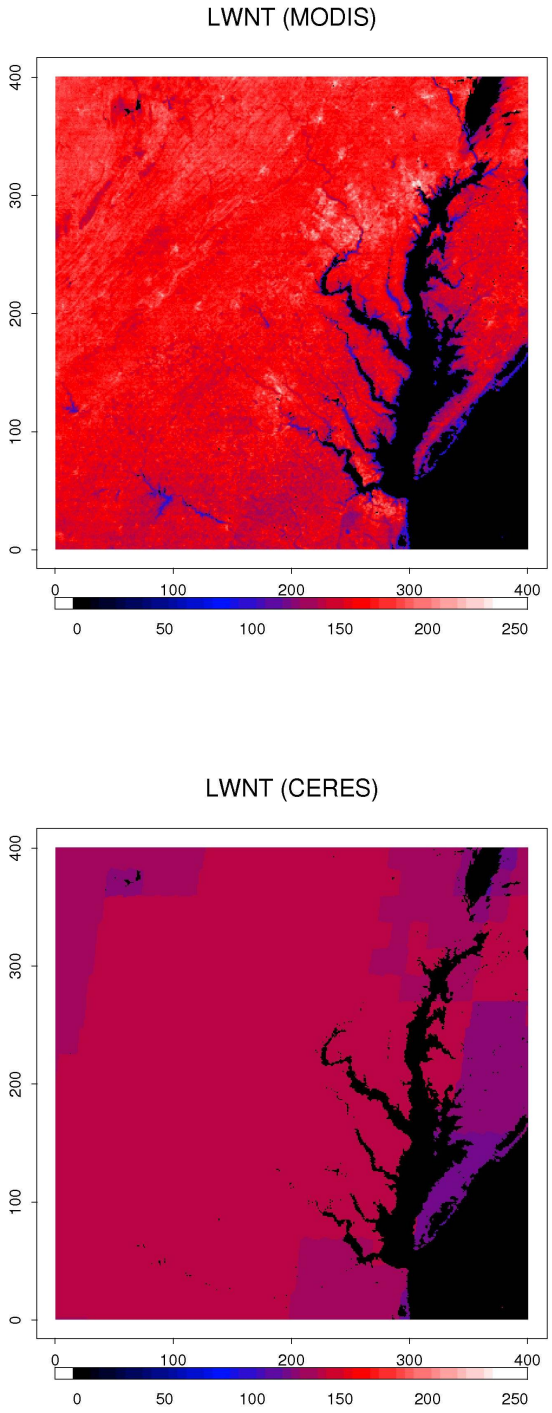

Figure 7-1 MODIS-derived versus CERES-derived instantaneous clear-sky LWNT images (400 x 400 pixels) over the Washington D.C. - Baltimore Metropolitan Area (April 10, 2007 18:10 UTC, unit W/m^2).

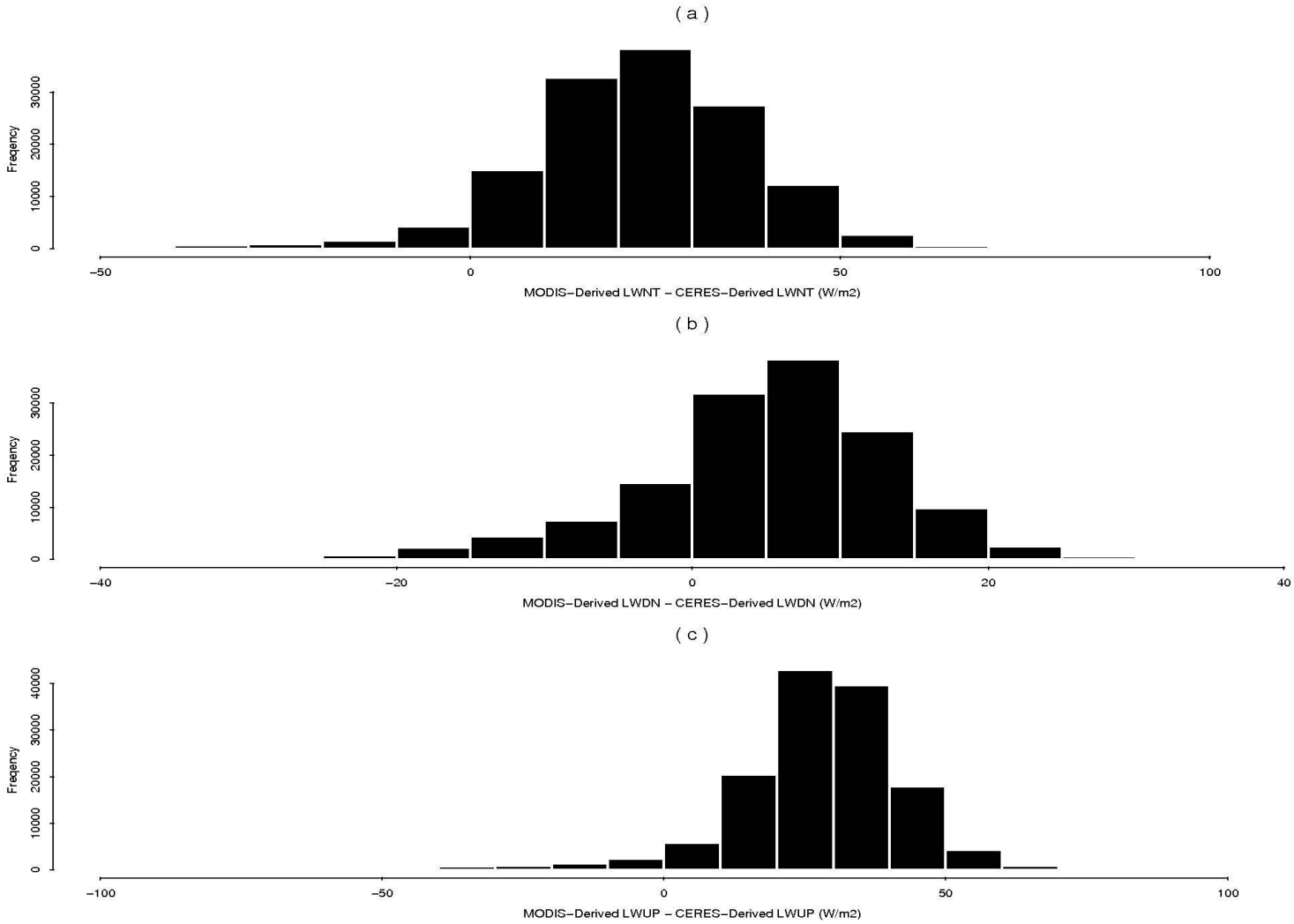

Figure 7-2 The differences between MODIS-derived and CERES-derived instantaneous clear-sky LWNT, LWDN, and LWUP.

MODIS- and CERES-derived LWDN and LWUP images were also compared to identify the potential factors that cause the difference between MODIS and CERES-derived LWNT. Figure 7-3 shows the LWDN images. The stripes in the MODIS LWDN image are caused by the systematic detector errors in MODIS channels 27, 28, and 33. The MODIS and CERES-derived LWDN images illustrated similar trends, with higher LWDN in the southwest portion of the images and lower LWDN in the northeast portion of the images. The MODIS LWDN image reveals more detailed variations within the scene. Figure 7-2 (b) shows the histograms of the differences between MODIS- and CERES-retrieved LWDN. Statistics show the differences between MODIS- and CERES-retrieved LWDN is small, with an average difference of ~ 5 W/m^2.

The difference between MODIS- and CERES-derived LWNT is mainly caused by LWUP. Figure 7-4 shows the LWUP images. Figure 7-2 (c) shows the histograms of the differences between MODIS- and CERES-retrieved LWUP. Although similar trends can be observed in the two LWUP images, the averaged difference between MODIS- and CERES-derived LWUP was ~27 W/m^2 , with the difference as large as 60 W/m^2 in some cases. LWUP has a much larger spatial variability compared with LWDN, especially during the day and over heterogeneous surfaces. The large difference in LWUP may be caused, at least partially, by the differences in instrument spatial resolutions. While MODIS-derived LWUP is capable to reveal detailed surface characteristics, CERES-derived LWUP obscures much of these variations. The methods used for deriving MODIS and CERES LWUP may also cause the differences in the two images. This issue was addressed in Section 7.2.

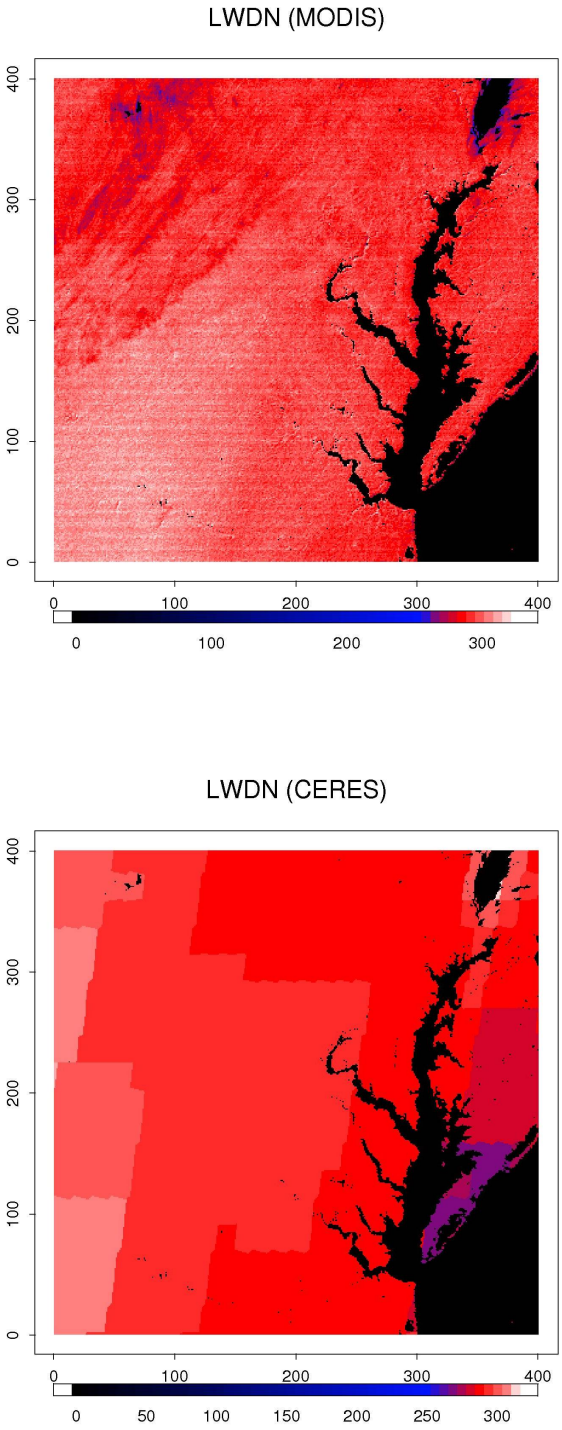

Figure 7-3 MODIS-derived versus CERES-derived instantaneous clear-sky LWDN images (400 x 400 pixels) over the Washington D.C. - Baltimore Metropolitan Area. (April 10, 2007 18:10 UTC, unit W/m^2). The stripes were caused by the systematic detector errors in MODIS channels 27, 28, and 33.

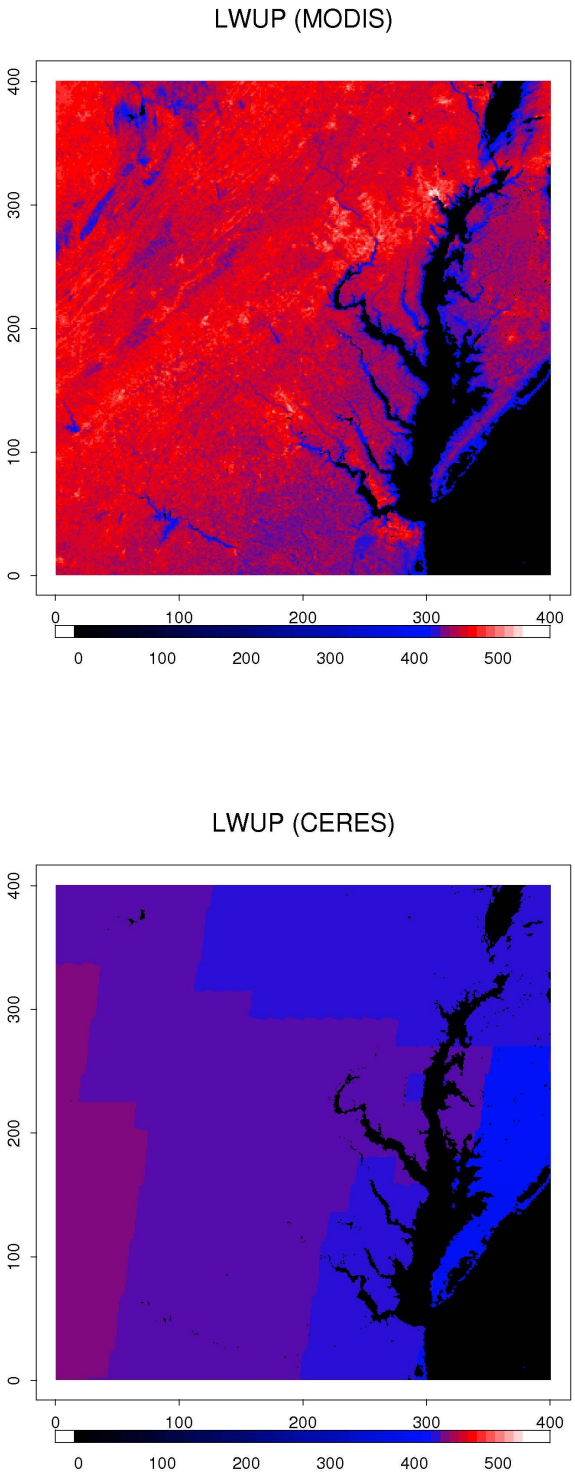

Figure 7-4 MODIS-derived versus CERES-derived instantaneous clear-sky LWUP images (400 x 400 pixels) over the Washington D.C. - Baltimore Metropolitan Area (April 10, 2007 18:10 UTC, unit W/m^2).

7.2 Comparing MODIS versus CERES Validation Results at SURFRAD sites

The case study in the previous subsection shows the MODIS-derived LWNT and LWUP are more than 20 W/m^2 larger than the CERES-derived values on average. CERES-derived instantaneous clear-sky LWDN and LWUP were validated at five SURFRAD sites (Bondville, Penn State, Desert Rock, Fort Peck, and Boulder) in 2005 (Charlock, 2006). The MODIS and CERES validation results were compared to investigate the underlying causes. Table 7-1 shows the accuracy of LWDN and LWUP evaluated at the five SURFRAD sites.

	LWDN (W/m^2)				**LWUP (W/m^2)**			
	MODIS		**CERES**		**MODIS**		**CERES**	
	Bias	**RMSE**	**Bias**	**RMSE**	**Bias**	**RMSE**	**Bias**	**RMSE**
Bondville	-2.55	19.15	-2.9	12.9	-5.44	14.09	7.6	20.3
Penn State	-1.54	15.49	-2.7	10.7	-4.34	10.92	2.2	14.8
Desert Rock	-8.46	17.87	-27.6	29.7	-15.97	18.27	-14.2	18.0
Fort Peck	-1.30	14.09	-9.9	15.6	-6.03	14.92	0.3	13.0
Boulder	7.56	18.35	-21.7	25.2	-4.51	17.00	-16.1	25.3

Table 7-1 Comparing MODIS and CERES validation results at five SURFRAD sites.

MODIS clear-sky LWDN validation results (using the nonlinear models) were compared to the CERES validation results. The RMSEs of CERES-derived LWDN are ~ 5 - 6 W/m^2 smaller at the Bondville and Penn State sites. However, the RMSEs of MODIS-derived LWDN are ~ 7 - 12 W/m^2 smaller than CERES at the Desert Rock and Boulder sites. The surface elevations of ~89% of pixels are lower than 500 meters in the study area. The difference between MODIS and CERES LWNT images showed in Section 7.1 is consistent with the difference in the SURFRAD validation results.

MODIS clear-sky LWUP validation results (using the ANN model method) were also compared to the CERES validation results at the five sites. The RMSEs of MODIS-derived LWUP are ~ 4 – 8 W/m^2 smaller than CERES RMSEs at the Bondville, Penn State, and Boulder sites. The differences between MODIS and CERES RMSEs are less than 2 W/m^2 at the Desert Rock and Fort Peck sites.

The MODIS and CERES LWUP validation comparison result is consistent with the validation results presented in Section 6.3. Under clear-sky conditions, CERES LWUP is estimated using MODIS-derived LST and emissivity products and aggregated to the CERES footprint (Gupta et al., 1997). The validation results in Section 6.3 indicated that the ANN model method outperforms the temperature-emissivity method. Moreover, the cloud-contamination problem is more severe in CERES because of its large footprint, which results in low LWUP retrieval. The extremely large differences (>50 W/m^2) may be caused by the fact that CERES can not detect fine scale hot and cold spots during the day. The comparison indicates that using CERES-derived surface longwave radiation budget in the high spatial resolution numerical models may cause large errors during the day.

7.3 GOES-12 Sounder

The GOES-12 Sounder is a 19 channel discrete-filter radiometer that senses specific data parameters for atmospheric vertical temperature and moisture profiles, surface and cloud top temperature, and O_3 distribution (Space Systems-Loral, 1996). Table 7-2 compares GOES-12 Sounder and MODIS TIR channels. Only the MODIS channels that were used to estimate LWDN or LWNT are listed. GOES-12 Sounder

provides more channels for retrieving temperature and moisture profiles compared with MODIS, however, with lower spatial resolution.

GOES 12 Sounder		MODIS		Primary Use
Band	**Wavelength (μm)**	**Band**	**Wavelength (μm)**	
1	14.71			Temperature sounding
2	14.37	36	14.235	
3	14.06	35	13.935	
4	13.64	34	13.635	
5	13.37	33	13.335	
6	12.66			
7	12.02	32	12.020	Surface temperature
8	11.03	31	11.030	
9	9.7	30	9.730	Total O_3
10	7.43	29	8.550	Water vapor sounding
11	7.02	28	7.325	
12	6.51	27	6.715	
13	4.57			Temperature Sounding
14	4.52			
15	4.45			
16	4.13			
17	3.98			Surface temperature
18	3.71			
19	0.7			cloud

Table 7-2 Comparing GOES-12 Sounder and MODIS TIR channels.

7.4 Hybrid Method for Estimating LWDN from GOES-12 Sounder Data

The hybrid method for estimating LWDN from GOES-12 Sounder TOA radiance and surface elevation is similar to that of MODIS. TOA radiance and LWDN were simulated using MODIS-retrieved atmosphere profiles and the MODTRAN4 radiative transfer model. The surface emissivity and surface pressure effects were accounted for in the same way as MODIS (see Chapter 5). Nonlinear linear models were developed using the simulated GOES-12 Sounder databases:

$$F_d = L_{tair}(a_0 + b_1 L_1 + b_2 L_3 + b_3 L_8 + b_4 L_{11} + b_5 L_{12} + c_1 \frac{L_7}{L_8} + c_2 \frac{L_5}{L_7} + c_3 \frac{L_{10}}{L_8} + d_1 H)$$
$$L_{air} = L_7 (daytime) \quad (7\text{-}1)$$
$$L_{air} = L_8 (nighttime)$$

where L_{Tair} equals to L_7 in the daytime models and equals to L_8 in the nighttime models; a_0, b_i, c_i, and d_1 are regression coefficients. The nonlinear models explain more than 93 % of variations in the simulated databases, with standard errors less than 15.51 W/m2. **Error! Reference source not found.** summarizes the model fitting results.**Error! Reference source not found.** GOES-12 Sounder nonlinear LDWN models regression coefficients.

The nonlinear LWDN models for estimating LWDN from GOES-12 Sounder TOA radiance were validated using half year's (July-December, 2007) SURFRAD ground measurements at the Bondville, Sioux Falls, Penn State, and Boulder sites. Clear-sky observations were identified using GOES cloud product (Minnis et al., 2004). No manual screening was applied to remove the undetected cloud-contaminated pixels. Validation results (see Figure 7-5) show the RMSEs of GOES-12 Sounder-derived range from 19.16 to 23.53 W/m^2; biases range from 0.05 to -2.17 W/m^2. The RMSEs for LWDN derived in this study is smaller than existing LWDN product derived using GOES 6,7, and 8 Sounder data (33.6 W/m^2, monthly) (ASDC, 2006).

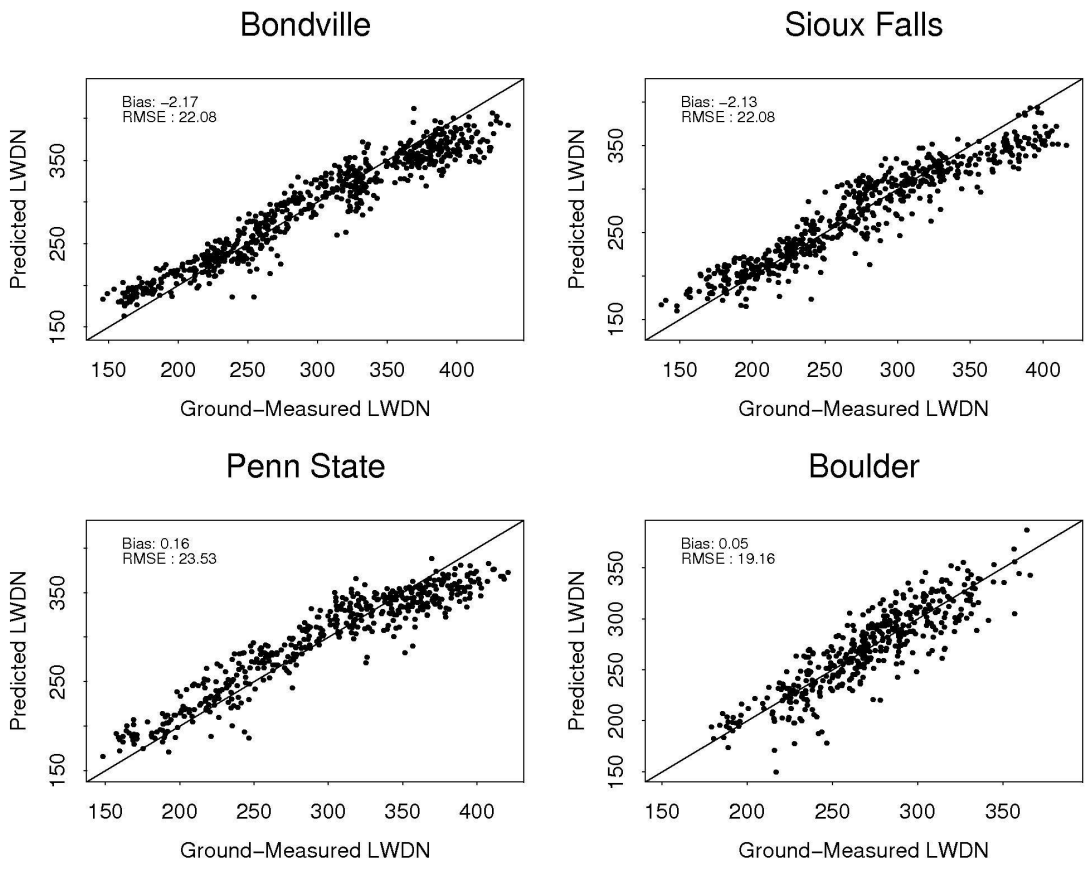

Figure 7-5 GOES-12 Sounder-derived LWDN validation results.

7.5 Hybrid Method for Estimating LWUP from GOES-12 Sounder Data

The hybrid method, similar to the MODIS LWUP hybrid method presented in Chapter 6, was developed for estimating LWUP from GOES-12 Sounder TOA radiance. GOES-12 Sounder channels 10, 8, 7 are corresponding MODIS channels 29, 31, and 32. These three channels were used for developing linear models for predicting LWUP from GOES-12 Sounder TOA radiance. The linear models can account for more than 99% of variations in the simulated dataset, with standard errors less than 5.42 W/m^2 for all sensor view zenith angles. Table 7-3 summarizes the model fitting results.

$$F_u = a_0 + \sum_i a_i L_i \quad \text{(i=7, 8, 10)} \tag{7-2}$$

	0º	**15º**	**30º**	**45º**	**60º**
R^2	0.9988	0.9987	0.9986	0.9982	0.9967
Std. Err.	2.991	3.038	3.205	3.640	4.947
a_0	124.8827	125.9401	128.9878	135.2046	148.1727
a_7	-130.4156	-132.0319	-137.2860	-148.0604	-170.4925
a_8	153.7796	155.1242	159.4967	168.4509	187.0587
a_{10}	4.6379	4.8304	5.4884	6.9761	10.5636

Table 7-3 GOES-12 Sounder LWUP model fitting results.

The linear LWUP models were also validated using SURFRAD ground measurements at the Bondville, Sioux Falls, Penn State, and Boulder sites. Figure 7-6 shows the validation results. The RMSEs range from 14.87 to 23.7 W/m^2; biases range from -13.13 to -0.63 W/m^2. The linear model fitting and validation results indicated that GOES-12 Sounder data can be used to estimate LWUP with improved accuracy than existing LWUP products using previous GOES Sounder data (ASDC, 2006). Nonlinear LWUP models were not developed in the current stage; they will be investigated in the future.

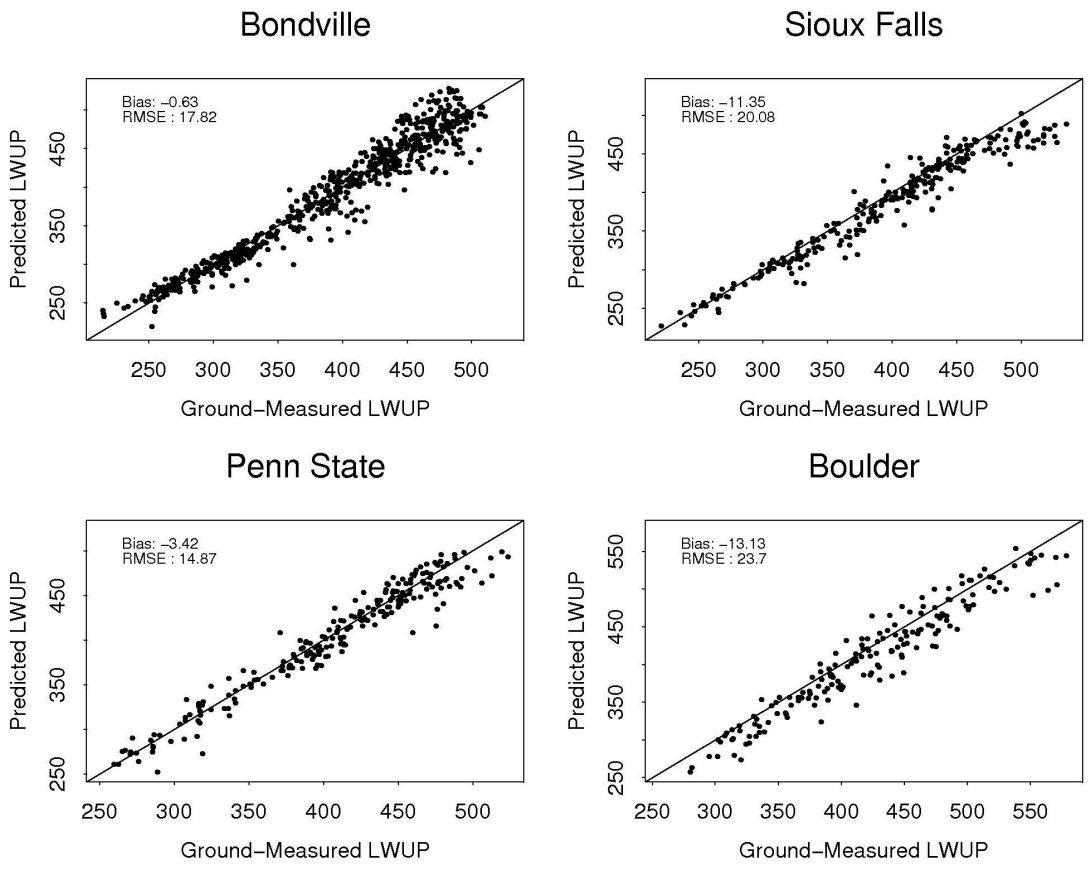

Figure 7-6 GOES-12 Sounder-derived LWUP validation results.

7.6 Estimating LWDN and LWUP from GOES-R ABI data

The first GOES-R series satellite, the next generation of NOAA geostationary satellite equipped with improved spacecraft and instrument technology, is scheduled to be launched in 2014. The ABI instrument onboard of the GOES-R satellite has similar band design as MODIS and GOES-12 Sounder in TIR spectrum. Table 7-4 compares GOES-R ABI and MODIS TIR channels. GOES-R ABI will have a spatial resolution of 2 km and a temporal resolution of 5 minutes (Schmit et al., 2005). Surface downwelling and upwelling longwave radiation are among the planed operational products of GOES-R program. Benefiting from the improved instrument technology, spatial resolution, and

temporal resolution, more timely and accurate surface longwave radiation budget products may be retrieved using the future GOES-R ABI data.

GOES-R ABI		MODIS	
Band Number	**Wavelength (μm)**	**Band Number**	**Wavelength (μm)**
7	3.9	22	3.96
8	6.15		
9	7.0	27	6.7
10	7.4	28	7.3
11	8.5	29	8.55
12	9.7	30	9.7
13	10.35		
14	11.2	31	11.0
15	12.3	32	12.0
16	13.3	33	13.3
		34	13.6
		35	13.9
		36	14.2

Table 7-4 GOES-R ABI TIR channels versus MODIS TIR channels.

A preliminary study was conducted to investigate the feasibility of using GOES-R ABI data to estimate the surface longwave radiation budget using the hybrid methods that are similar to the method developed for MODIS and GOES-12 Sounder. The radiative transfer simulation for GOES-R ABI was similar to MODIS and GOES-12 Sounder. The simulated GOES-R ABI spectral response function from the Space Science and Engineering Center at the University of Wisconsin was used in the study (Dr. Tim Schmit, personal communication, 2007). The surface emissivity and surface pressure effects were considered in the same way as MODIS. GOES-R ABI channels 7-16 TOA radiance, LWDN, and LWUP were simulated for each MODIS-retrieved atmosphere profiles.

In the current stage, only linear models were fitted for predicting LWDN and LWUP from the GOES-R ABI data due to the lack of official spectral response functions.

No separate models were fitted for estimating LWDN during daytime and nighttime. Equations 7-3 and 7-4 show the linear models developed for estimating LWDN and LWUP from GOES-R ABI data:

$$F_{d,GOES-R} = a_0 + \sum_i a_i L_i + bH \qquad \text{i= 7, 8, 9, 10, 11, 13, 14, and 15} \tag{7-3}$$

$$F_{u,GOES-R} = a_0 + \sum_i a_i L_i \quad \text{(i=11, 13, 14, 15)} \tag{7-4}$$

Figure 7-7 shows the LWDN model fitting results. Similar to MODIS, the GOES-R ABI linear models can explain more than 93% of variations in the simulated databases, with standard errors less than 15.51 W/m^2. The model fitting results indicated GOES-R ABI data may be used to estimate LWDN. However, one major concern is that GOES-R ABI only has one channel for retrieving air temperature profile at 13.3 µm and beyond. Two or more temperature profile channels from 13 – 15 µm were used to develop the hybrid methods for MODIS and GOES 12 Sounder.

Figure 7-8 shows the LWUP model fitting results. The linear models can explain more then 99% of variations in the simulated databases, with standard errors less than 4.97 W/m^2. Besides the TIR channels that are corresponding to MODIS channels 29, 31, and 32, GOES-R ABI has an additional window channel at 10.35 µm (channel 13) that may be used for estimating LWUP. No major concerns exists for deriving LWUP using GOES-R ABI data if the current proposed channels are retained at sensor launch.

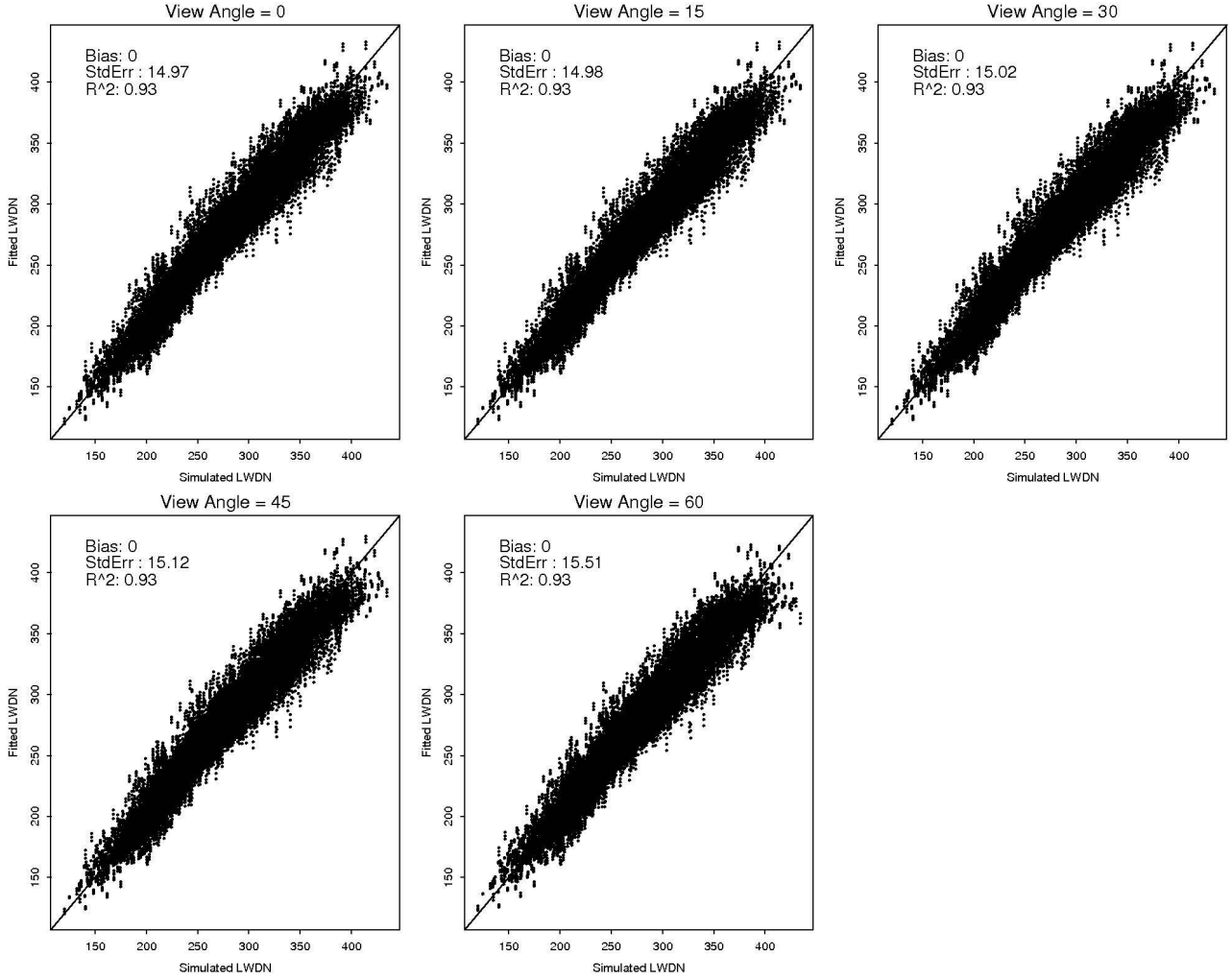

Figure 7-7 The linear LWDN model fitting results for GOES-R ABI.

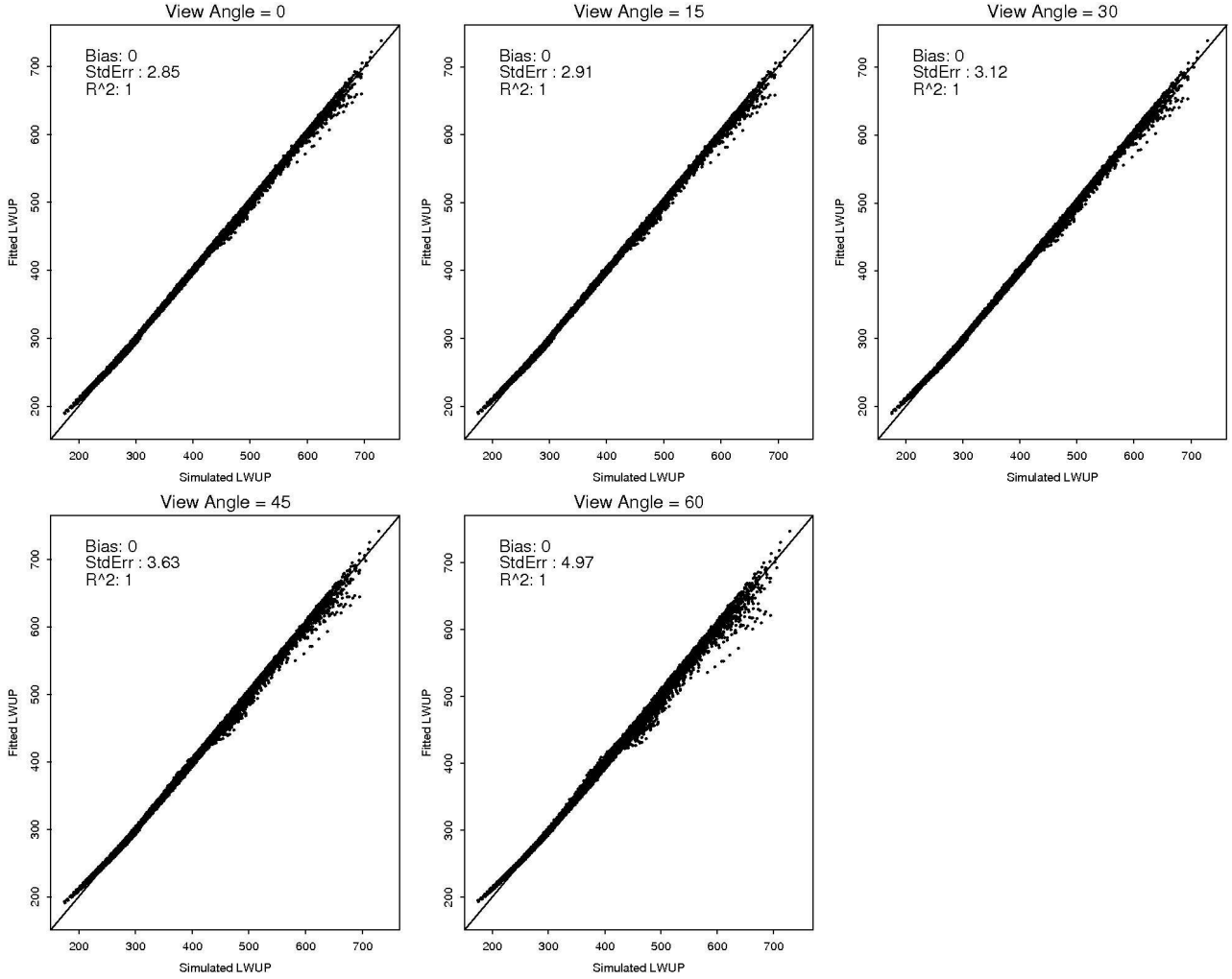

Figure 7-8 The linear LWUP model fitting results for GOES-R ABI.

7.7 Summary

The MODIS-derived surface longwave radiation budget was compared to CERES. MODIS-derived LWDN is similar to CERES-derived LWDN over low elevation surfaces, with the RMSEs of CERES-derived LWDN ~ 5 - 6 W/m^2 smaller than MODIS. However, the RMSEs of MODIS-derived LWDN are ~ 7 - 12 W/m^2 smaller than CERES at higher elevation sites. The RMSEs of MODIS-derived LWUP are smaller than CERES in general.

New hybrid methods were developed for estimating instantaneous clear-sky LWDN and LWUP from GOES-12 Sounder data. The methods were validated using half-year's ground measurements at four SURFRAD sites, with RMSEs less than 23.7 W/m^2 in all cases. The accuracy of GOES-12 Sounder-derived LWDN and LWUP is better than existing surface longwave radiation budget dataset derived using GOES data. It may be further improved after the models are refined in the future.

The preliminary study also indicated that the hybrid method can be used to estimate LWUP using the future GOES-R ABI TOA radiance. The hybrid method may also be used to estimate LWDN from the GOES-R ABI data. However, there is a concern about the lack of sufficient air temperature profile channel in the current ABI instrument design.

Chapter 8 Summary and Suggestions for Future Research

The surface radiation budget is valuable in addressing a variety of scientific and application issues related to climate trends, hydrological and biogeophysical modeling, and agriculture. The three longwave components of the surface radiation budget, LWDN, LWUP, and LWNT, are important input and/or diagnostic parameters for land surface models and numerical weather prediction models. However, existing satellite-derived surface longwave radiation budget products have coarse spatial resolutions and their accuracy needs to be greatly improved. In this study, new hybrid methods were developed for estimating instantaneous clear-sky high spatial resolution surface longwave radiation budget using MODIS, GOES-12 Sounder, and the future GOES-R ABI data at 1 - 10 km spatial resolution.

8.1 Estimating Surface Longwave Radiation Budget from MODIS Data

MODIS onboard of the NASA EOS Terra and Aqua satellites provides a unique opportunity for estimating surface longwave radiation budget at high spatial resolution. However, no study has been conducted to estimate surface longwave budget at 1 km spatial resolution using MODIS data. New hybrid methods have been developed to estimate instantaneous clear-sky LWDN and LWUP from MODIS TOA radiance (and surface elevation in the case of LWDN). LWNT was derived using LWDN and LWUP.

A new hybrid method was developed for estimating instantaneous clear-sky land LWDN from 1 km MODIS TOA radiance and surface elevation. Linear and nonlinear LWDN models were developed based on extensive radiative transfer simulations and

statistical analysis. The linear models explain more than 92 % of variations of the simulated databases, with standard errors less than 16.27 W/m^2 for all sensor view zenith angles. The nonlinear models explain more than 93.6 % of variations, with standard error less than 15.20 W/m^2. The LWDN models were validated using two years of ground measurements at six SURFRAD sites. The nonlinear models outperform the linear models, with mean RMSE of 17.60 (Terra) and 16.17 (Aqua) W/m^2. The mean RMSE of the nonlinear models is ~2.5 W/m^2 smaller than that of the linear models. Figure 8-1 shows the nonlinear models validation result using two years (2005 and 2006) of Terra and Aqua clear-sky observations at all six SURFRAD sites.

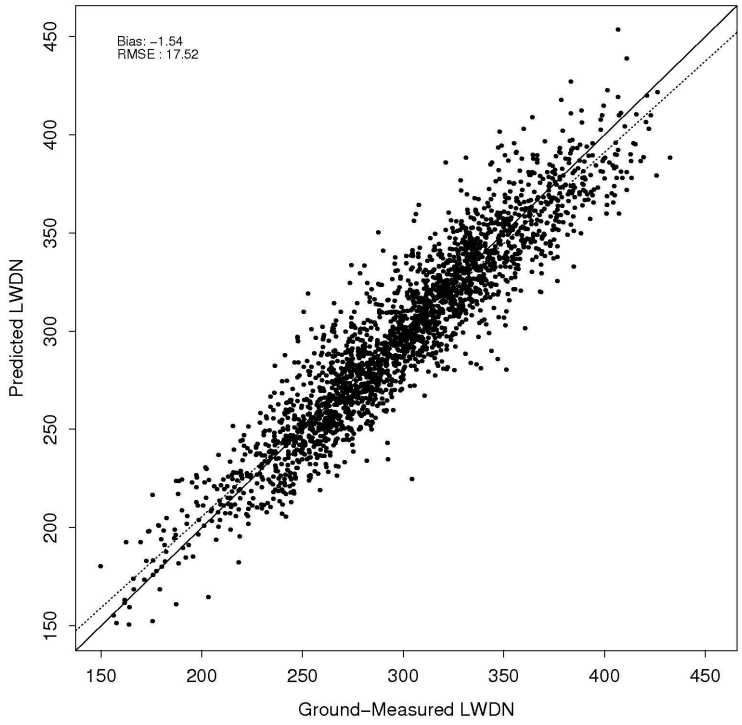

Figure 8-1 MODIS LWDN hybrid method (nonlinear models) validation results using two years (2005 and 2006) of Terra and Aqua clear-sky observations at all six SURFRAD sites.

A new hybrid method was developed for estimating LWUP from MODIS TOA radiance at 1 km spatial resolution. Linear and ANN models were developed using the simulated databases. Three methods were evaluated: 1) the temperature-emissivity method, 2) the linear model method, and 3) the ANN model method. The linear LWUP models explain more than 99% of variation, with standard errors less than 6.11 W/m^2. The ANN models explain more than 99.6% of variations in the simulated databases, with standard errors less than 3.70 W/m^2. The three methods were validated using two years (2005 and 2006) of ground measurements from six SURFRAD sites. The ANN model method outperforms the other two methods, with mean RMSE of 15.89 (for Terra) and 14.57 (for Aqua data) W/m^2. The temperature-emissivity method has the largest biases and RMSEs at all sites. The mean bias and RMSE of the ANN model method is ~5 W/m^2 smaller than that of the temperature-emissivity method and ~2.5 W/m^2 smaller than that of the linear model method. Figure 8-2 shows the ANN model method validation result using two years (2005 and 2006) of Terra and Aqua clear-sky observations at all six SURFRAD sites.

LWNT was derived using LWUP (hybrid method, ANN models) and LWDN (hybrid method, nonlinear models). MODIS-derived LWNT was validation at the same SURFRAD sites that were used to validate LWDN and LWUP. The averaged RMSEs were 17.72 W/m^2 (Terra) and 16.88 W/m^2 (Aqua); the averaged biases are -2.08 W/m^2 (Terra) and 1.99 W/m^2 (Aqua). Figure 8-3 shows the LWNT validation result using two years (2005 and 2006) of Terra and Aqua clear-sky observations at all six SURFRAD sites.

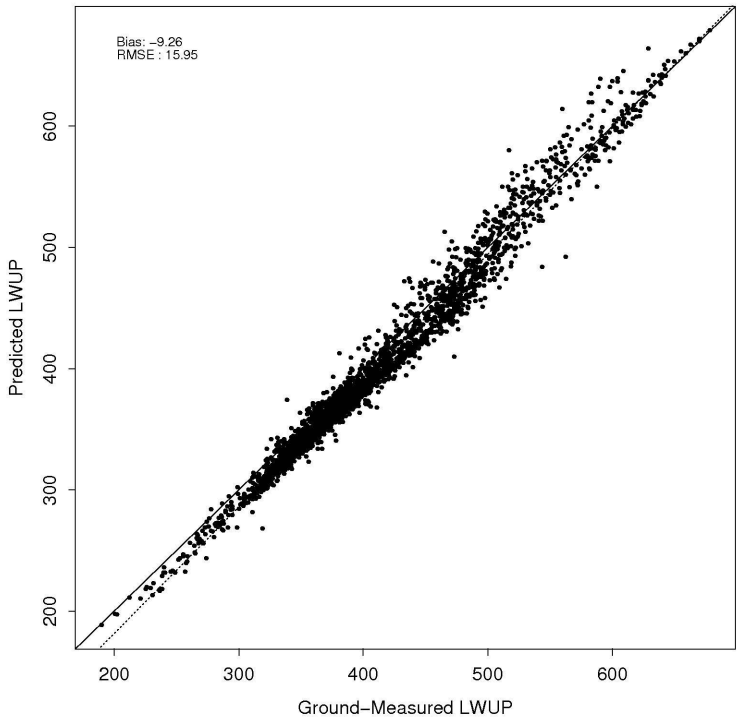

Figure 8-2 MODIS LWUP hybrid method (ANN models) validation results using two years (2005 and 2006) of Terra and Aqua clear-sky observations at all six SURFRAD sites.

The MODIS-derived surface longwave radiation budget was compared to CERES using image-based comparison and SURFRAD validation results. MODIS-derived LWDN is similar to CERES-derived LWDN over low elevation surfaces, with the RMSEs of CERES-derived LWDN ~ 5 - 6 W/m^2 smaller than MODIS. However, the RMSEs of MODIS-derived LWDN are ~ 7 - 12 W/m^2 smaller than CERES at higher elevation sites. The RMSEs of MODIS-derived LWUP are smaller than CERES in general.

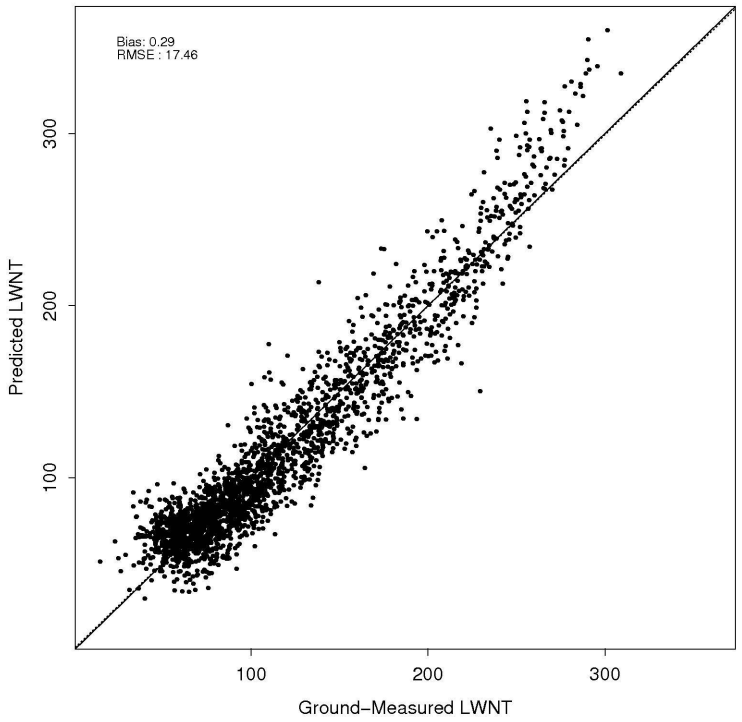

Figure 8-3 MODIS LWNT (LWUP-LWDN) validation results using two years (2005 and 2006) of Terra and Aqua clear-sky observations at all six SURFRAD sites.

8.2 Estimating Surface Longwave Radiation Budget from GOES Data

Surface longwave radiation budget components estimated from MODIS data alone are inadequate for deriving the diurnal cycle. Preliminary hybrid methods, similar to the MODIS hybrid methods, were developed for estimating instantaneous clear-sky LWDN and LWUP from the current GOES-12 Sounder and the future GOES-R ABI data. The GOES-12 Sounder hybrid methods were validated using half-year's ground measurements at four SURFRAD sites, with RMSEs less than 23.7 W/m^2 at all sites. The accuracy of GOES-12 Sounder-derived LWDN and LWUP is better than the existing surface longwave radiation budget dataset derived using GOES data. Figure 8-4 shows the GOES-12 Sounder LWDN hybrid method overall validation results using all clear-

sky observations from the four sites. Figure 8-5 shows the GOES-12 Sounder LWUP hybrid method overall validation results. The preliminary study also indicates that hybrid methods may also be used to estimate LWDN and LWUP from the future GOES-R ABI data.

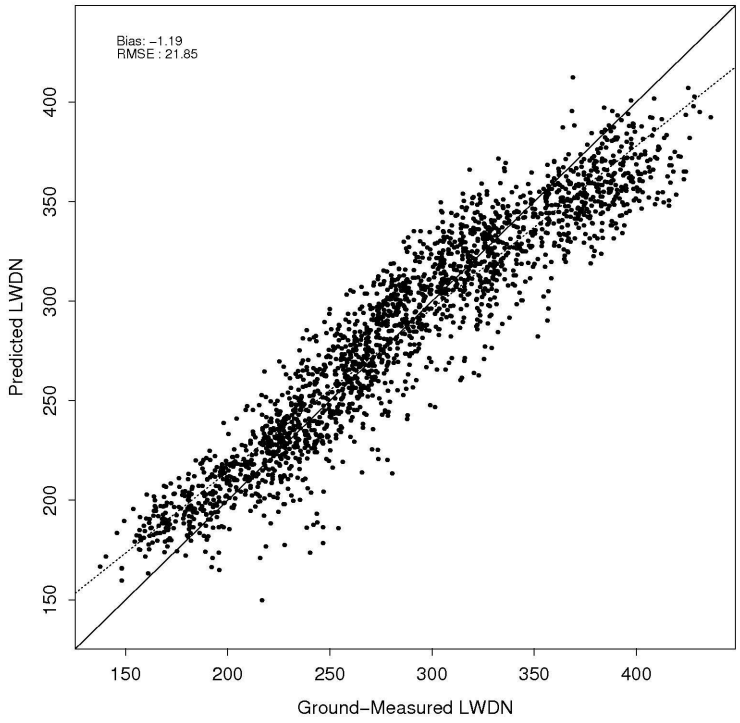

Figure 8-4 GOES-12 Sounder LWDN hybrid method (nonlinear models) validation results using half-year of clear-sky observations from the four sites (Bondville, Sioux Falls, Penn State, and Boulder).

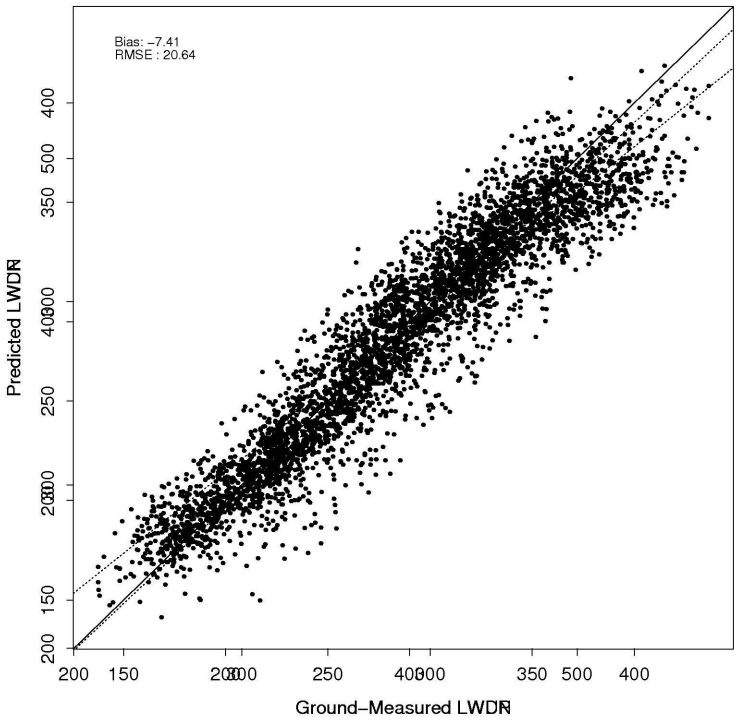

Figure 8-5 GOES-12 Sounder LWUP hybrid method (linear models) validation results using half-year of clear-sky observations from the four SURFRAD sites (Bondville, Sioux Falls, Penn State, and Boulder).

8.3 Significance of This Study

This study is the first effort for estimating surface longwave radiation budget using high spatial resolution MODIS and GOES-12 Sounder data. Compared with previous studies, the new hybrid methods developed in this study are focused on land surfaces and are unique in at least two other aspects: (1) land surface emissivity effect was considered explicitly in the new hybrid methods; (2) surface pressure effect was accounted for by incorporating surface elevation in the statistical models for prediction LWDN.

Validation results indicated that the hybrid methods developed in this study can be used to estimate land surface longwave radiation budget with an improved accuracy than existing satellite-derived datasets. MODIS-derived surface longwave radiation budget can capture more detailed variations. It can be used as input or diagnostic parameters to better support high resolution land surface models and numerical prediction models.

The new hybrid methods developed in this study are computationally efficient and are easy to be implemented to generate operational products. Although sophisticated procedures were involved in the methods development process, only the resulted statistical models, TOA radiance, and surface elevation (in case of LWDN) are needed to produce surface longwave radiation products. Alternative methods, i.e., the physical method for estimating LWDN and the temperature-emissivity method for estimating LWUP, require more satellite derived products (atmosphere profiles, LST and emissivity) and are sensitive to the errors in these input parameters. The hybrid methods are not affected by the errors in other satellite derived products.

8.4 Suggestions for Future Research

8.4.1 Further Evaluation of the Hybrid Methods

The new hybrid methods developed in this study were only evaluated using SURFRAD sites at the current stage. Although SURFRAD sites have a wide variety of land cover types, all sites are located within the continental U.S. Sites from other areas are needed to further evaluate the accuracy of the hybrid methods developed. Surface pressure is an important factor in land LWDN. SURFARAD site elevations do not exceed

1700 meters above sea level. Ground sites with higher surface elevation, such as the Tibet sites (~4700 m) of the Asian Automatic Weather Station Network Project, are needed to further evaluate the LWDN hybrid methods.

8.4.2 Using Atmosphere Infra-Red Sounder Atmosphere (AIRS) Profiles

MOIDS-Retrieved atmospheric temperature and moisture profiles were used in radiative transfer simulation required by the hybrid methods. MODIS-retrieved atmosphere profiles have coarse vertical resolution and can not provide sufficient information about the atmosphere close to the surface, where the majority of LWDN originated. Using high vertical resolution satellite-retrieved atmosphere profiles to replace MODIS-retrieved profiles may further improve the accuracy of the hybrid methods developed in this study.

The AIRS onboard of the NASA Aqua EOS satellite is a high spectral resolution spectrometer with 2378 bands in the thermal infrared (3.7 - 15.4 μm). The retrieved atmosphere profiles available from the AIR supporting product have 100 levels (Susskind et al., 1998; Aumann et al., 2003). Although the spatial resolution of AIRS atmosphere product is coarser than that of MODIS, the retrieved profiles may be used to simulate more realistic TOA radiance. Better LWDN and LWUP models may be derived from the simulated databases.

8.4.3 Estimating Cloudy-Sky Surface Longwave Radiation Budget from MODIS and GOES data

The hybrid methods presented in the dissertation are focused on estimating instantaneous clear-sky LWUP and LWDN. Instantaneous cloudy-sky LWUP and LWDN are required to generate the daily and monthly averaged surface longwave

radiation budget. Large errors exist in satellite-derived cloudy-sky surface longwave radiation budget because of the challenges in estimating cloud base height, cloud base temperature, atmosphere and surface conditions under the clouds using thermal remote sensing techniques. Future research is needed to develop methods for estimating the cloudy-sky surface longwave radiation budget from MODIS and GOES data and estimating daily and monthly averaged surface longwave radiation budget components.

References

Ackerman, Steve, Kathleen Strabala, Paul Menzel, Richard Frey, Chris Moeller, Liam Gumley, Bryan Baum, Suzanne Wetzel Seeman, and Hong Zhang. (2002). Discriminating clear-sky from cloud with MODIS: algorithm theoretical basis document (MOD35). *Cooperative Institute for Meteorological Satellite Studies, University of Wisconsin-Madison; NOAA/NESDIS, NASA/LaRC, Hampton, VA*.

Albrecht, B., and S. K. Cox. (1977). Procedures for improving pyrgeometer performance. *Journal of Applied Meteorology*, 16(2), 188-197.

ASDC. (2006). http://eosweb.larc.nasa.gov/HPDOCS/projects/rad_budg.html [visited Dec. 22,, 2006].

Augustine, John A., John J. DeLuisi, and Charles N. Long. (2000). SURFRAD—A national surface radiation budget network for atmospheric research. *Bulletin of the American Meteorological Society*, 81(10), 2341-2357.

Augustine, John A., Gary B. Hodges, Christopher R. Cornwall, Joseph J. Michalsky, and Carlos I. Medina. (2005). An update on SURFRAD—The GCOS Surface Radiation Budget Network for the continental United States. *Journal of Atmospheric and Oceanic Technology*, 22(10), 1460-1472.

Aumann, H.H., M.T. Chahine, C. Gautier, M.D. Goldberg, E. Kalnay, L.M. McMillin, H. Revercomb, P.W. Rosenkranz, W.L. Smith, D.H. Staelin, L.L. Strow, and J. Susskind. (2003). AIRS/AMSU/HSB on the Aqua mission: design, science objectives, data products, and processing systems. *Geoscience and Remote Sensing, IEEE Transactions on*, 41(2), 253-264.

Barnes, William L., Thomas S. Pagano, and Vincent Salomonson. (1998). Prelaunch characteristics of the Moderate Resolution Imaging Spectroradiometer (MODIS) on EOS-AM1. *IEEE Transactions on Geoscience and Remote Sensing*, 36(4), 1088-1100.

Berk, A., G. P. Anderson, P. K. Acharya, J. H. Chetwynd, L. S. Bernstein, E. P. Shettle, M. W. Matthew, and S. M. Adler-Golden. (1999). MODTRAN4 user's manual. *Air Force Research Laboratory, Space Vehicles Directorate, and Air Force Materiel Command*.

CEOS, and WMO. (2000). http://192.91.247.60/sat/aspscripts/Requirementsearch.asp [visited Feb. 7, 2007].

Charlock, Thomas. (2006). http://www-cave.larc.nasa.gov/cave/ [visited Dec 22, 2006].

Curry, Judith A., William B. Rossow, David Randall, and Julie L. Schramm. (1996). Overview of arctic cloud and radiation characteristics. *Journal of Climate*, 9, 1731-1764.

Darnell, Wayne L., Shashi K. Gupta, and W. Frank Staylor. (1983). Downward longwave radiation at the surface from satellite measurements. *Journal of Applied Meteorology*, 22(11), 1956-1960.

Diak, George R., William L. Bland, John R. Mecikalski, and Martha C. Anderson. (2000). Satellite-based estimates of longwave radiation for agricultural applications. *Agricultural and Forest Meteorology*, 103(4), 349-355.

Ellingson, Robert G. (1995). Surface longwave fluxes from satellite observations: a critical review. *Remote Sensing of Environment*, 51(1), 89-97.

Fang, Hongliang, Shunlin Liang, Hye-Yun Kim, John R. Townshend, Crystal L. Schaaf, Alan H. Strahler, and Robert E. Dickinson. (2007). Developing a spatially continuous 1 km surface albedo dataset over North America from Terra MODIS products. *Journal of Geophysical Research*, 112(D20206)

Francis, J., and J. Secora. (2004). A 22-year dataset of surface longwave fluxes in the Arctic. *Fourteenth ARM Science Team Meeting Proceedings*, March 22-26, at Albuquerque, New Mexico.

Gabarró, C., M. Vall-Llossera, J. Font, and A. Camps. (2004). Determination of sea surface salinity and wind speed by L-band microwave radiometry from a fixed platform. *International Journal of Remote Sensing 25*, (1)

GCOS. (2006). Systematic observation requirements for satellite-based products for climate-supplemental details to the satellite-based component of the implementation plan for the global observing system for climate in support of the UNFCCC. *The Global Climate Observation System*. GCOS-107. http://www.wmo.ch/web/gcos/Publications/gcos-107.pdf.

GEWEX. (2002). Global Enery and Water Cycle Experiment: Phase I. *GEWEX*. http://www.gewex.org.

Gillespie, A. R., S. Rokugawa, S. J. Hook, T. Matsunaga, and A. B. Kahle. (1999). Temperature/emissivity separation algorithm theoretical basis document (version 2.4). http://eospso.gsfc.nasa.gov/eos_homepage/for_scientists/atbd/docs/ASTER/atbd-ast-05-08.pdf.

Gillespie, A., S. Rokugawa, T. Matsunaga, J.S. Cothern, S. Hook, and A.B. Kahle. (1998). A temperature and emissivity separation algorithm for Advanced Spaceborne

Thermal Emission and Reflection Radiometer (ASTER) images. *IEEE Transactions on Geoscience and Remote Sensing*, 36(4), 1113-1126.

Guenther, B., G. D. Godden, X. Xiong, E. J. Knight, S.-Y. Qiu, H. Montgomery, M. M. Hopkins, M. G. Khayat, and Z. Hao. (1998). Prelaunch algorithm and data format for the level 1 calibration product for the EOS-AM1 Moderate Resolution Imaging Spectroradiometer (MODIS). *IEEE Transactions on Geoscience and Remote Sensing*, 36(4), 1142-1151.

Gupta, Shashi K. (1989). A parameterization for longwave surface radiation from sun-synchronous satellite data. *Journal of Climate*, 2(4), 305-320.

Gupta, Shashi K., David P. Kratz, and Anne C. Wilber. (2004). Validation of parameterized algorithms used to derive TRMM–CERES surface radiative fluxes. *Journal of Atmospheric and Oceanic Technology*, 21(5), 742–752.

Gupta, Shashi K., Charles H. Whitlock, Nancy A. Ritchey, and Anne C. Wilber. (1997). Clouds and the Earth's Radiant Energy System (CERES) algorithm theoretical basis document: an algorithm for longwave surface radiation budget for total skies (subsystem 4.6.3). http://asd-www.larc.nasa.gov/ATBD/pdf_docs/r2_2/ceres-atbd2.2-s4.6.3.pdf.

Inamdar, A. K., and V. Ramanathan. (1997). Clouds and the Earth's Radiant Energy System (CERES) algorithm theoretical basis document: estimation of longwave surface radiation budget from CERES (subsystem 4.6.2). http://asd-www.larc.nasa.gov/ATBD/pdf_docs/r2_2/ceres-atbd2.2-s4.6.2.pdf.

———. (1997). On monitoring the atmospheric greenhouse effect from space. *Tellus Ser. B-Chem. Phys. Meteorol.*, 49

———. (1998). Tropical and global scale interactions among water vapor, atmospheric greenhouse effect, and surface temperature. *Journal of Geophysical Research-Atmosphere*, 103(D24), 32177-32194.

Insightful. (2005). http://www.insightful.com/support/splus70unix/unixug.pdf [visited May 1, 2007].

Lee, H. -T. (1993). Development of a statistical technique for estimating the downward longwave radiation at the surface from satellite observations. PhD Dissertation. *Dept. of Meteorology*, *University of Maryland*, College Park, Maryland.

Lee, Hai-Tien, and Robert G. Ellingson. (2002). Development of a nonlinear statistical method for estimating the downward longwave radiation at the surface from satellite observations. *Journal of Atmospheric and Oceanic Technology*, 19(10), 1500-1515.

Liang, Shunlin. (2004). Quantitative remote sensing of land surfaces. Edited by J. A. Kong, *Wiley series in remote sensing*. Jew Jersey: John Wiley & Sons.

Liu, Ronggao G., Jiyuan Y. Liu, and Shunlin Liang. (2006). Estimation of systematic errors of MODIS thermal infrared bands. *IEEE Geoscience and Remote Sensing Letters*, 3(4), 541-545.

Meerkoetter, H., and Hartmut Grassl. (1984). Longwave net flux at the ground from radiance at the top. *IRS '84 current problems in atmospheric radiation; proceedings of the International Radiation Symposium*, 21-28 August 1984, at Perugia, Italy.

Menzel, W. Paul, Suzanne W. Seemann, Jun Li, and Liam E. Gumley. (2002). MODIS atmospheric profile retrieval algorithm theoretical basis document. *University of Wisconsin-Madison*. http://modis-atmos.gsfc.nasa.gov/JOINT/atbd.html.

Minnis, P., L. Nguyen, W. L. Smith Jr., M. M. Khaiyer, R. Palikonda, D. A. Spangenberg, D. R. Doelling, D. Phan, G. D. Nowicki, P. W. Heck, and C. Wolff. (2004). Real-time cloud, radiation, and aircraft icing parameters from GOES over the USA. In *Proc. 13th AMS Conf. Satellite Oceanogr. and Meteorol.* Norfolk, VA.

Morcrette, J. J., and P. Y. Deschamps. (1986). Downward longwave radiation at the surface in clear sky atmospheres: comparison of measured, satellite-derived and calculated fluxes. *Proc. ISLSCP Conf*, at Rome, ESA SO-248M Darmstadt, Germany.

Philipona, Rolf, Ellsworth G. Dutton, Tom Stoffel, Joe Michalsky, Ibrahim Reda, Armin Stifter, Peter Wendling, Norm Wood, Shepard A. Clough, Eli J. Mlawer, Gail Anderson, Henry E. Revercomb, and Timothy R. Shippert. (2001). Atmospheric longwave irradiance uncertainty: Pyrgeometers compared to an absolute sky-scanning radiometer, atmospheric emitted radiance interferometer, and radiative transfer model calculations. *Journal of Geophysical Research*, 106(D22), 28,129 –28,141.

Philipona, Rolf, Claus Fröhlich, Klaus Dehne, John DeLuisi, John Augustine, Ellsworth dutton, Don Nelson, Bruce Forgan, Peter Novotny, John Hickey, Steven P. Love, Steven Bender, Bruce McArthur, Atsumu Ohmura, John H. Seymour, John S. Foot, Masataka Shiobara, Francisco P. J. Valero, and Anthony W. Strawa. (1998). The Baseline Surface Radiation Network pyrgeometer round-bobin calibration experiment. *Journal of Atmospheric and Oceanic Technology*, 15(3), 687-696.

Prata, Fred. (2002). Land surface temperature measurement from space: AATSR algorithm theoretical basis document. *CSIRO Atmospheric Research*. http://earth.esa.int/pub/ESA_DOC/LST-ATBD.pdf.

Schmetz, Johannes. (1989). Towards a surface radiation climatology: retrieval of downward irradiances from satellites. *Atmospheric Research*, 23(3-4), 287-321.

Schmit, T.J., M.M. Gunshor, W.P. Menzel, J.J. Gurka, and J. Li. (2005). Introducing the next-generation Advanced Baseline Imager on GOES-R. *Bulletin of the American Meteorological Society*, 86(1079-1096)

Seemann, Suzanne W., Jun Li, W. Paul Menzel, and Liam E. Gumley. (2003). Operational retrieval of atmospheric temperature, moisture, and ozone from MODIS infrared radiances. *Journal of Applied Meteorology*, 42(8), 1072-1091.

Smith, W. L., and H. M. Wolfe. (1983). Geostationary satellite sounder (VAS) observations of longwave radiation flux. *The Satellite Systems to Measure Radiation Budget Parameters and Climate Change Signal*, 29 Aug - 2 Sep, at Igls, Austria.

Sobrino, J. A., and M. Romaguera. (2004). Land surface temperature retrieval from MSG1-SEVIRI data. *Remote Sensing of Environment*, 92(2), 247-254.

Sobrino, Jose A., Juan C. Jimenez-Munoz, and Leonardo Paolini. (2004). Land surface temperature retrieval from LANDSAT TM 5. *Remote Sensing of Environment*, 90(4), 434-440.

Space Systems-Loral. (1996). GOES I-M Data Book. DRL 101-08.

Strahler, Alan, Doug Muchoney, Jordan Borak, Mark Friedl, Sucharita Gopal, Eric Lambin, and Aaron Moody. (1999). MODIS Land Cover Product Algorithm Theoretical Basis Document (ATBD) Version 5.0. *Boston University*. http://modis.gsfc.nasa.gov/data/atbd/atbd_mod12.pdf.

Susskind, Joel, Chris Barnet, and John Blaisdell. (1998). Determination of atmospheric and surface parameters from simulated AIRS/AMSU/HSB sounding data: Retrieval and cloud clearing methodology. *Advances in Space Research*, 21(3), 369-384.

The Eppley Laboratory. (2007). http://www.eppleylab.com/ [visited Dec. 4, 2007].

Toller, Gary N., Alice Isaacman, James Kuyper, and Vincent Salomonson. (2006). MODIS Level 1B Product User's Guide. *NASA/Goddard Space Flight Center*.

Wan, Zhengmin, and J. Dozier. (1996). A generalized split-window algorithm for retrieving land-surface temperature from space. *IEEE Transactions on Geoscience and Remote Sensing*, 34(4), 892-905.

Wan, Zhengming. (1999). MODIS land-surface temperature algorithm theoretical basis document (LST ATBD):version 3.3. *University of California, Santa Barbara*. http://modis.gsfc.nasa.gov/data/atbd/atbd_mod11.pdf.

———. (2008). New refinements and validation of the MODIS Land-Surface Temperature/Emissivity products. *Remote Sensing of Environment*, 112, 59–74.

Wan, Zhengming, and Zhao-Liang Li. (1997). A physics-based algorithm for retrieving land-surface emissivity and temperature from EOS/MODIS data. *IEEE Transactions on Geoscience and Remote Sensing*, 35(4), 980-996.

Wan, Zhengming, Yulin Zhang, Zhao-liang Li, Ruibo Wang, Vincent V. Salomonson, Arnaud Yves, Roland Bosseno, and Jean Francois Hanocq. (2002). Preliminary estimate of calibration of the moderate resolution imaging spectroradiometer thermal infrared data using Lake Titicaca. *Remote Sensing of Environment*, 80(3), 497-515.

Wang, K., Z. Wan, P. Wang, M. Sparrow, J. Liu, and S. Haginoya. (2007). Evaluation and improvement of the MODIS land surface temperature/emissivity products using ground-based measurements at a semi-desert site on the western Tibetan Plateau. *International Journal of Remote Sensing*, 28(11), 2549 - 2565.

Wang, Kaicun, Zhengming Wan, Pucai Wang, Michael Sparrow, Jingmiao Liu, Xiuji Zhou, and Shigenori Haginoya. (2005). Estimation of surface long wave radiation and broadband emissivity using Moderate Resolution Imaging Spectroradiometer (MODIS) land surface temperature/emissivity products. *Journal of Geophysical Research*, 110(D11109)

Wang, Wenhui, and Shunlin Liang. (2008). Estimating high spatial resolution clear-sky surface downwelling longwave radiation and net longwave radiation from MODIS Data. *Remote Sensing of Environment*, submitted

Wang, Wenhui, Shunlin Liang, and John A. Augustine. (2008). Estimating high spatial resolution clear-sky land surface upwelling longwave radiation from MODIS Data. *IEEE transactions on geoscience and remote sensing*, revised

Wang, Wenhui, Shunlin Liang, and Tilden Meyers. (2008). Validating MODIS land surface temperature products using long-term nighttime ground measurements. *Remote Sensing of Environment*, 112(3), 623-635.

Wielicki, Bruce A., Bruce R. Barkstrom, Edwin F. Harrison, Robert B. Lee III, G. Louis Smith, and John E. Cooper. (1996). Clouds and the Earth's Radiant Energy System (CERES): an earth observation system experiment. *Bulletin of the American Meteorological Society*, 77(5), 853-868.

Wild, Martin, Atsumu Ohmura, and Hans Gilgen. (2001). Evaluation of downward longwave radiation in general circulation models. *Journal of climate*, 14, 3227-3238.

Zhang, Y.-C., and W. B. Rossow. (2002). New ISCCP global radiative flux data products. *GEWEX News*, 12(4), 7.

Zhang, Y.-C., W. B. Rossow, and A. A. Lacis. (1995). Calculation of surface and top of atmosphere radiative fluxes from physical quantities based on ISCCP datasets: 1.

Method and sensitivity to input data uncertainties. *Journal of Geophysical Research*, 100(D1), 1149–1165.

Zhang, Yuanchong, William B. Rossow, Andrew A. Lacis, Valdar Oinas, and Michael I. Mishchenko. (2004). Calculation of radiative fluxes from the surface to top of atmosphere based on ISCCP and other global datasets: Refinements of the radiative transfer model and the input data. *Journal of Geophysical Research*, 109(D19105)

Zhou, Yaping, and Robert D. Cess. (2001). Algorithm development strategies for retrieving the downwelling longwave flux at the Earth's surface. *Journal of Geophysical Research*, 106(D12), 12477-12488.

Zhou, Yaping, David P. Kratz, Anne C. Wilber, Shashi K. Gupta, and Robert D. Cess. (2007). An improved algorithm for retrieving surface downwelling longwave radiation from satellite measurements. *Journal of Geophysical Research*, 112(D15102)